Electronic Thesis and Dissertation Repository

12-15-2020 10:30 AM

Development of Multi-Functional Molecular Systems for Applications on Nanomaterial Surfaces

Jun Hyeong Park, *The University of Western Ontario*

Supervisor: Workentin, Mark S., *The University of Western Ontario*
A thesis submitted in partial fulfillment of the requirements for the Master of Science degree in Chemistry
© Jun Hyeong Park 2020

Abstract

The glutathione-mediated, retro Michael-type addition reaction is demonstrated to take place at the interface of water-soluble, maleimide-functionalized gold nanoparticles (Maleimide-AuNP). The retro Michael-type addition can be blocked by hydrolyzing the Michael addition thioether adduct at the nanoparticle's interface. This procedure "locks" the molecule of interest onto the Maleimide-AuNP template, ensuring no loss of the molecular cargo from the nanocarrier. On the other hand, the glutathione-mediated retro Michael-type addition reaction can be exploited for delivering a molecular payload. The Michael donor, 4-mercaptophenylacetic acid was modified with a terminal azide, allowing for addition of cargo through strain-promoted alkyne azide cycloadditions with various functional alkynes. The resulting AuNPs are versatile platforms for the integration of multiple functionalities within a single construct, enabling their use in complex biotic environments. As a proof of concept, a fluorogenic molecular cargo was incorporated onto a Maleimide-AuNP and delivered via the glutathione-mediated, retro Michael-type addition reaction.

Keywords

Summary for Lay Audience

Nanomaterials are extremely tiny materials that are typically between 1-100 nm in diameter and have unique characteristics and properties compared to the bulk material. They have been identified as promising candidates for application in optics, electronics, and medicine. Gold nanoparticles (AuNPs) are one type of nanomaterial that have been previously used in optical sensing, cancer therapy, and drug delivery due to their compatibility with biological environments and high stability. Flexible, linker chemicals attached to various functional molecules can be bound to the surface of AuNPs to change their physical and chemical properties. Further function (drug, imaging agent, etc.) can be introduced to AuNPs through the manipulation of the peripheral molecules using click reactions. Click chemistry, defined as highly efficient reactions that proceed under mild conditions, is becoming increasingly popular in the materials chemistry field due to its ease of purification and lack of undesired by-products. Previously our research group has demonstrated this reactivity by binding fluorescent molecules to AuNPs, then releasing them under biological conditions. The release was triggered by the addition of glutathione (GSH), a compound commonly found in cancer cells. Therefore, this research helped to develop a "click & release" system on AuNPs to deliver chemical cargo to GSH rich environments, however the system was poorly understood, and potential applications were largely unexplored. The goal of this thesis was to further investigate and improve this "click & release" system to expand its practicality and to widen the scope of its application. By implementing more bio-compatible click reactions in this system, a functional chemical cargo can be attached and released more effectively. The molecular system will be responsive towards GSH concentrations (which varies in tumor cells and healthy cells) and can therefore be exploited for selective release in biological environments. Overall, the goal of this research is to engineer functional and responsive materials that will provide exciting new applications across the sciences.

Co-Authorship Statement

The work discussed in this thesis contains contributions from the author, the supervisor Prof. Mark S. Workentin, and a colleague Jonathan Wong. The contributions of each are described below.

Chapter 1 was written by the author and edited by Prof. Mark S. Workentin.

Chapter 2 describes a series of small molecule compounds that were synthesized and characterized by the author. The chapter was written by the author and edited by Prof. Mark S. Workentin.

Chapter 3 describes the synthesis, characterization, and surface modifications of various AuNPs. The electrochemical studies were performed by Jonathan Wong from the Ding group. All other experiments and measurements were conducted by the author. The chapter was written by the author and edited by Prof. Mark. S. Workentin.

Chapter 4 was written by the author and edited by Prof. Mark S. Workentin.

Acknowledgments

First, I would like to express my gratitude to my supervisor, mentor and friend, Dr. Mark Workentin! You have truly been a great role model for me in academia and in my personal life. You have inspired me to pursue further education, worked tirelessly to open several opportunities for me, spurred me on to be a well-rounded person, and much, much more. From your passion for learning, to your support and patience with me in stressful, trying times; you have made a massive, positive impact on my life! I am so thankful and excited to continue working with you in my PhD program!

A special thank you to Dr. Pierangelo Gobbo from The University of Bristol, who welcomed me into his research group in 2019 and for my PhD program. A big thank you to my committee members; Prof. Robert Hudson, Prof. James Wisner, and Prof. Vera Tai for taking the time to read this thesis. I am extremely grateful to the professors in the department I have had the opportunity to work with: Prof. Johanna Blacquiere, Prof. Paul Ragogna, Prof. Michael Kerr, Prof. Brian Pagenkopf, Prof. James Wisner, Prof. Zhifeng Ding, and Prof. Joe Gilroy. I would also like to thank the rest of the Department of Chemistry's faculty, support staff, and administration: Mathew Wilans, Doug Hairsine, Yves Rambour, John Vanstone, Jon Aukema, Barakat Misk, Monica Chirigel, and more.

Next, and in no particular order, I'd like to acknowledge all past and present Workentin Research Group members I've had the opportunity to work with: Wilson Luo, Praveen Gunawardene, Tommaso Romagnoli, Alexander Van Belois, Rajeshwar Vasdev, Kyle Classen, Sydney Legge, Andy Lim, Christian Petrozza, Komal Patel, Grace Lee, Johanna de Jong, Julia Martin, and Jake Rosati. A special shout out for Kyle Classen, thanks for being a great friend, roommate, and co-worker these past few years! I know you will kill it in law school and that you will do great things! Additionally, I would like to add Jonathan Wong, Benjamin Bridge, Michael Anghel, Meagan Kindervater, and Suendues Noori from other groups. A thanks to all my roommates over the years as well! Thank you all for the coffee runs, the meals shared together, the support and comradery, and the fun times and memories we have shared together!

Table of Contents

List of Figures

List of Schemes

List of Appendices

List of Abbreviations

°C	degree Celsius
^{13}C	carbon-13
^{1}H	proton
μL	microliter
AAC	alkyne-azide cycloaddition
AuNPs	gold nanoparticles
ATR	attenuated total reflectance
BCN	bicyclononyne
br	broad
Bu	butyl
cm^{-1}	wavenumber
COD	cyclooctadiene
CuAAC	copper(I)-assisted alkyne-azide cycloaddition
d	doublet
Da	dalton
DCC	N,N'-dicyclohexylcarbodiimide
dd	doublet of doublets
DIAD	diisopropyl azodicarboxylate
DIBAC	dibenzoazacyclooctyne

DIBO	dibenzocyclooctyne
DIFO	difluorinated cyclooctyne
DIPEA	N,N-diisopropylethylamine
DMAP	4-dimethylaminopyridine
DMF	dimethylformamide
DMSO	dimethylsulfoxide
dt	doublet of triplets
ESI-MS	electrospray ionization-mass spectrometry
Fc	ferrocene
FT	Fourier-transform
g	gram
GSH	glutathione
h	hours
hv	light
*hv*DIBO	cyclopropenone-caged dibenzocyclooctyne
HBTU	2-(1H-benzotriazol-1-yl)-1,1,3,3-tetramethyluronium hexafluorophosphate)
Hz	hertz
iPr	isopropyl
IR	infrared
J	coupling constant

K	degrees Kelvin
LCST	lower critical solution temperature
m	multiplet
M	molar
MHz	megahertz
min	minutes
mL	milliliter
mmol	millimole
mol	mole
MPA	4-mercaptophenylacetic acid
MWCO	molecular weight cutoff
NHS	N-hydroxysuccinimide
NIR	near-infrared
nm	nanometer
NMM	N-methylmaleimide
NMR	nuclear magnetic resonance
OCT	cyclooctyne
PBS	phosphate buffer solution
Ph	phenyl
pNIPAM	poly(N-isopropylacrylamide)

ppm	parts per million
q	quartet
ROS	reactive oxygen species
rpm	revolutions per minute
r.t.	room temperature
s (in NMR data)	singlet
s	second
SCE	saturated calomel electrode
SPAAC	strain-promoted alkyne-azide cycloaddition
SPANC	strain-promoted alkyne-nitrone cycloaddition
t	triplet
TBAF	tetrabutylammonium fluoride
TBAP	tetrabutylammonium perchlorate
TBDMS	tert-butyldimethylsilyl
TBDMSCl	tert-butyldimethylsilyl chloride
TEM	transmission electron microscopy
TFA	trifluoroacetic acid
THF	tetrahydrofuran
TIPS	triisopropylsilane
tt	triplet of triplets

UV-A	ultraviolet A
UV-Vis	ultraviolet-visible
λ	wavelength
λ_{em}	wavelength of emission
λ_{ex}	wavelength of excitation
λ_{max}	wavelength of maximum absorption

Chapter 1

1 Introduction

Over the past few decades, researchers have extensively studied nanotechnology and material sciences to synthesize a vast variety of nanomaterials, varying in morphology, solubility, and in size.[1-2] These structurally unique materials are generally inert and difficult to functionalize; however, they can be specifically altered to become useful in several applications including drug delivery, biolabeling, and electrochemistry.[3-4] Bioorthogonal click chemistry enables the facile introduction of functional moieties to nanomaterial surfaces. The incorporation of these transformations decreases reaction times, increases selectivity in complex environments, and provides greater molecular control when synthesizing functional nanomaterials for use in biological environments. To functionalize these materials, substituents with specific functions are conjugated to the nanomaterial surface or a reactive group is interfacially introduced, which can then be further functionalized. These functional moieties can then be displaced off the nanomaterial interface in the presence of glutathione, present in high concentrations in cancer cells.[5] Therefore, these bioorthogonal click reactions can be manipulated to develop a highly modular, multi-functional molecular system on nanomaterials for targeted biotic delivery of drugs, fluorophores, and redox active molecules.[6]

Click chemistry has become an established category of reactions characterized by rapid, high yielding, and atom economic transformations that require minimal purification and can be carried out under ambient conditions.[7] Click reactions tend to incorporate highly selective, reactive partners that make click chemistry very advantageous for complex chemical systems and a powerful tool in materials sciences.[8-10] One of the most utilized click moieties in the field is the maleimide group. Maleimides are versatile compounds that can be easily modified using a wide range of click reactions, including Diels Alders (Scheme 1 A), Michael additions (Scheme 1 B), and 1,3-dipolar cycloadditions (Scheme 1 C).[11] This group is commonly tethered onto the periphery of materials to gain access to several routes of functionalization on a single template. As depicted in Scheme 1, multiple distinct transformations can install a single R group on the maleimide, allowing for several

different methods to incorporate the same functionality. Conversely, several different functionalities can be introduced to maleimides using only one click reaction: a Michael addition. A Michael addition is a reaction where a nucleophile participates in a 1,4-conjugate addition to an α, β-unsaturated carbonyl.[12] The nucleophile is referred to as a Michael donor and can be derived from an anion or a heteroatom with a lone pair. The α, β-unsaturated carbonyl is the electrophile in the reaction and is referred to as a Michael acceptor.[13]
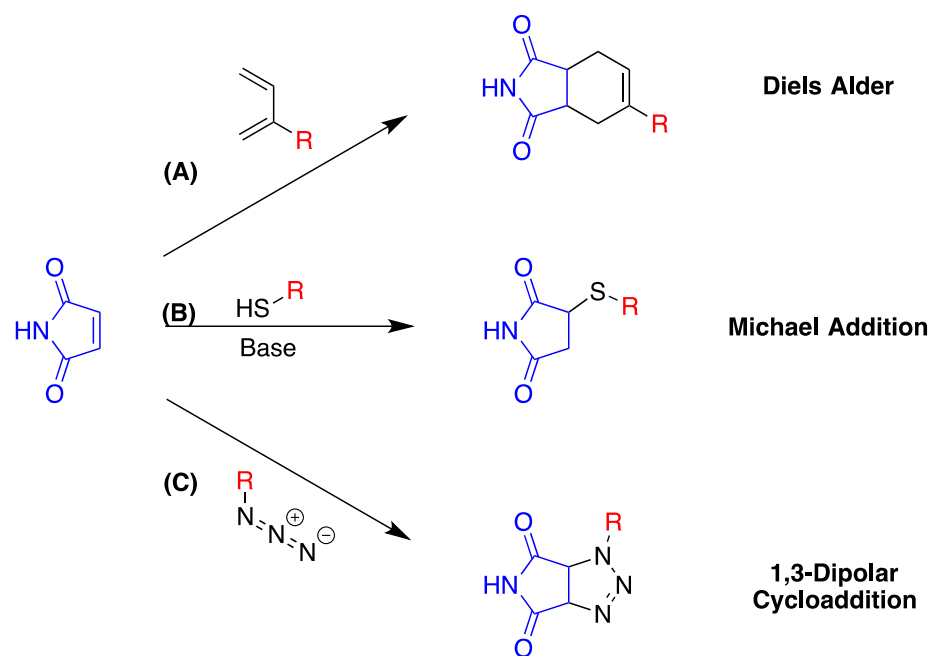
Scheme 1: The introduction of a R group onto a maleimide through in multiple reactions; Diels Alder cycloaddition (**A**), thiol Michael addition (**B**), and a dipolar cycloaddition with an azide (**C**).

Another set of transformations prominent in the field of click chemistry are alkyne-azide cycloadditions (AACs) where an azide reacts with an alkyne to form a stable triazole ring (Scheme 2 A).[14] However, this reaction is not a click reaction as high reaction temperatures are required. Although, with the use of copper (I) salts to catalyze this reaction, Sharpless and Meldal found that the cycloaddition occurs at r.t. (Scheme 2 B).[15-16] This click reaction was called the Cu(I)-assisted alkyne-azide cycloaddition (CuAAC). CuAACs enabled the construction of more advanced and complex structures that were previously difficult or impossible to obtain, however, its use in living systems was limited due to the cytotoxicity of Cu(I) that mediates the generation of reactive oxygen species

(ROS), which degrades delicate biomolecules.[17-19] In 2004, Bertozzi and coworkers established a copper free AAC by utilizing strained alkynes (Scheme 2 C).[20] These alkynes did not require catalysts for AACs because they were more reactive due to ring strain and bond angle deformation. With this new click reaction, named the strain-promoted alkyne-azide cycloaddition (SPAAC), Bertozzi et al. demonstrated covalent modifications to biomolecules in living systems, overcoming the toxicity problem with CuAACs.[20] Therefore, SPAACs caught the attention of material scientists to be a viable chemical tool for the assembly of materials with more functional or complex architectures. This research is so impactful that it is a topic of discussion to be potentially awarded a Nobel Prize in Chemistry.
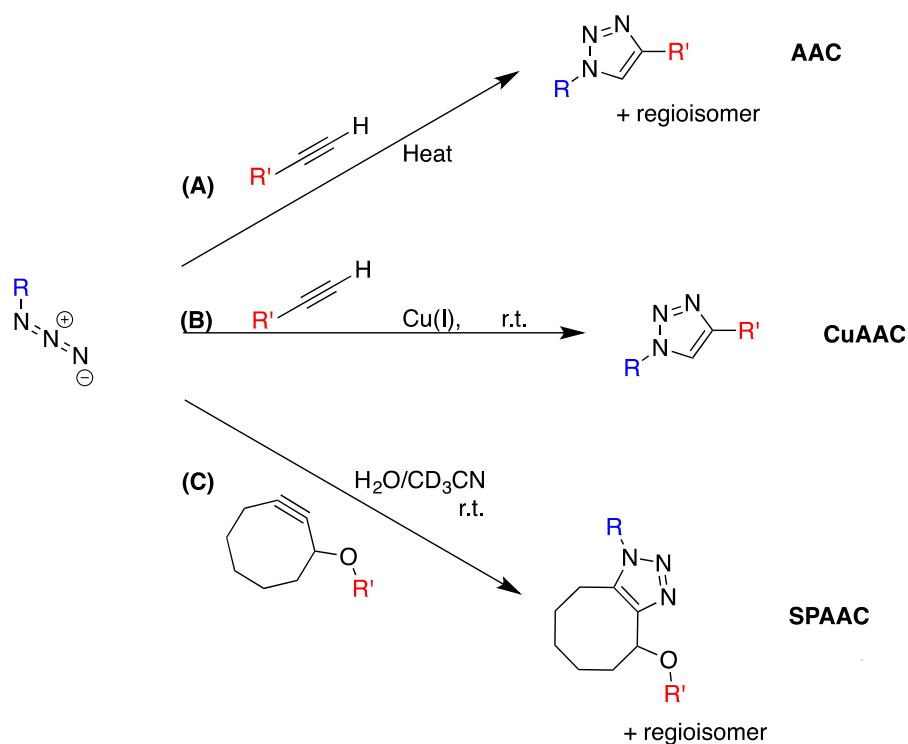
Scheme 2: An azide participating in multiple reactions with alkynes; alkyne-azide cycloaddition (**A**), Cu(I)-assisted alkyne-azide cycloaddition (**B**), and a strain promoted alkyne-azide cycloaddition (**C**).

The successful implementation SPAACs with cyclooctyne (OCT) in biomaterials led to the development of improved or alternative strained alkynes. The objective of synthetic chemists is to design and yield strained alkynes with more rapid reaction kinetics than OCT by making the alkyne electron deficient and sterically rigid (Figure 1). The two

fluoro groups on difluorinated cyclooctyne (DIFO) are electron withdrawing, thus pulling electron density away from the alkyne and yielding a less stable, more reactive click partner for azides. Bicyclononyne (BCN) is a bicyclic compound with less steric encumbrance than OCT due to its substituent positioning being further from the strained alkyne. Dibenzoazacyclooctyne (DIBAC) and dibenzocyclooctyne (DIBO) introduced more sp^2 hybridized carbons into the cyclooctyne ring, causing more ring strain on the alkyne and blocking lower energy conformations from ring buckling. As the reaction kinetics of the strained alkynes improved, the stability of these derivatives decreased. To circumvent degradation and unwanted side reactivity of the strained alkyne, a cyclopropenone-masked dibenzocyclooctyne (*hv*DIBO) can be used. The Popik group was able to synthesize this molecule in 2009, and demonstrated the facile unmasking of the strained alkyne using ultraviolet A light.[21] When *hv*DIBO is irradiated with 350 nm light, the cyclopropenone ring is opened and carbon monoxide is released via a radical process to cleanly yield the deprotected strained alkyne (Scheme 3). The rapid deprotection can be performed *in situ* and the resulting alkyne is then free to selectively react with an azide in a SPAAC. Along with its great stability and simple deprotection method, the application of *hv*DIBO in multi-functional molecular systems introduces spatial and temporal control due to the sensitivity of the cyclopropenone group to 350 nm UV-A light.[22-24] Electronically and sterically distinct azides have not been extensively studied due to the explosiveness of many small azides and expensive synthesis costs. However, one alternative to SPAACs are strain-promoted alkyne-nitrone cycloadditions (SPANCs), where a strained alkyne and a nitrone combine to form a stable isooxazoline.[25-27]
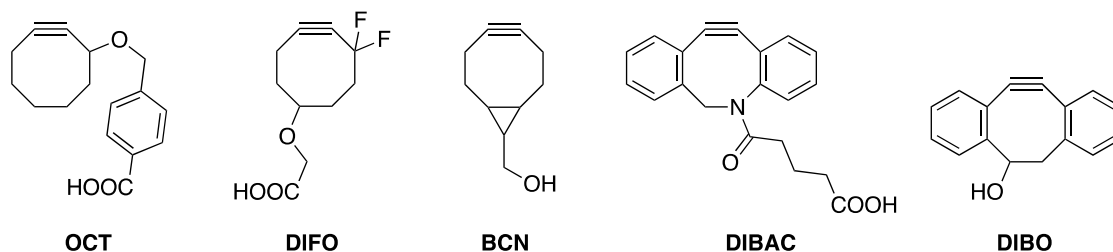
Figure 1: Various structurally unique, strained alkynes used in SPAACs. From left to right: cyclooctyne (**OCT**), difluorinated cyclooctyne (**DIFO**), bicyclononyne (**BCN**), dibenzoazacyclooctyne (**DIBAC**), and dibenzocyclooctyne (**DIBO**).
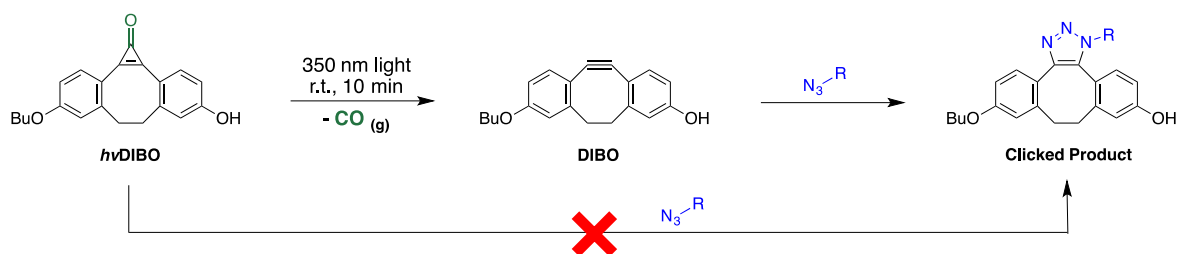
Scheme 3: The photochemical deprotection of *hv*DIBO via irradiation with 350 nm UV-A light. Carbon monoxide gas is liberated, yielding a strained alkyne which can form a triazole ring in a reaction with an azide. The cyclopropenone group of *hv*DIBO is unreactive in the presence of azides.

Bioorthogonal reactions are a subset of click reactions, but with the added constraint of biocompatibility.[28-31] These highly selective transformations can occur under physiological conditions (H_2O, 37 °C, pH 6 – 8) and are inert in the presence of many other functional groups in biological systems.[28] Bioorthogonal click reactions frequently involve organic azides as one of the click partners due to their small size, inert nature to many biological processes, and versatility (Figure 2).[32-33] There are other moieties suitable for this class of reactions, but with nucleophiles, oxidants, and reductants so prevalent in living systems, these functionalities are quite rare. Despite these challenges, bioorthogonal click reactions have been extensively employed in a wide range of fields in chemical biology to form robust linkages.[34-35] These transformations enable the facile introduction of functional moieties to biologically active nanomaterials as well.
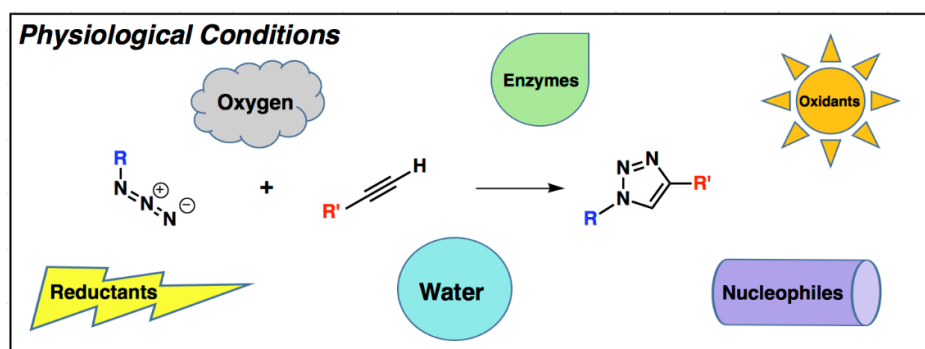
Figure 2: The stability of azides in physiological conditions (H_2O, 37 °C, pH 6 – 8) in the presence of water, oxygen, enzymes, nucleophiles, oxidants, and reductants.

Nanomaterials are nanoscale materials that are typically between 1-100 nm in diameter and have unique properties and reactivity, compared to the bulk material.[36] They have been identified as promising candidates for application in optics, electronics, and biomedicine.[37-38] The properties of these nanomaterials utilized for their applications are largely determined by the material itself, which may depend on the size, morphology, and the functional groups at the interface of the material.[39] In addition, nanomaterials provide a platform for the integration of multiple functionalities within a single construct, which permits their use in complex environments that require specific interactions at their interface. Manipulating the chemistry at the interface of these materials can alter the properties and allow them to be utilized in many applications; surface modifications have resulted in materials used in fluorescence imaging, drug delivery, and electrochemistry.[40-42] The Workentin Group has made efforts to incorporate SPAACs, along with other bioorthogonal click reactions into intricate molecular systems on gold nanoparticles (AuNPs) as a model reactive nanomaterial template to showcase chemical modifications in a facile and robust manner. AuNPs are one type of nanomaterial that have been previously used in optical sensing, cancer therapy, and drug delivery due to their biocompatibility and high stability.[43-44] AuNPs are composed of a metallic gold core and an organic ligand corona that stabilizes the metal core and prevents aggregation of individual particles. Due to this stabilization, AuNPs are very stable and can be stored for long periods of time with minimal degradation.[45] AuNPs have a strong binding affinity to thiols and their solubilities can be tuned to be organic or aqueous soluble (Scheme 4). These advantageous attributes of AuNPs can be controlled to engineer biocompatible nanoparticles; this is achieved by carefully selecting the thiol linker chains on the interface of the particles to be soluble in PBS buffer, by obtaining good particle stability at 37 °C, and by functioning at physiological pH.[45] One can also control the size of AuNPs based on the nanoparticle synthetic method selected and the varying ratio of the concentrations of the gold salt to the thiol ligand.[46] The high binding affinity between gold and sulfur allows for the conjugation of particles with organic ligands through thiol linker chains.[47] These organic ligands can modify the interface of AuNPs with various functional groups in order to change the physical and chemical properties of the particles.[48]
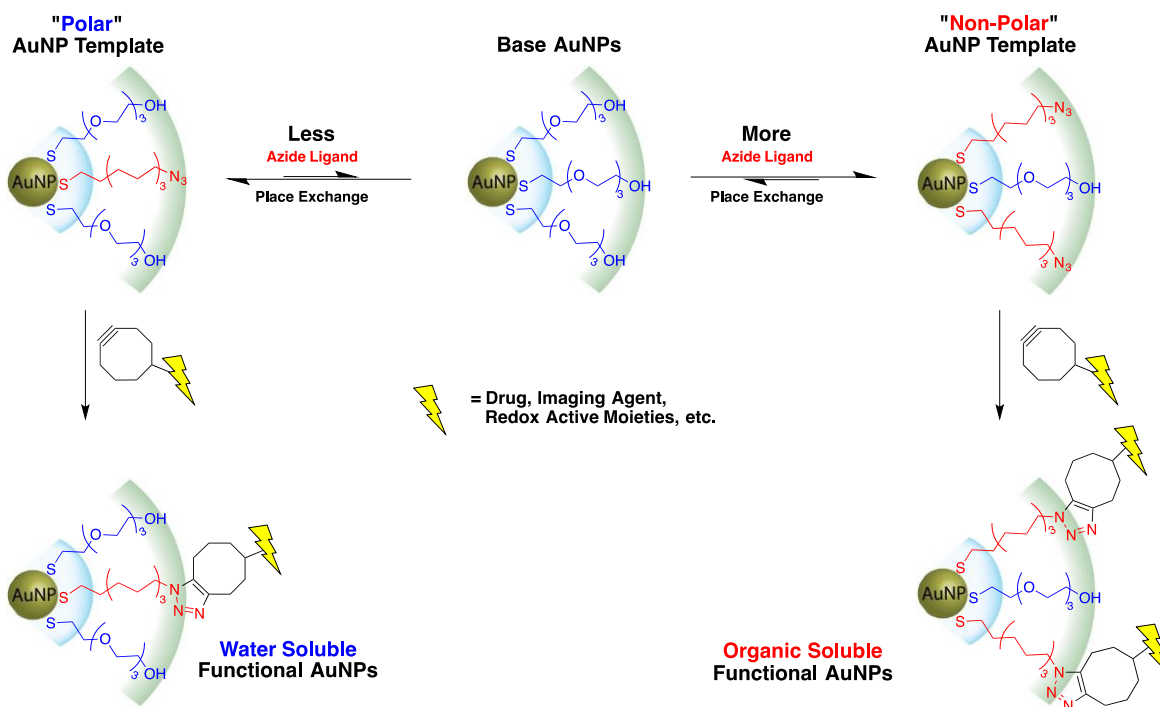
Scheme 4: Tuning solubilities of hydroxyl-terminated AuNPs via place exchange reactions with varying quantities of the nonpolar ligand (red). Equilibria of bound stabilizing ligands to the metallic gold cores are established between the polar hydroxyl-terminated ligands (blue) and the nonpolar azide-terminated ligands to both give polar and nonpolar AuNP templates. These templates can be functionalized with strained alkynes to produce water soluble and organic soluble functional AuNPs.

There are three main methods to add functionality onto AuNPs: direct synthesis, ligand displacement, and interfacial reactions. The direct synthesis method involves the addition of function to the particles during the initial synthesis of the particles (Scheme 5 A), while the ligand displacement method introduces function to inert base AuNPs (Scheme 5 B). Base AuNPs are synthesized with non-functional thiolates that form a stable monolayer of tightly packed ligands and although these particles are inert, they can easily be functionalized via place exchange reactions. These reactions introduce a second thiol ligand but with functionality to the base AuNPs and the functional thiol displaces the inert ligands until an equilibrium is reached with different concentrations of the two ligands bound on the surface of the AuNPs.[49] The third method is similar to the second, where inert base AuNPs are reacted with an additional thiol ligand in a place exchange reaction, but this thiol incorporates an intermediate reactive functionality (e.g. azides), not function (Scheme 5 C). The functionality is introduced during a second interfacial reaction, where

the functionality is bound to a reactive partner for the intermediate reactive functionality previously installed to combine with.[50] Another great advantage of working with AuNPs is the ease of characterization, as these nanomaterials may be characterized with a wide range of powerful techniques, including: NMR, UV-Vis, IR, TGA, etc. Thus, AuNPs were chosen as a model nanomaterial to modify in this work because of their stability, biocompatibility, solubility, ease of synthesis and characterization.
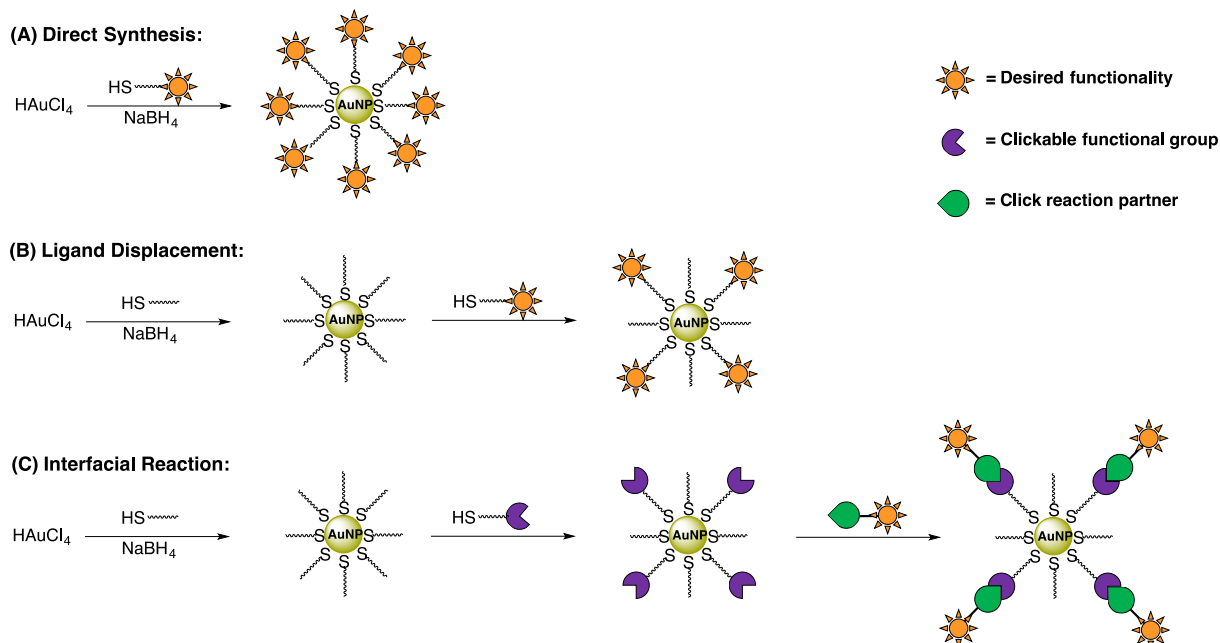
Scheme 5: Synthetic methods to introduce functionality (sun) to AuNPs; direct synthesis (**A**), ligand displacement (**B**), and interfacial reactions (**C**).

Previously, our group has demonstrated the use of Michael additions on maleimide-terminated AuNPs with mercaptophenylacetic acid (MPA) derivatives. Our group demonstrated that in the presence of glutathione (GSH), MPA is able to undergo a retro-Michael addition when bound to maleimide under physiological conditions (Scheme 6).[51] In this paper, a fluorescent dye was conjugated onto the carboxylic acid group of MPA as an imaging agent and the release of the dye in the presence of GSH and PBS buffer at 37 °C was studied. This molecular system showed promise for a new complex, multi-functional system on nanomaterial surfaces, however there were limitations. High temperatures were required to remove the furan groups off the protected maleimide-AuNPs via retro-Diels Alder reactions. Due to the increased temperatures, the desired AuNPs

began to aggregate, producing low yields and costly intermediate synthesis steps. The interfacial reactions on the resulting maleimide-AuNPs were time consuming and required several reagents that were difficult to separate from the desired AuNP products as well.
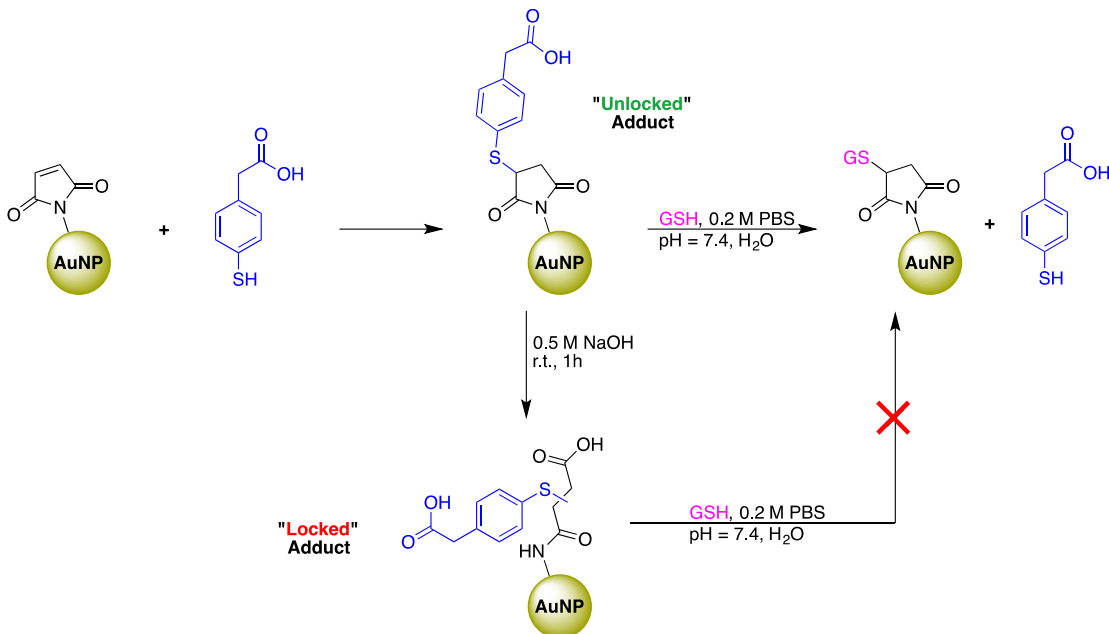
Scheme 6: The manipulation of maleimide-terminated AuNPs. MPA (blue) is bound to the maleimides through Michael additions to yield the "unlocked" adduct. The "unlocked" adduct is then reacted with GSH, which displaced off MPA in a retro-Michael addition under physiological conditions. On the contrary, the "locked" adduct can be formed via hydrolysis of the maleimide of the "unlocked" adduct, which does not react with GSH to release MPA.

Therefore, this thesis expands upon the previous system by utilizing more bioorthogonal click reactions and by incorporating 3-azido-1-propanamine onto the carboxylic acid moiety of MPA to form an amide that links to an azide. This modified MPA acts as a Michael donor and combines with maleimide and the azide can be used to introduce desired functionalization through SPAACs with strained alkynes. This new component opens the system up for facile, clean additions of various molecular cargo onto AuNPs with maleimide groups on the interface. Using SPAACs with azides to introduce functionality is much simpler than performing amide coupling reactions on carboxylic acids on the interface of AuNPs. As a result, this new molecular system is more adaptable to a versatile range of applications through cleaner transformations than the previous

system. Similarity, in the presence of GSH under physiological conditions, GSH can displace the cargo-loaded MPA groups off the MPA-maleimide-AuNPs to yield GSH-maleimide-AuNPs and released free cargo. The aim of this work is to incorporate bioorthogonal click reactions to develop a multifunctional nanomaterial template, which can undergo SPAACs with various cargo loaded strained alkynes. This system will use thiol-Michael additions with an azide modified MPA derivative to reversibly functionalize the interface of the AuNPs. Consequently, synthesizing a single nanomaterial that can undergo an assortment of functionalization with strained alkyne derivatives generates a molecular system capable of participating in a wide scope of applications (Scheme 7). Some of the potential applications include fluorescence imaging agents, drug delivery systems, electrochemical catalysis, and more. By exploring the physical and chemical properties of a system such as this, we hope to expand the synthetic toolbox of material sciences.
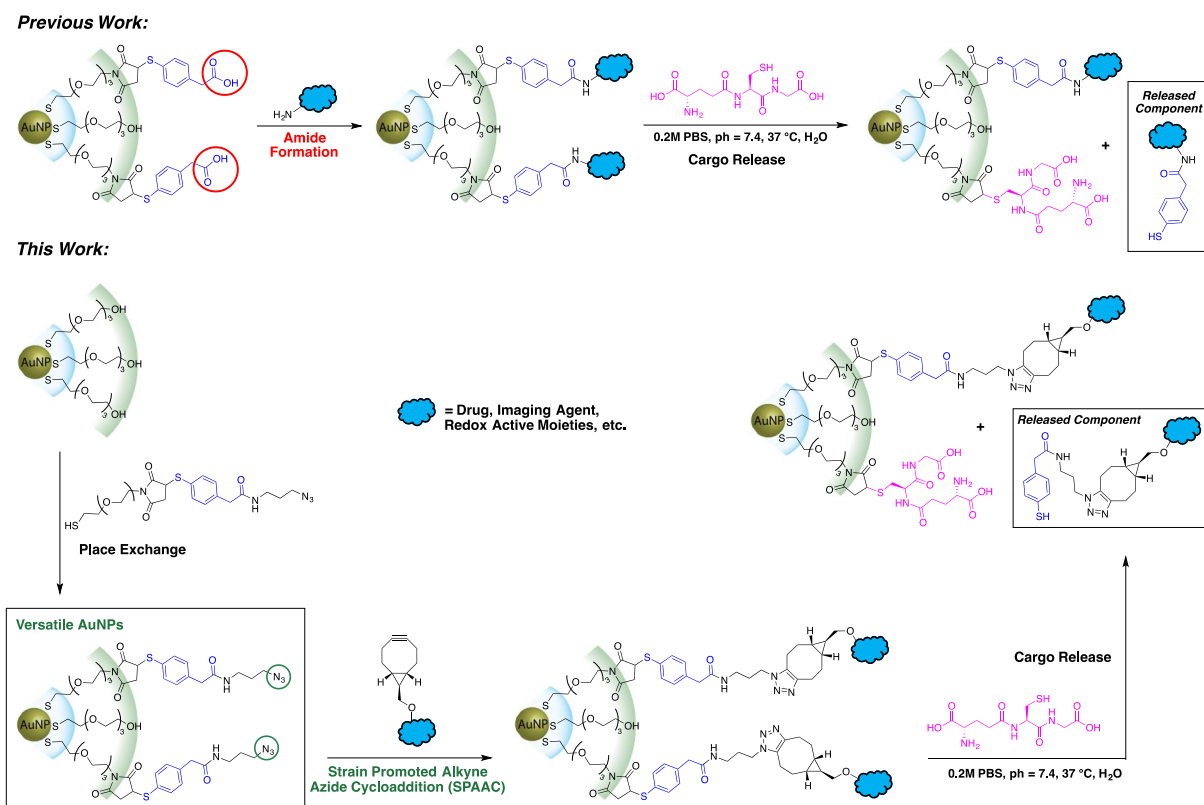
Scheme 7: A comparison between the previous molecular system and the versatile molecular system utilized in this work on AuNPs in order to develop a click and release system. MPA is depicted in blue, GSH is depicted in pink, and the cloud moiety symbolizes a drug, imaging agent, redox active molecules, etc.

Chapter 2

2 Small Molecule Studies

2.1 AuNP Ligand Synthesis

To begin this project, a plan was devised to synthesize thiol ligand (**11**); which incorporated the multi-functional system, in order to bind it onto the AuNP surface. The first reaction carried out was the furan protection of maleimide. This reaction was necessary to prevent Michael additions into maleimide by nucleophiles used in the next steps of the synthesis. After successfully isolating compound **1**, a small amount of 3-azidopropylamine (**2**) was prepared from (3-bromopropyl)ammonium bromide to be used later in the synthesis as an azide bound to a good nucleophile. This amine was used to modify the carboxylic acid group of MPA to add the clickable azide group to molecular system. Next, tetraethylene glycol was used as the starting compound for the synthesis of thiol **11**. This molecule was chosen because the ether groups give better water solubility to the AuNPs it is bound to when compared to using a purely carbon chain like *n*-dodecane. Water solubility is extremely important for this project, as we want to utilize these particles in aqueous PBS buffer to mimic physiological conditions. The first modification to tetraethylene glycol was a ditosylation of the two hydroxyl groups at both ends of the chain. Then, one of the tosyl groups was substituted with a S-trityl group in a S_N2 reaction using triphenylmethanethiol. The S-trityl group was used to install a protected thiol that can be easily deprotected at the end of the thiol **11** synthesis to yield the desired thiol. In this reaction, compound **4** was used in a large excess to statistically only substitute one end of the ligand with a S-trityl group. Next, the other tosyl group was substituted with the protected maleimide moiety to give compound **5** and then the product was refluxed in toluene to deprotect the maleimide group in a retro-Diels Alder reaction.

The MPA portion of thiol **11** was then synthesized. First, the thiol of MPA was trityl protected to prevent dimerization from disulfide formation. The carboxylic group was then converted to an amide using compound **2** as the amine and HBTU as the coupling agent. This transformation covalently bound an azide useful in click reactions to MPA to yield compound **8**. Then the molecule was subject to TFA and TIPS in CH_2Cl_2 to cleave

the trityl group off MPA. Immediately after purification, compound **9** was added to a solution of compound **6** in $Ar_{(g)}$ purged CH_3OH to participate in a thiol-Michael addition and yield compound **10**. Finally, thiol **11** was made by deprotecting the trityl group on compound **10** (Scheme 8).
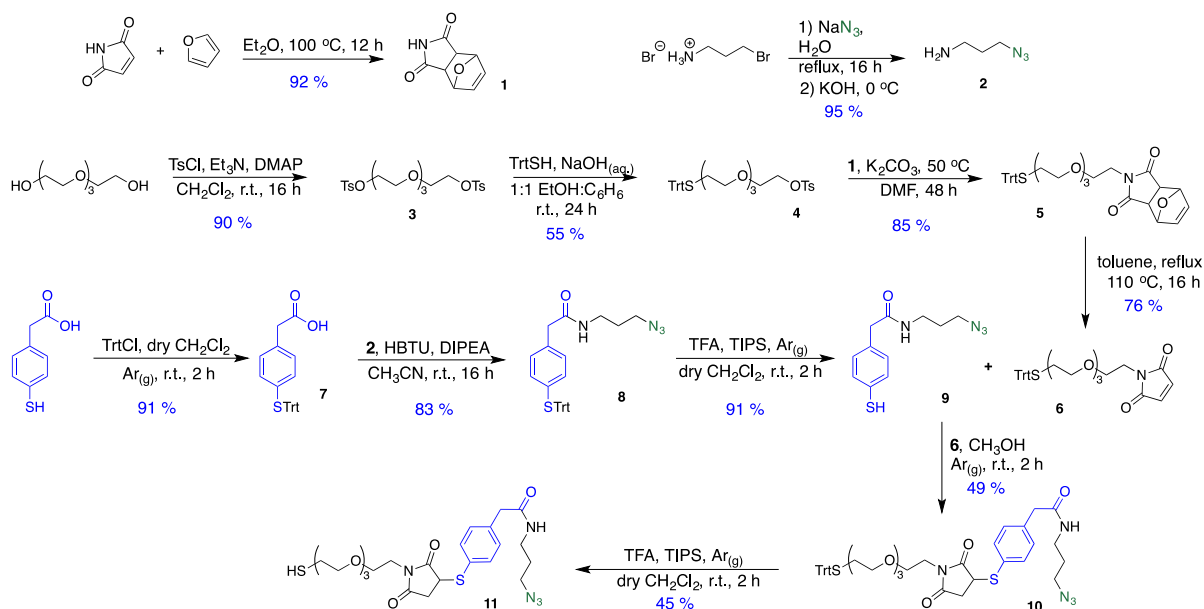
Scheme 8: Synthetic pathway to produce thiol **11** to be used to introduce an azide as a ligand on AuNPs. These azides will allow for the AuNPs to participate in interfacial SPAAC reactions.

2.2   BCN Molecular Cargo Synthesis

In the next phase of this project, several molecular cargoes covalently bound to bicyclononyne (BCN), a strained alkyne, were prepared. This process began by synthesizing BCN from cyclooctadiene (COD) and ethyl diazoacetate using a literature procedure developed by Dommerholt and coworkers (Scheme 9).[53] In the first reaction step, COD and ethyl diazoacetate were reacted together to form a cyclopropane group off the eight membered ring by liberating nitrogen gas. This transformation was catalyzed with a rhodium catalyst to yield compound **12a/b** as a regioisomeric mixture of 35:65 exo:endo. The two isomers were separated using column chromatography and only the isolated exo isomer was moved forward to the next synthetic step. Next, compound **12a** was treated with $LiAlH_4$ for 15 mins to reduce its ester to a primary alcohol and give compound **13**. Then compound **13** was reacted with bromine in an alkene dibromination reaction and these

two newly installed bromo groups were added to function as good leaving groups in the next reaction. Potassium *tert*-butoxide was slowly added to a solution of compound **14** in dry THF, until all of **14** was converted to compound **15** in a double E2 reaction to yield the strained alkyne, BCN.
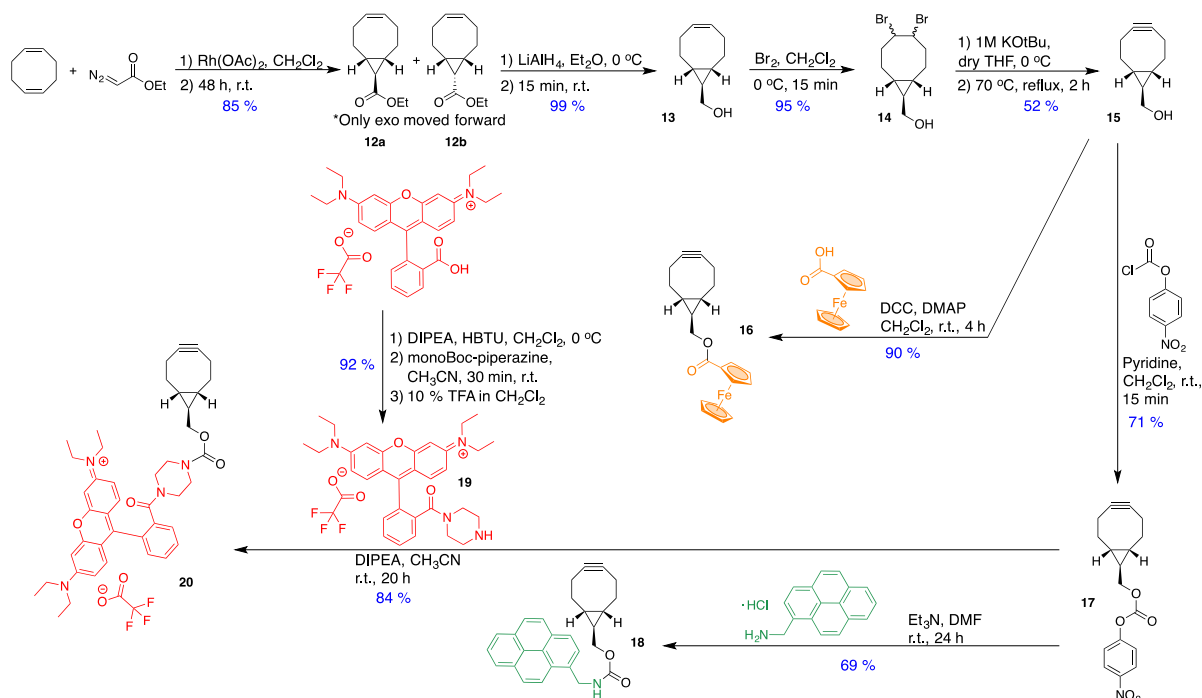
Scheme 9: Synthetic pathway to synthesize a strained alkyne in BCN (**15**) and its modification with several different molecular cargoes to be utilized to deliver functionality to materials with an azide group through interfacial SPAAC reactions.

After a bulk sample of BCN was accumulated, several different moieties that add functionality to the strained alkyne were attached to it (Scheme 9). First, a small portion of **15** was converted to BCN-ferrocene **16** and reacted the rest with 4-nitrophenyl chloroformate to change the nucleophilic alcohol of BCN to an electrophilic carbonate **17**. To conjugate BCN with a ferrocene group, **15** was stirred at r.t. with ferrocenecarboxylic acid, DCC, and DMAP in CH_2Cl_2 for 4 h. Compound **16** was a bright yellow solid that was synthesized to be used as a strained alkyne that delivers a redox active functionality to any material that it is reacted with. Next, the electrophilic BCN **17** was modified with 1-pyrenemethylamine hydrochloride to form a stable amide and adhere the fluorescent pyrene group to the strained alkyne. Compound **18** is a white solid that fluoresces bright

blue light when under UV-visible light and this molecule can now deliver the ability to be used in applications such as fluorescence imaging to materials. Compound **20** was prepared following a previous literature procedure published by our group in 2015.[54] This compound is a strained alkyne with a modified rhodamine B group attached. The compound is a shiny purple solid that fluoresces bright pink in solution when exposed to UV-visible light and can also be used to introduce fluorescent character

2.3   *hv*DIBO Molecular Cargo Synthesis

To demonstrate that BCN is not the only strained alkyne capable of delivering functionality to materials, another strained alkyne named photo-dibenzocyclooctyne (*hv*DIBO) was synthesized following a literature procedure outlined by Popik et al. in 2014.[55] The "photo" component of this compound arises from the cyclopropenone protecting group that masks the strain alkyne in order to prevent undesirable side reactions. This protecting group introduces an additional advantage in spatial and temporal control because the deprotection of the strained alkyne only required 350 nm light and light can be controlled to be focused into many different shapes and sizes. The first transformation in the synthesis of *hv*DIBO was a substitution reaction to replace a primary alcohol on 3-methoxybenzyl alcohol with a bromo group (Scheme 10). Next, the product was treated with triphenylphosphine (PPh$_3$) to yield a phosphonium salt as compound **22**. Next, a Mitsunobu reaction was performed on 3-hydroxybenzaldehyde using 1-butanol to synthesize compound **23**. Then, compound **22** was converted to an ylide with n-BuLi at –78 °C to give a Wittig reagent. Aldehyde **23** was added to a solution of the Wittig reagent in dry THF to yield a mixture of regioisomers of the alkene.
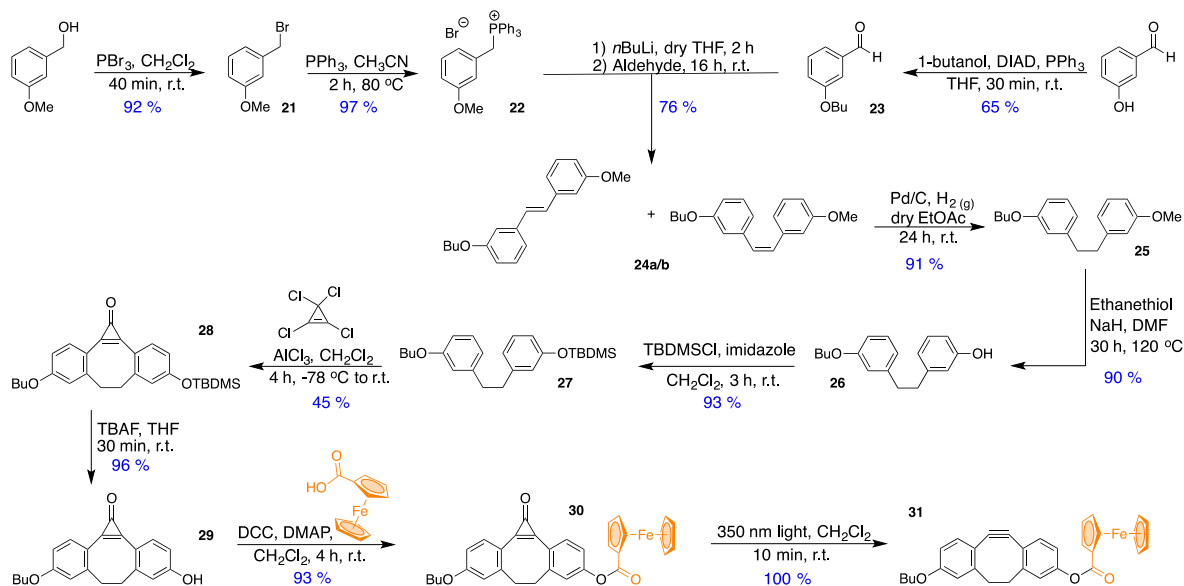
Scheme 10: Synthetic pathway to synthesize an alternative strained alkyne to BCN as *hv*DIBO (**29**) and its modification with ferrocenecarboxylic acid to be utilized to deliver redox functionality to materials with an azide group through interfacial SPAAC reactions.

Both isomers were suspended in a solution of Pd/C and EtOAc under an atmosphere of hydrogen gas in a hydrogenation reaction to give the alkane product **25**. Then, sodium hydride and ethanethiol was used to cleave the methyl group of the alkane **25** to yield compound **26** with a hydroxyl group. The hydroxyl group was then TBDMS protected to remove all the acidic protons before the next transformation; a double Friedel-Crafts alkylation. In this step, compound **27** was reacted with tetrachlorocyclopropene and aluminum chloride followed by a hydrolysis to yield compound **28** as TBDMS-*hv*DIBO. To deprotect the TBDMS group, TBAF was added to a solution of compound **28** in THF and the reaction was stirred at r.t. for 30 mins, yielding *hv*DIBO **29**. Before the photo-deprotection of *hv*DIBO **29**, the hydroxyl group was reacted with ferrocenecarboxylic acid, DCC, and DMAP in CH_2Cl_2 for 4 h to install a ferrocene group onto the compound. The product of this reaction (**30**) was then photo-deprotected by irradiating a solution of compound **30** with 350 nm light at r.t. for 10 mins to yield DIBO-ferrocene as a strained alkyne. This compound can be used as an alternative for compound **16** to deliver redox activity to materials containing azides.

2.4   Small Molecule Studies

After the thiol ligand (**11**) containing the mutli-functional system and all the molecular cargoes were prepared, the project moved onto small molecule studies to determine the reaction conditions and parameters required to successfully carry out the interfacial reactions on AuNPs. These experiments were also conducted to obtain ^{1}H NMR spectra of the molecular system with the molecular cargoes attached. These spectra were collected to be compared to the analogous system on the AuNPs. The comparison of the small molecule studies to the nanomaterial modifications aided in the analysis of the all the AuNP ^{1}H NMR spectra. Signals in the ^{1}H NMR spectra of AuNPs appear broad with minimal resolvable splitting patterns which renders complex molecules on particles difficult to analyze. The morphology of AuNPs are actually non-spherical, they are polyhedral in character in a face-centered cubic lattice with gold atoms occupying edges, terraces, and verticies.[52-53] This characteristic causes the broadening of AuNP NMR spectra because the thiol ligands are bound to inequivalent gold atoms on the surface of the metal core. To conserve the amount of compound **6**, N-methylmaleimide (NMM) was chosen as a substitute for the small molecule studies. The first step of these experiments was to monitor the thiol-Michael addition of compound **9** into NMM (Scheme 11).
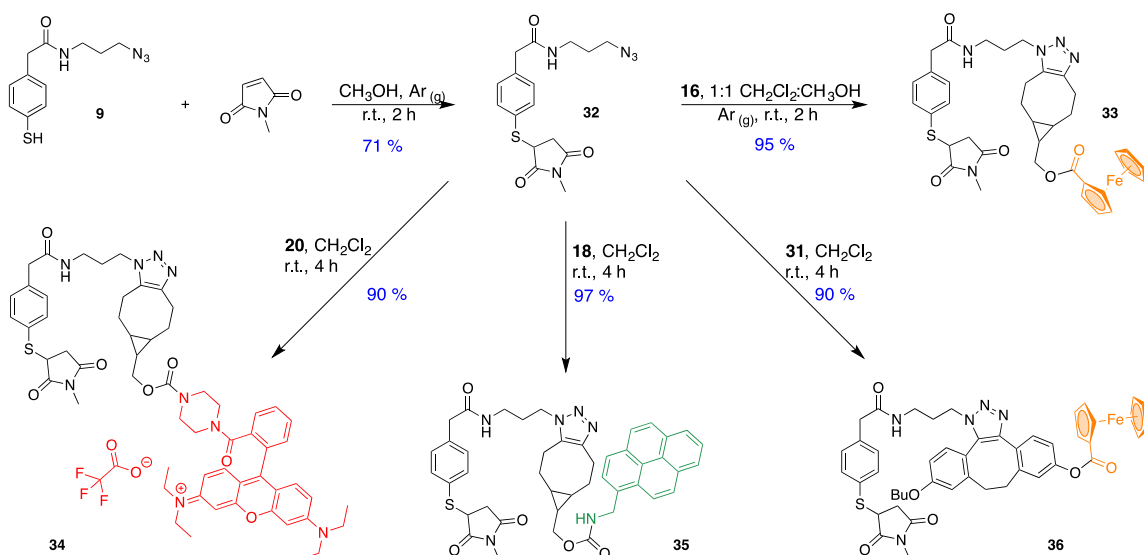
Scheme 11: Small molecule studies reacting the azide of adduct **32** with four strained alkynes carrying several molecular cargoes using SPAACs. These reactions were carried out to study the reaction conditions and parameters required to successfully carry out similar reactions on AuNPs.

The reagents were added to a round bottom flask and were stirred at r.t. in argon purged methanol to avoid disulfide formation. The Michael addition was complete after two hours to yield compound **32** as a white solid. The ^{1}H NMR spectrum of this stable adduct displayed an interesting splitting pattern of the individual maleimide protons in the 5-membered ring (Figure 3). Compound **32** was then reacted with each of the molecular cargoes separately using SPAACs to form stable triazole rings (Scheme 11). The first molecular cargo reacted with the adduct **32** was BCN-ferrocene **16**. By simply adding compounds **32** and **16** into a vial with 1:1 CH_2Cl_2:CH_3OH as the solvent and stirring at r.t. for 2 hours, product **33** is formed with minimal purification required. Similar conditions were used to yield compounds **34** and **35** by adding compounds **20** and **18,** respectively. The ^{1}H NMR spectra of compounds **33**, **34**, and **35** exhibited broadening of signals due to each of the products being regioisomeric mixtures that are not easily isolatable. The regioisomers are formed because in SPAACs, the azide can react with the strained alkyne in two different orientations to form the triazole ring. The last molecular cargo reacted with adduct **32** was DIBO-ferrocene **31**. Some of the signals in the ^{1}H NMR spectrum of product **36** were duplicated. The reason for this change in the spectrum is also due to the product being a regioisomeric mixture, but the rigidity of DIBO helps to produce sharper signals than BCN, hence reducing the broadening (Figure 4). Thus, with the small molecules test reactions completed and all the molecular cargo successfully synthesized, the project progressed onto the AuNP synthesis and interfacial modifications.
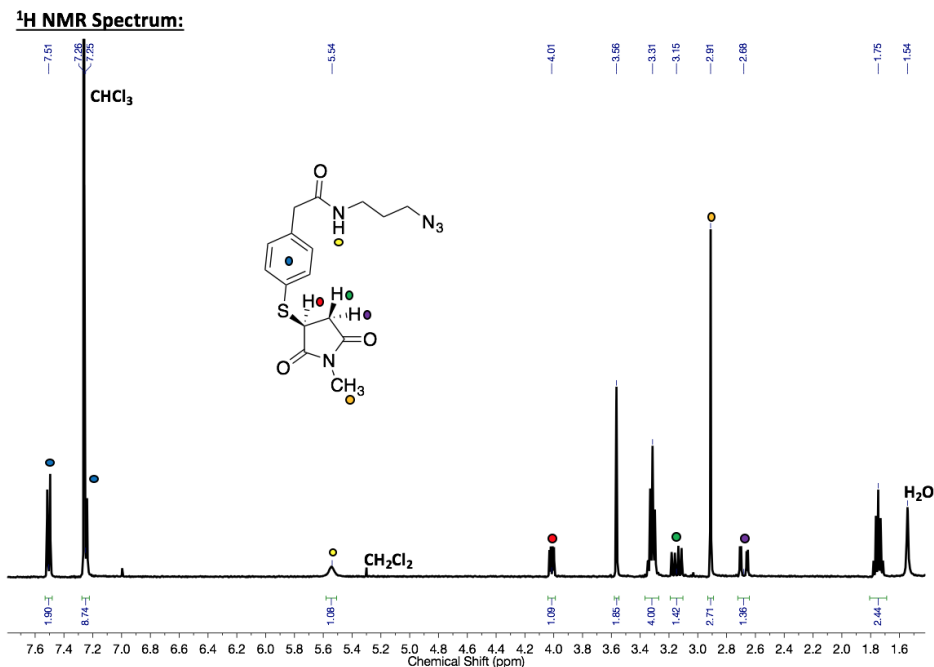
Figure 3: ¹H NMR spectrum of compound **32** with labelled chemical shifts, integrations, and characteristic proton assignments. The red, green, and purple circles represent the maleimide ring protons and each signal corresponds to a doublet of doublets.
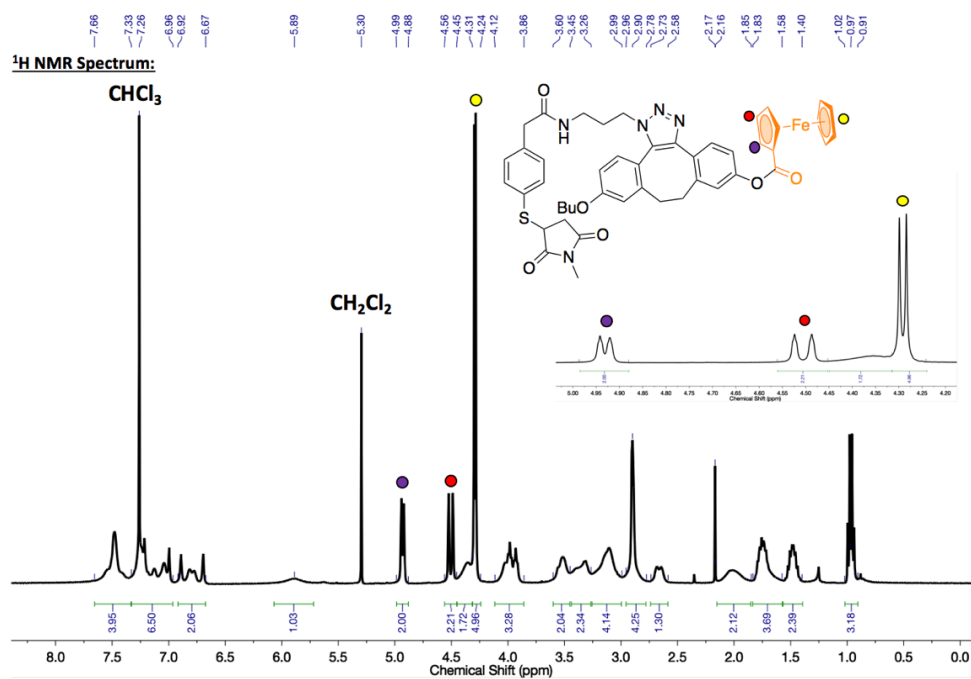
Figure 4: ¹H NMR spectrum of compound **36** with labelled chemical shifts, integrations, and diagnostic proton assignments. The red, yellow, and purple circles represent the duplicated ferrocene protons.

2.5   Small Molecule Studies Experimental

2.5.1   Materials and Methods

All reagents, unless otherwise stated, were purchased from Sigma-Aldrich and used as received. All common solvents, triethylamine (Et_3N), and trifluoroacetic acid (TFA) were purchased from Caledon. Ethanol (EtOH) was purchased from Commercial Alcohols. Dialysis membranes (MWCO 6000-8000 Da) were purchased from Spectra/Por. Glutathione was purchased from Alfa Aesar.

^{1}H and ^{13}C{^{1}H} NMR spectra were recorded on Varian INOVA 400 (or 600) or Bruker AvIII HD 400 spectrometers using $CDCl_3$, CD_2Cl_2 or CD_3OD as solvent. ^{1}H NMR spectra that were recorded in $CDCl_3$ were referenced against residual protonated solvent at 7.27 ppm. ^{13}C NMR spectra that were run in $CDCl_3$ were referenced to 77.00 ppm. NMR spectra are reported as follows: s (singlet), d (doublet), t (triplet), q (quartet), dd (doublet of doublets), dt (doublet of triplets), tt (triplet of triplets), m (multiplet), bs (broad signal). Coupling constants are reported as J values in Hertz (Hz). The number of protons for a given resonance is indicated as nH and is based on spectral integration values. FT-IR spectra were recorded using an attenuated total reflectance (ATR) attachment using a Bruker Vector 33 FT-IR spectrometer and using standard quartz cells (1 cm path length) with a scan range of 200 to 800 nm. Ultraviolet (UV)-visible spectra were recorded using a Varian Cary 300 Bio spectrometer. ESI MS spectra were recorded on a Micromass LCT mass spectrometer. Photolysis were conducted in a Luzchem LZC-4V photoreactor equipped with 14 UVA (350 nm) 8-watt lamps.

2.5.2   Preparation and Characterization of Compounds (1 – 36)

2.5.2.1   Compounds 1 – 11
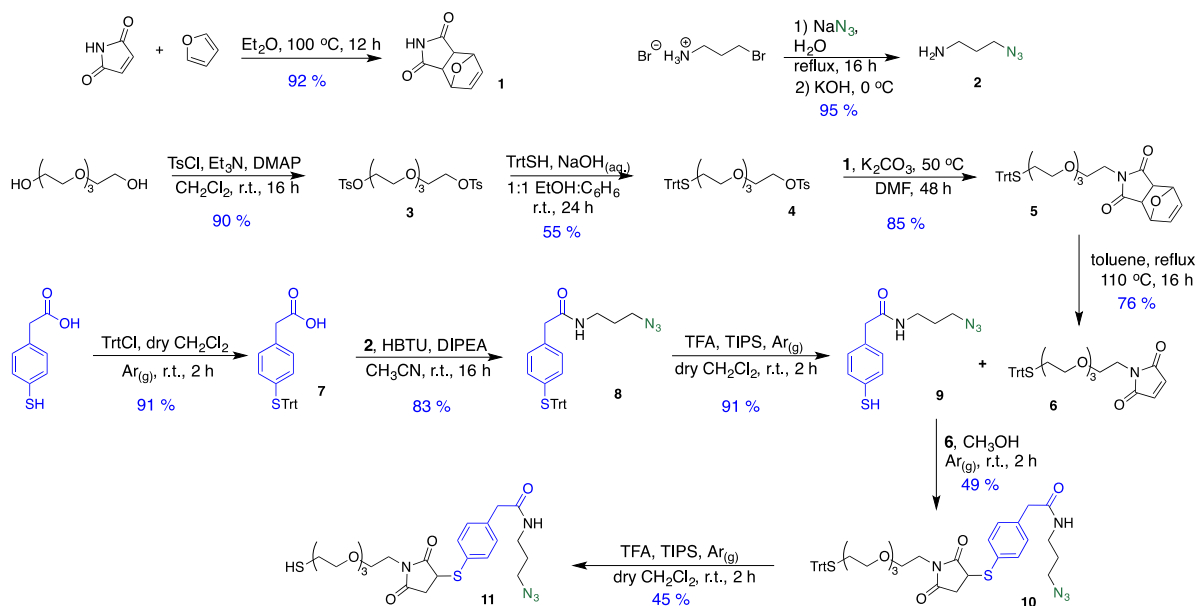
Synthesis of Compound 1:

To a pressure tube containing maleimide (0.500 g, 5.15 mmol) was added furan (0.526 mL, 7.73 mmol) and Et_2O (25 mL). The tube was sealed and heated to 100 °C and stirred for 16 h. The pressure tube was then cooled to r.t. After, the precipitate was isolated using Buchner filtration and washed with cold Et_2O (3 x 25 mL). The solid was then dried to afford compound **1** as a white solid (0.782 g, 92%). ^1H NMR (CDCl$_3$, 400 MHz): δ 7.92 (bs, 1H), 6.52 (dd, J = 1 Hz, J = 1 Hz, 2H), 5.32 (dd, J = 1 Hz, J = 1 Hz, 2H), 2.89 (s, 2H). $^{13}C\{^1H\}$ NMR (CDCl$_3$, 101 MHz): δ 175.9, 136.7, 81.1, 48.9. FT-IR (ATR, ν, cm^{-1}): 3147, 3067, 3012, 2998, 2751, 1771, 1717, 1704, 1700, 1695, 1683, 1675, 1652, 1398, 1288, 1204, 1188, 1143, 1091, 1020, 937, 928, 906, 897, 855, 841, 822, 791, 734, 690, 636, 632, 583. ESI-MS calcd for $C_8H_7NO_3^+$ [M]$^+$ 165.0426, found 165.0420; difference +3.64 ppm.

Synthesis of Compound 2:

To a flask containing (3-bromopropyl)ammonium bromide (1.64 g, 7.49 mmol) was added sodium azide (1.63 g, 25.0 mmol) and H_2O (25 mL). The reaction mixture was refluxed at 100 °C and stirred for 16 h. The flask was then cooled to r.t. and Et_2O (50 mL)

was added. After, the flask was placed in an ice bath and KOH (2.00 g, 89.1 mmol) in H_2O (5 mL) was slowly added while stirring. The reaction mixture was then extracted with Et_2O (3 x 30 mL) and the organic fraction was dried with K_2CO_3. The solid was then filtered out using gravity filtration was the excess solvent was removed to yield compound **2** (0.710 g, 95%) as a clear colourless oil. ^{1}H NMR ($CDCl_3$, 400 MHz): δ 3.38 (t, J = 7 Hz, 2H), 2.81 (t, J = 7 Hz, 2H), 1.73 (tt, J = 7 Hz, J = 7 Hz, 2H), 1.24 (bs, 2H). The ^{1}H NMR spectrum corresponded with the literature.[54]

Synthesis of Compound 3:

To a flask containing tetraethylene glycol (10.0 g, 51.5 mmol) was added tosyl chloride (58.9 g, 309 mmol), Et_3N (21.5 mL, 154 mmol), DMAP (1.26 g ,10.3 mmol), and CH_2Cl_2 (400 mL). The flask was stirred at r.t. for 16 h. The crude product was extracted with H_2O (3 x 200 mL) and brine (50 mL), dried with $MgSO_4$, and filtered using gravity filtration. After, the solvent was removed using rotary evaporation and the crude product was purified by column chromatography on silica gel using 3:1 EtOAc: hexanes as the eluent to afford compound **3** as a pale yellow oil (23.3 g, 90%). ^{1}H NMR ($CDCl_3$, 400 MHz): δ 7.79 (d, J = 4 Hz, 4H), 7.33 (d, J = 4 Hz, 4H), 4.17 – 4.13 (m, 4H), 3.70 – 3.65 (m, 4H), 3.59 – 3.52 (m, 8H), 2.44 (s, 6H). ^{13}C{^{1}H} NMR ($CDCl_3$, 101 MHz): δ 144.9, 133.1, 130.0, 128.1, 70.9, 70.7, 69.4, 68.8, 21.8. ESI-MS calcd for $C_{22}H_{30}O_9S_2^+$ $[M]^+$ 502.1331, found 502.1340; difference -1.75 ppm.

Synthesis of Compound 4:

To a flask containing compound **3** (12.1 g, 24.1 mmol) was added a mixture of 1:1 EtOH: Benzene (100 mL) and was stirred at r.t. Then, NaOH (5.00 g, 12.0 mmol) and triphenylmethanethiol (3.33 g, 12.0 mmol) was dissolved in 1:1 EtOH: Benzene (40 mL) was slowly added to the reaction flask. The flask was stirred at r.t. for 24 h. Then, the solvent was removed, and the crude product was dissolved in CH_2Cl_2 (100 mL). The solution was filtered using gravity filtration and the CH_2Cl_2 was evaporated. The crude product was purified by column chromatography on silica gel using 1:1 EtOAc: hexanes as the eluent to afford compound **4** as a pale-yellow oil (4.02 g, 55%). ^{1}H NMR ($CDCl_3$, 400 MHz): δ 7.79 (d, J = 4 Hz, 2H), 7.45 – 7.39 (m, 6H), 7.35 – 7.17 (m, 11H), 4.17 – 4.10

(m, 2H), 3.69 – 3.63 (m, 2H), 3.57 – 3.50 (m, 6H), 3.45 – 3.40 (m, 2H), 3.30 (t, J = 7 Hz, 2H), 2.44 (s, 3H), 2.42 (t, J = 7 Hz, 2H). $^{13}C\{^1H\}$ NMR (CDCl$_3$, 101 MHz): δ 145.0, 144.9, 133.2, 130.0, 129.8, 128.1, 128.0, 126.8, 70.9, 70.7, 70.6, 70.3, 69.8, 69.4, 68.8, 66.7, 31.8, 21.8. ESI-MS calcd for $C_{34}H_{38}NaO_6S_2^+$ [M+Na]$^+$ 629.2008, found 629.2008; difference 0.00 ppm.

Synthesis of Compound 5:

To a flask containing compound **4** (2.30 g, 3.79 mmol) was added compound **1** (0.480 g, 2.92 mmol), K$_2$CO$_3$ (0.806, 5.83 mmol), and DMF (50 mL). The flask was stirred at 60 °C for 48 h. The volume was reduced, and the reaction mixture was dissolved in CH$_2$Cl$_2$ (50 mL). The crude product was extracted with H$_2$O (3 x 200 mL) and brine (50 mL), dried with MgSO$_4$, and filtered using gravity filtration. After, the solvent was removed using rotary evaporation and the crude product was purified by column chromatography on silica gel using EtOAc as the eluent to afford compound **5** as a pale-yellow oil (1.49 g, 85%). ^{1}H NMR (CDCl$_3$, 400 MHz): δ 7.44 – 7.38 (m, 6H), 7.31 – 7.17 (m, 9H), 6.48 (s, 2H), 5.25 (s, 2H), 3.70 – 3.51 (m, 10H), 3.45 – 3.41 (m, 2H), 3.29 (t, J = 7 Hz, 2H), 2.83 (s, 2H), 2.42 (t, J = 7 Hz, 2H). $^{13}C\{^1H\}$ NMR (CDCl$_3$, 101 MHz): δ 176.2, 145.0, 136.7, 129.8, 128.0, 126.8, 81.0, 70.7, 70.6, 70.3, 70.2, 69.8, 67.3, 66.7, 47.6, 38.3, 31.8. FT-IR (ATR, ν, cm^{-1}): 3059, 2923, 2096, 1780, 1706, 1652, 1541, 1490, 1444, 1397, 1334, 1189, 1120, 746, 702. ESI-MS calcd for $C_{35}H_{37}NNaO_6S^+$ [M+Na]$^+$ 622.2239, found 622.2216; difference +3.74 ppm.

Synthesis of Compound 6:

To a flask containing compound **5** (1.49 g, 2.48 mmol) was toluene (50 mL). The flask was stirred and refluxed at 110 °C for 16 h. After, the solvent was removed using rotary evaporation and the crude product was purified by column chromatography on silica gel using 1:1 EtOAc: hexanes as the eluent to afford compound **6** as a clear yellow oil (1.00 g, 76%). ^{1}H NMR (CDCl$_3$, 400 MHz): δ 7.44 – 7.38 (m, 6H), 7.32 – 7.23 (m, 6H), 7.23 – 7.17 (m, 3H), 6.67 (s, 2H), 3.75 – 3.67 (m, 2H), 3.45 – 3.41 (m, 2H), 3.30 (t, J = 7 Hz, 2H), 2.42 (t, J = 7 Hz, 2H). $^{13}C\{^1H\}$ NMR (CDCl$_3$, 101 MHz): δ 170.8, 145.0, 134.3, 129.8, 128.0, 126.8, 70.7, 70.6, 70.3, 70.2, 69.8, 68.0, 66.7, 37.3, 31.8. FT-IR (ATR, ν, cm^{-1}):

3464, 3055, 2867, 1958, 1710, 1706, 1704, 1700, 1695, 1683, 1652, 1594, 1489, 1443, 1436, 1404, 1389, 1350, 1320, 1178, 1101, 1034, 1002, 972, 933, 888, 827, 767, 743, 695, 677, 667, 635, 629, 622, 616, 576, 524, 506, 486, 472, 463, 458. ESI-MS calcd for $C_{31}H_{33}NNaO_sS^+$ [M+Na]$^+$ 531.2079, found 554.1972; difference +0.99 ppm.

Synthesis of Compound 7:

To a flask containing MPA (1.00 g, 5.94 mmol) was added trityl chloride (1.99 g, 7.13 mmol), and Ar$_{(g)}$ purged CH_2Cl_2 (30 mL). The flask was stirred at r.t. under inert atmosphere for 2 h. After, the solvent was removed using rotary evaporation and the crude product was purified by column chromatography on silica gel using 7:1 CH_2Cl_2:acetone as the eluent to afford compound **7** as a yellow-white solid (2.22 g, 91%). ^{1}H NMR (CDCl$_3$, 400 MHz): δ 7.43 – 7.37 (m, 6H), 7.26 – 7.15 (m, 9H), 6.91 (s, 4H), 3.51 (s, 2H). ^{13}C{^{1}H} NMR (CDCl$_3$, 101 MHz): δ 176.1, 144.6, 134.8, 133.8, 132.9, 130.1, 129.2, 127.8, 126.8, 70.9, 40.5. FT-IR (ATR, ν, cm^{-1}): 3200-2500 (bs), 2900, 1700, 1594, 1485, 1441, 1298, 1155, 1020, 946, 802, 767, 734, 694, 673, 654, 615, 532, 513, 467. ESI-MS calculated for $C_{27}H_{22}O_2S^+$ [M+H]$^+$ 410.1341, found 410.1338; difference +0.54 ppm.

Synthesis of Compound 8:

To a flask containing compound **7** (2.00 g, 4.87 mmol) was added compound **2** (0.536 g, 5.35 mmol), HBTU (2.53 g, 6.67 mmol), DIPEA (1.73 g, 13.4 mmol), and CH_3CN (100 mL). The flask was stirred at r.t. for 16 h. After, the solvent was removed using rotary evaporation and the crude product was purified by column chromatography on silica gel using 3:2 EtOAc: hexanes as the eluent to afford compound **8** as a white solid (1.99 g, 83%). ^{1}H NMR (CDCl$_3$, 400 MHz): δ 7.44 – 7.38 (m, 6H), 7.28 – 7.16 (m, 9H), 6.98 – 6.84 (m, 4H), 5.34 (bs, 1H), 3.42 (s, 2H), 3.30 – 3.22 (m, 4H), 1.70 (tt, J = 7 Hz, J = 7 Hz, 2H). ^{13}C{^{1}H} NMR (CDCl$_3$, 101 MHz): δ 170.9, 144.6, 135.0, 134.2, 134.1, 130.1, 129.3, 127.8, 126.9, 71.1, 49.5, 43.5, 37.5, 28.8. FT-IR (ATR, ν, cm^{-1}): 3271, 3054, 2897, 2090, 1642, 1594, 1546, 1487, 1441, 1320, 1264, 1198, 1150, 1081, 1033, 1017, 838, 809, 763, 740, 696, 620, 582, 528, 502, 428. ESI-MS calcd for $C_{30}H_{28}N_4NaOS^+$ [M+Na]$^+$ 515.1882, found 515.1881; difference +0.11 ppm.

Synthesis of Compound 9:

To a flask containing compound **8** (0.200 g, 0.406 mmol) was added CH_2Cl_2 (20 mL). The flask was stirred at r.t. and purged with $Ar_{(g)}$ for 20 min in the dark. Then, TIPS (0.420 mL, 2.03 mmol) and TFA (0.620 mL, 8.12 mmol) were added to the reaction flask and the reaction mixture was stirred at r.t. for 2 h. After, the solvent was removed using rotary evaporation and the crude product was quickly purified by column chromatography on silica gel using 2:1 EtOAc: hexanes as the eluent. The product is a thiol, which are prone to disulfide formation in the presence of $O_{2\ (g)}$. Therefore, the column must be run quickly and with $Ar_{(g)}$ purged eluent to afford compound **9** as a cloudy white oil (0.928 g, 91%). The product was stored in a vial purged with $Ar_{(g)}$ in the freezer. ^{1}H NMR ($CDCl_3$, 400 MHz): δ 7.29 – 7.25 (m, 2H), 7.15 – 7.11 (m, 2H), 5.72 (bs, 1H), 3.50 (s, 2H), 3.47 (s, 1H), 3.33 – 3.26 (m, 4H), 1.72 (tt, J = 7 Hz, J = 7 Hz, 2H). ^{13}C{^{1}H} NMR ($CDCl_3$, 101 MHz): δ 171.0, 132.3, 130.3, 130.2, 128.2, 49.7, 43,4, 37.7, 28.7. FT-IR (ATR, ν, cm^{-1}): 3290, 2931, 2888, 2555, 2088, 1644, 1594, 1538, 1491, 1438, 1416, 1402, 1337, 1294, 1239, 1200, 1106, 1016, 956, 845, 800, 743, 676, 570, 493, 440. ESI-MS calcd for $C_{11}H_{14}N_4OS^+$ [M]$^+$ 250.0888, found 250.0896; difference -2.88 ppm.

Synthesis of Compound 10:

To a flask containing compound **6** (0.525 g, 0.989 mmol) was added CH_3OH (30 mL). The flask was stirred at r.t. and purged with $Ar_{(g)}$ for 20 min. Then, compound **9** (0.225 g, 0.899 mmol) was added to the reaction flask and the reaction was stirred at r.t. and under inert atmosphere for 2 h. After, the solvent was removed using rotary evaporation and the crude product was purified by column chromatography on silica gel using 5% CH_3OH in CH_2Cl_2 as the eluent to afford compound **10** as a pale yellow oil (0.344 g, 49%). ^{1}H NMR ($CDCl_3$, 400 MHz): δ 7.51 – 7.47 (m, 2H), 7.43 – 7.38 (m, 6H), 7.31 – 7.17 (m, 11H), 5.62 (bs, 1H), 4.01 (dd, J = 4 Hz, J = 9 Hz, 1H), 3.68 – 3.50 (m, 12H), 3.45 – 3.40 (m, 2H), 3.32 – 3.26 (m, 6H), 3.13 (dd, J = 9 Hz, J = 13 Hz, 1H), 2.64 (dd, J = 4 Hz, J = 13 Hz, 1H), 2.42 (t, J = 7 Hz, 2H), 1.73 (tt, J = 7 Hz, J = 7 Hz, 2H). ^{13}C{^{1}H} NMR ($CDCl_3$, 101 MHz): δ 175.6, 174.5, 170.5, 145.0, 136.2, 134.8, 130.5, 130.0, 129.8, 128.0, 126.8, 70.7, 70.6, 70.3, 70.0, 69.8, 67.0, 66.8, 49.6, 44.0, 43.5, 38.4, 37.7, 36.2, 31.8, 28.7.

FT-IR (ATR, ν, cm^{-1}): 3405, 3309, 3055, 2867, 2096, 1779, 1700, 1656, 1652, 1539, 1490, 1443, 1394, 1349, 1332, 1265, 1189, 116, 1034, 1019, 768, 742, 700, 677, 667, 629, 622, 616, 506. ESI-MS calcd for $C_{42}H_{47}N_5NaO_6S_2^+$ [M+Na]$^+$ 804.2866, found 804.2834; difference +3.88 ppm.

Synthesis of Compound 11:

To a flask containing compound **10** (0.140 g, 0.179 mmol) was added CH_2Cl_2 (20 mL). The flask was stirred at r.t. and purged with Ar$_{(g)}$ for 20 min in the dark. Then, TIPS (0.183 mL, 0.895 mmol) and TFA (0.274 mL, 3.58 mmol) were added to the reaction flask and the reaction mixture was stirred at r.t. for 2 h. After, the solvent was removed using rotary evaporation and the crude product was quickly purified by column chromatography on silica gel using EtOAc as the eluent. The product is a thiol, which are prone to disulfide formation in the presence of O$_{2 (g)}$. Therefore, the column must be run quickly and with Ar$_{(g)}$ purged eluent to afford compound **11** as a pale-yellow oil (0.043 g, 45%). The product was stored in a vial purged with Ar$_{(g)}$ in the freezer. ^{1}H NMR (CDCl$_3$, 400 MHz): δ 7.53 – 7.49 (m, 2H), 7.27 – 7.22 (m, 2H), 5.62 (bs, 1H), 4.04 (dd, J = 4 Hz, J = 9 Hz, 1H), 3.68 – 3.54 (m, 16H), 3.68 – 3.54 (m, 4H), 3.16 (dd, J = 9 Hz, J = 13 Hz, 1H), 2.72 – 2.62 (m, 3H), 1.74 (tt, J = 7 Hz, J = 7 Hz, 2H), 1.59 (t, J = 8 Hz, 1H). ^{13}C{^{1}H} NMR (CDCl$_3$, 101 MHz): δ 175.6, 174.5, 170.6, 136.1, 134.8, 130.5, 130.2, 73.0, 70.7, 70.7, 70.4, 70.1, 67.1, 49.7, 44.0, 43.5, 38.5, 37.8, 36.2, 28.7, 24.4. ESI-MS calcd for $C_{23}H_{34}N_5O_6S_2^+$ [M+H]$^+$ 540.1951, found 540.1951; difference -3.70 ppm.

2.5.2.2　Compounds 12 – 20
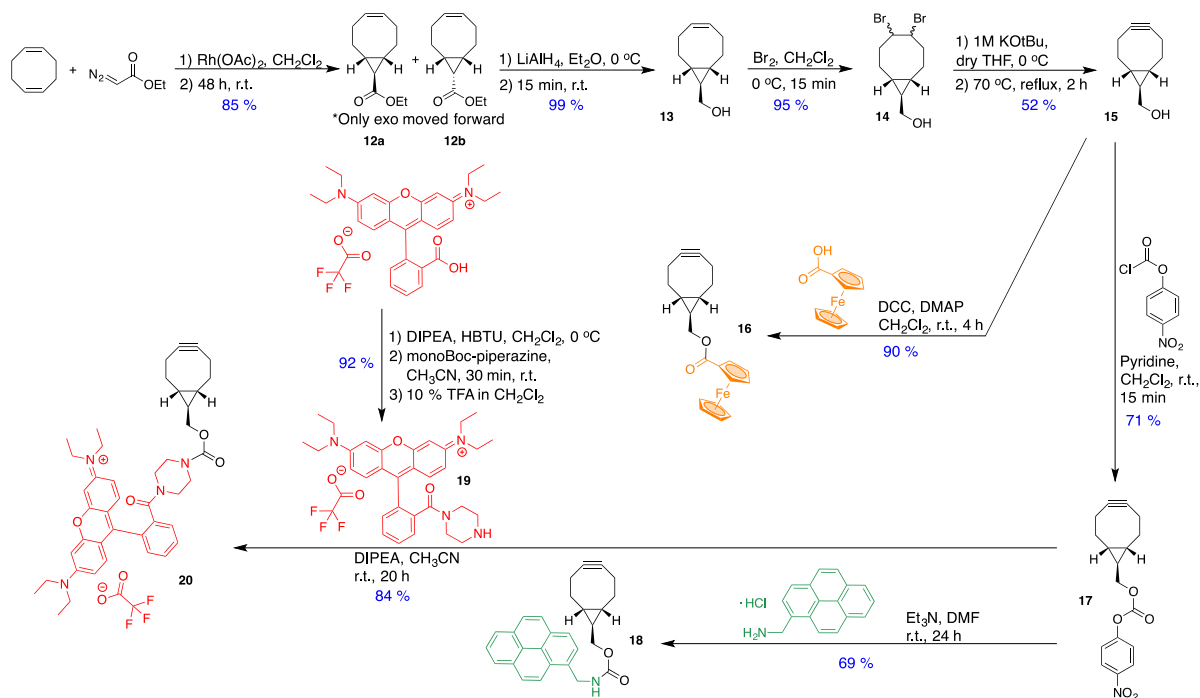
Synthesis of Compound 12a/b:

To a flask containing $Rh_2(OAc)_4$ (0.776 g, 1.76 mmol) was added dry CH_2Cl_2 (20 mL) and cyclooctadiene (40 mL, 330 mmol). In a separate flask containing ethyl diazoacetate (4.30 mL, 41.0 mmol) was added dry CH_2Cl_2 (20 mL) and was then added to the flask containing $Rh_2(OAc)_4$. The flask was stirred at r.t. for 48 h. After, the solvent was removed using rotary evaporation and the crude product was purified by column chromatography on silica gel using hexanes as the eluent to remove the excess cyclooctadiene. Then, the crude was purified again by column chromatography on silica gel using 0.5:9 EtOAc: hexanes as the eluent to separate the two isomers **12a** (*exo*) and **12b** (*endo*) as clear, colourless oils (Total: 6.77 g, 85%, 35% *exo* and 65% *endo*). ^{1}H NMR (CDCl₃, 400 MHz): δ 5.68 – 5.60 (m, 2H), 4.10 (q, J = 7 Hz, 2H), 2.35 – 2.25 (m, 2H), 2.25 – 2.14 (m, 2H), 2.14 – 2.03 (m, 2H), 1.62 – 1.41 (m, 4H), 1.25 (t, J = 7 Hz, 3H), 1.18 (t, J = 5 Hz, 1H). The ^{1}H NMR spectrum corresponded with the literature.[55]

Synthesis of Compound 13:

A flask containing a suspension of LiAlH$_4$ (0.862 g, 22.7 mmol) in dry Et$_2$O (70 mL) was cooled to 0 °C in an ice bath. To a separate flask containing compound **12a** (5.80 g, 29.9 mmol) was added dry Et$_2$O (80 mL) and was also cooled to 0 °C. This solution was then added dropwise to the flask with LiAlH$_4$. The flask was stirred at r.t. for 40 min and then cooled again to 0 °C. Then, H$_2$O was added dropwise to the reaction flask until a white solid formed. The crude product was dried with Na$_2$SO$_4$, filtered using gravity filtration, and washed with cold Et$_2$O (3 x 20 mL). After, the solvent was removed using rotary evaporation to afford compound **13** as a clear, colourless oil (3.80 g, 99%). ^{1}H NMR (CDCl$_3$, 400 MHz): δ 5.68 – 5.59 (m, 2H), 3.47 (d, J = 7 Hz, 2H), 2.35 – 2.23 (m, 2H), 2.23 – 2.12 (m, 2H), 2.12 – 2.01 (m, 2H), 1.47 – 1.36 (m, 2H), 0.83 – 0.73 (m, 2H), 0.70 – 0.62 (m, 1H). The ^{1}H NMR spectrum corresponded with the literature.[55]

Synthesis of Compound 14:

To a flask containing compound **13** (3.70 g, 24.3 mmol) was added dry CH$_2$Cl$_2$ (100 mL) and was also cooled to 0 °C. Then, bromine (1.60 mL, 31.6 mmol) was added to the flask dropwise until a yellow colour persisted in the flask. After, the reaction was quench with Na$_2$S$_2$O$_4$ (aq) and it was added to the flask until the reaction mixture became colourless. The crude product was extracted with CH$_2$Cl$_2$ (3 x 20 mL) and brine (50 mL), dried with MgSO$_4$, and filtered using gravity filtration. After, the solvent was removed using rotary evaporation to afford compound **14** as a white solid (7.21 g, 95%). ^{1}H NMR (CDCl$_3$, 400 MHz): δ 4.89 – 4.77 (m, 2H), 3.76 (d, J = 7 Hz, 2H), 2.76 – 2.61 (m, 2H), 2.34 – 2.10 (m, 2H), 2.00 – 1.84 (m, 2H), 1.72 – 1.50 (m, 2H), 1.29 – 1.04 (m, 3H). The ^{1}H NMR spectrum corresponded with the literature.[55]

Synthesis of Compound 15:

To a flask containing compound **14** (7.00 g, 22.4 mmol) was added dry THF (100 mL) and was cooled to 0 °C. Then, a 1.0 M solution of KOtBu in THF (74 mL, 73.9 mmol) was added dropwise to the flask at 0 °C. The flask was then stirred and refluxed at 70 °C for 2 h. Next, the flask was cooled to r.t. and quenched with NH$_4$Cl (aq) (10 mL). The crude

product was extracted with CH_2Cl_2 (3 x 30 mL), dried with Na_2SO_4, and filtered using gravity filtration. After, the solvent was removed using rotary evaporation and the crude product was purified by column chromatography on silica gel using 3:1 Et_2O:hexanes as the eluent to afford compound **15** as a white solid (1.75 g, 52%). ^{1}H NMR (CDCl_3, 400 MHz): δ 3.73 (d, J = 7 Hz, 2H), 2.38 – 2.16 (m, 6H), 1.69 – 1.52 (m, 2H), 1.41 – 1.29 (m, 1H), 1.00 – 0.87 (m, 2H). The ^{1}H NMR spectrum corresponded with the literature.[55]

Synthesis of Compound 16:

To a flask containing ferrocenecarboxylic acid (0.577 g, 2.51 mmol) was added DCC (0.400 g, 1.93 mmol), DMAP (0.120 g, 0.965 mmol), and CH_2Cl_2 (40 mL). The flask was stirred at r.t. for 15 min. Then, compound **15** (0.290 g ,1.93 mmol) was added and the reaction mixture was stirred at r.t. for 4 h. The crude product was filtered using gravity filtration. After, the solvent was removed using rotary evaporation and the crude product was purified by column chromatography on silica gel using CH_2Cl_2 as the eluent to afford compound **16** as an orange solid (0.656 g, 90%). ^{1}H NMR (CDCl_3, 400 MHz): δ 4.82 (t, J = 2 Hz, 2H), 4.39 (t, J = 2 Hz, 2H), 4.30 (d, J = 8 Hz, 2H), 4.20 (s, 5H), 2.40 – 2.18 (m, 6H), 1.76 – 1.60 (m, 2H), 1.54 – 1.44 (m, 1H), 1.07 – 0.97 (m, 2H). ^{13}C{^{1}H} NMR (CDCl_3, 101 MHz): δ 171.9, 98.9, 77.2, 71.6, 71.3, 70.3, 69.8, 62.3, 29.4, 21.6, 20.4, 17.8. FT-IR (ATR, ν, cm^-1): 2911, 2809, 2064, 1696, 1467, 1373, 1346, 1275, 1135, 1054, 1022, 1001, 943, 894, 815, 791, 776, 736, 670, 665, 559, 525, 478. ESI-MS calcd for $C_{37}H_{41}N_5NaO_5SFe^+$ [M+Na]$^+$ 746.2094, found 746.2076; difference +2.47 ppm. UV-Vis in CH_2Cl_2 (λ_{max} = 309, 348, 444 nm).

Synthesis of Compound 17:

To a flask containing compound **15** (0.700 g, 4.66 mmol) was added 4-nitrophenyl chloroformate (1.03 g, 5.13 mmol), pyridine (0.950 mL, 11.6 mmol), and CH_2Cl_2 (50 mL). The flask was stirred at r.t. for 20 min and then was quenched with NH_4Cl $_{(aq)}$ (10 mL). The crude product was extracted with CH_2Cl_2 (3 x 20 mL) and brine (50 mL), dried with $MgSO_4$, and filtered using gravity filtration. After, the solvent was removed using rotary evaporation and the crude product was purified by column chromatography on silica gel using 1:1 EtOAc: hexanes as the eluent to afford compound **17** as a white solid (1.05 g,

71%). ^{1}H NMR (CDCl$_3$, 400 MHz): δ 8.31 – 8.25 (m, 2H), 7.42 – 7.36 (m, 2H), 4.41 (d, J = 8 Hz, 2H), 2.41 – 2.19 (m, 6H), 1.69 – 1.45 (m, 3H), 1.12 – 1.01 (m, 2H). The ^{1}H NMR spectrum corresponded with the literature.[55]

Synthesis of Compound 18:

To a flask containing compound **17** (0.075 g, 0.238 mmol) was added 1-pyrenemethylamine hydrochloride (0.058 g, 0.216 mmol), Et$_3$N (0.060 mL, 0.432 mmol), and DMF (5 mL). The flask was stirred at r.t. for 24 h. Then, the DMF was removed and the crude product was dissolved in Et$_2$O (10 mL) and extracted with NaHCO$_3$ (5 x 10 mL), dried with MgSO$_4$, and filtered using gravity filtration. After, the solvent was removed using rotary evaporation and the crude product was purified by column chromatography on silica gel using 1:2 EtOAc: hexanes as the eluent to afford compound **18** as a white solid (0.061 g, 69%). ^{1}H NMR (CDCl$_3$, 400 MHz): δ 8.33 – 8.26 (m, 2H), 8.23 – 8.18 (m, 2H), 8.18 – 8.12 (m, 2H), 8.10 – 7.95 (m, 4H), 5.10 (bs, 3H), 4.24 (d, J = 8 Hz, 2H), 2.33 – 2.10 (m, 6H), 1.67 – 1.57 (m, 2H), 1.43 – 1.30 (m, 1H), 0.99 – 0.88 (m, 2H). ^{13}C{^{1}H} NMR (CDCl$_3$, 101 MHz): δ 156.5, 131.4, 131.3, 131.2, 130.7, 128.2, 127.5, 127.4, 126.8, 126.1, 125.4, 125.3, 125.1, 124.8, 124.7, 122.8, 122.7, 98.8, 63.1, 43.4, 29.1, 21.4, 20.2, 17.8. FT-IR (ATR, ν, cm^{-1}): 3302, 3092, 2939, 1773, 1702, 1699, 1695, 1684, 1675, 1652, 1604, 1558, 1539, 1520, 1495, 1436, 1374, 1245, 1185, 1118, 1040, 954, 849, 817, 769, 732, 694, 668, 584, 516, 472, 458. ESI-MS calcd for C$_{28}$H$_{25}$NO$_2$$^+$ [M]$^+$ 407.1885, found 407.1884; difference +0.34 ppm. UV-Vis in CH$_2$Cl$_2$ (λ$_{max}$ = 300, 321, 323, 326, 334 nm).

Synthesis of Compound 19:

To a flask containing Rhodamine B (1.00 g, 2.10 mmol) was added DIPEA (0.420 mL, 2.40 mmol), and CH$_2$Cl$_2$ (200 mL). Then, HBTU (0.910 g, 2.40 mmol) was added dropwise to the flask at 0 °C. The flask was stirred at 0 °C for 30 min and then monoBoc-piperazine (0.450 g, 2.4 mmol) in CH$_3$CN (20 mL) was added dropwise to the reaction flask. The flask was warmed to r.t. and then stirred for 16 h. After, the solvent was removed using rotary evaporation and the crude product was purified by column chromatography on silica gel using 15:1 CH$_2$Cl$_2$: EtOH 95% as the eluent. Next, to deprotect the piperazine moiety, the reaction mixture was dissolved in 10% TFA in CH$_2$Cl$_2$ (20 mL) and stirred at

r.t. for 2 h. After, the solvent was removed using rotary evaporation and the crude product was purified by column chromatography on silica gel using 3:1 CH_2Cl_2:EtOH 95% as the eluent to afford compound **19** as a shiny purple solid (1.21 g, 92%). ^{1}H NMR (CDCl$_3$, 400 MHz): δ 7.71 – 7.62 (m, 2H), 7.60 – 7.55 (m, 1H), 7.35 – 7.30 (m, 1H), 7.21 (d, J = 8 Hz, 2H), 6.94 (dd, J = 2 Hz, J = 9 Hz, 2H), 6.77 (d, J = 2 Hz, 2H), 3.69 – 3.51 (m, 12H), 2.89 (bs, 4H), 1.32 – 1.29 (t, J = 7 Hz, 12H). The ^{1}H NMR spectrum corresponded with the literature.[56]

Synthesis of Compound 20:

To a flask containing compound **17** (0.070 g, 0.218 mmol) was added compound **19** (0.170 g, 0.272 mmol), DIPEA (0.129 mL, 0.741 mmol), and CH$_3$CN (20 mL). The flask was stirred at r.t. for 20 h. After, the solvent was removed using rotary evaporation and the crude product was purified by column chromatography on silica gel using 7:3 CH_2Cl_2:iPrOH as the eluent to afford compound **20** as a shiny purple solid (0.213 g, 84%). ^{1}H NMR (CDCl$_3$, 400 MHz): δ 7.73 – 7.65 (m, 2H), 7.57 – 7.50 (m, 1H), 7.39 – 7.33 (m, 1H), 7.31 – 7.17 (m, 2H), 7.09 – 6.67 (m, 4H), 4.14 (d, J = 8 Hz, 2H), 3.70 – 3.54 (m, 8H), 3.36 (bs, 8H), 2.34 – 2.13 (m, 6H), 1.61 – 1.45 (m, 2H), 1.32 (t, J = 7 Hz, 12H), 0.99 – 0.89 (m, 2H). The ^{1}H NMR spectrum corresponded with the literature.[56]

2.5.2.3   Compounds 21 – 31
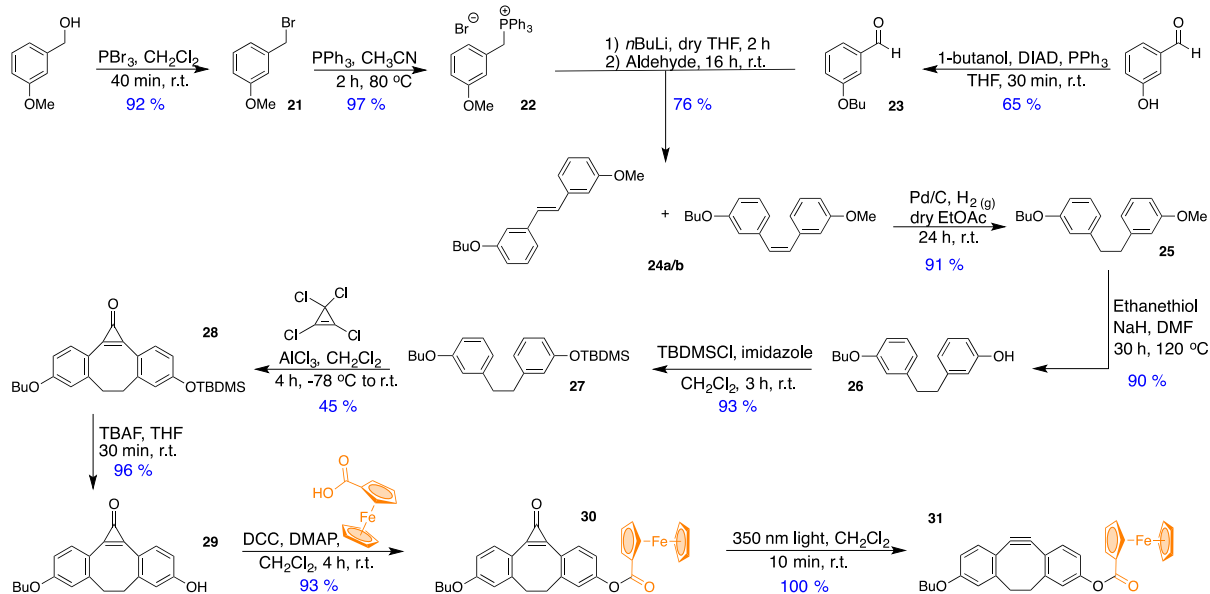
Synthesis of Compound 21:

To a flask containing 3-methoxybenzyl alcohol (20.0 g, 145 mmol) was added CH_2Cl_2 (400 mL) and the flask was stirred at 0 °C for 10 min. Next, PBr_3 (29.4 g, 109 mmol) was added dropwise to the flask over 10 min. The flask was stirred at r.t. for 40 min and then quenched with $NaHCO_3$ (aq) (50 mL). The crude product was extracted with Et_2O (3 x 100 mL), $Na_2S_2O_3$ (3 x 50 mL) and brine (50 mL). Then the organic fraction was dried with $MgSO_4$ and filtered using gravity filtration. After, the solvent was removed using rotary evaporation to afford compound **21** as a colourless oil (26.7 g, 92%). ^{1}H NMR ($CDCl_3$, 400 MHz): δ 7.26 (t, J = 8 Hz, 1H), 7.00 – 6.96 (m, 1H), 6.95 – 6.92 (m, 1H), 6.86 – 6.82 (m, 1H), 4.47 (s, 2H), 3.82 (s, 3H). The ^{1}H NMR spectrum corresponded with the literature.[57]

Synthesis of Compound 22:

To a flask containing compound **21** (16.0 g, 79.6 mmol) was added PPh_3 (59.5 g, 227 mmol) and CH_3CN (250 mL). The reaction mixture was refluxed at 80 °C and stirred for 2 h. The flask was then cooled to r.t. and the solvent was reduced using rotary evaporation. Toluene (500 mL) was then added to the flask to precipitate out the product

as a solid. The solid was collected using Buchner filtration and was washed with cold toluene (3 x 50 mL). After, the solid was dried to afford compound **22** as a white solid (35.9 g, 97%). ^{1}H NMR (CDCl$_3$, 400 MHz): δ 7.71 – 7.78 (m, 9H), 7.60 – 7.65 (m, 6H), 6.99-7.03 (m, 1H), 6.74 – 6.78 (m, 2H), 6.63 – 6.65 (m, 1H), 5.36 – 5.33 (d, J = 12 Hz, 1H), 3.53 (s, 3H). The ^{1}H NMR spectrum corresponded with the literature.[57]

Synthesis of Compound 23:

To a flask containing 3-hydroxybenzaldehyde (12.0 g, 98.0 mmol) was added 1-butanol (9.00 mL, 98.0 mmol), PPh$_3$ (28.8 g, 98.0 mmol), and THF (200 mL). The flask was stirred at 0 °C and diisopropyl azodicarboxylate (19.9 g, 98.0 mmol) was added dropwise. The reaction mixture was stirred at r.t. for 30 min. After, the solvent was removed using rotary evaporation and the crude product was purified by column chromatography on silica gel using 1:10 EtOAc: hexanes as the eluent to afford compound **23** as a colourless oil (11.4 g, 65%). ^{1}H NMR (CDCl$_3$, 400 MHz): δ 9.97 (s, 1H), 7.38 – 7.44 (m, 3H), 4.00 – 4.04 (t, J = 7 Hz, 2H), 176 – 1.83 (m, 2H), 1.46 – 1.55 (m, 2H), 0.97 – 1.01 (t, J = 7 Hz, 3H). The ^{1}H NMR spectrum corresponded with the literature.[57]

Synthesis of Compound 24a/b:

To a flask containing compound **22** (22.0 g, 47.5 mmol) was added dry THF (300 mL) and the mixture was stirred at – 78 °C (dry ice in acetone) for 15 min. The flask was purged with Ar$_{(g)}$ and a THF solution of nBuLi (5.05 mL, 54.6 mmol) was added dropwise at – 78 °C over 15 min. The reaction mixture was stirred at – 78 °C for 2 h. Next, compound **23** (8.45 g, 47.5 mmol) in dry THF (20 mL) was added dropwise to the reaction flask. Then, the dry ice bath was removed, and the reaction flask was stirred at r.t. for 16 h. The reaction was quenched with H$_2$O (50 mL) and the THF was removed using rotary evaporation. The crude product was extracted with EtOAc (3 x 100 mL) and brine (50 mL), dried with MgSO$_4$, and filtered using gravity filtration. After, the solvent was removed using rotary evaporation and the crude product was purified by column chromatography on silica gel using 1:4 EtOAc: hexanes as the eluent to afford compounds **24a** and **24b** as colourless oils (10.2 g, 76%). ^{1}H NMR (CDCl$_3$, 400 MHz): δ 7.24 – 7.33 (m, 3H), 7.03 – 7.17 (m, 6H), 6.78 – 6.86 (m, 5H), 6.71 – 6.75 (m, 1.5H), 6.57 (s, 2H), 3.99 – 4.02 (t, J = 7 Hz,

1.5H), 3.85 (s, 2H), 3.78 – 3.81 (t, J = 7 Hz, 2H), 3.66 (s, 3H), 1.75 – 1.82 (m, 2 H), 1.64 – 1.71 (m, 2H), 1.38 – 1.57 (m, 3H), 0.92 – 1.01 (m, 5H). The ^{1}H NMR spectrum corresponded with the literature.[57]

Synthesis of Compound 25:

To a flask containing compounds **24a** and **24b** (1.03 g, 3.64 mmol) was added 10% Pd/C (0.0388 g, 0.364 mmol) and dry EtOAc (100 mL). The flask was stirred at r.t. and was purged with $Ar_{(g)}$ for 10 min. An outlet needle and a balloon of $H_{2\ (g)}$ was attached to the flask using a metal needle. The metal needle was lowered into the solution in order to bubble $H_{2\ (g)}$ throughout the reaction mixture. The flask was stirred at r.t. for 24 h and the balloon was refilled with $H_{2\ (g)}$ after the first and second hours. Then, the reaction mixture was filtered over celite using gravity filtration. After, the solvent was removed using rotary evaporation and the crude product was purified by column chromatography on silica gel using 1:10 EtOAc: hexanes as the eluent to afford compound **25** as a colourless oil (0.942 g, 91%). ^{1}H NMR (CDCl$_3$, 400 MHz): δ 7.16 – 7.23 (m, 2H), 6.73 – 6.80 (m, 6H), 3.91 – 3.94 (t, J = 7 Hz, 2H), 3.77 (s, 3H), 2.88 (s, 4H), 1.72 – 1.79 (m, 2H), 1.44 – 1.56 (m, 2H), 0.96 – 0.99 (t, J = 7 Hz, 3H). The ^{1}H NMR spectrum corresponded with the literature.[57]

Synthesis of Compound 26:

To a flask containing compound **25** (2.80 g, 9.85 mmol) was added ethanethiol (6.05 mL, 79.0 mmol) and DMF (25 mL). The flask was stirred at 0 °C and a suspension of 60% NaH in oil (2.76 g, 69 mmol) was added dropwise to the reaction flask over 10 min. The flask was stirred at r.t. for 30 min and then at 120 °C for 30 h. Then, the reaction flask was cooled to r.t., diluted with Et$_2$O (100 mL), quenched with H$_2$O (50 mL), and acidified by added 5% HCl $_{(aq)}$ (50 mL). The crude product was extracted with H$_2$O (3 x 100 mL) and brine (50 mL), dried with MgSO$_4$, and filtered using gravity filtration. After, the solvent was removed using rotary evaporation and the crude product was purified by column chromatography on silica gel using 1:10 EtOAc: hexanes as the eluent to afford compound **26** as a colourless oil (2.40 g, 90%). ^{1}H NMR (CDCl$_3$, 400 MHz): δ 7.15 – 7.23 (m, 2H), 6.75 – 6.80 (m, 4H), 6.68 – 6.69 (m, 2H), 4.93 (s, 1H), 3.94 – 3.97 (t, J = 7 Hz,

2H), 2.88 (s, 4H), 1.74 – 1.81 (m, 2H), 1.46 – 1.56 (m, 2H), 0.98 – 1.02 (t, J = 7 Hz, 3H). The ^{1}H NMR spectrum corresponded with the literature.[57]

Synthesis of Compound 27:

To a flask containing compound **26** (2.10 g, 7.77 mmol) was added imidazole (0.582 g, 8.55 mmol), TBDMSCl (1.29 g, 8.55 mmol), and CH_2Cl_2 (50 mL). The flask was stirred at r.t. for 3 h and was then quenched with NH_4Cl $_{(aq)}$ (5 mL). Then, the reaction mixture was diluted with Et_2O (50 mL) and the organic layer was washed with H_2O (3 x 30 mL) and brine (50 mL). The organic fraction was dried with $MgSO_4$ and filtered using gravity filtration. After, the solvent was removed using rotary evaporation and the crude product was purified by column chromatography on silica gel using 1:10 EtOAc: hexanes as the eluent to afford compound **27** as a colourless oil (2.77 g, 93%). ^{1}H NMR ($CDCl_3$, 400 MHz): δ 7.13 – 7.22 (m, 2H), 6.74 – 6.82 (m, 4H), 6.68 – 6.71 (m, 2H), 3.93 – 3.97 (t, J = 7 Hz, 2H), 2.89 (s, 4H), 1.74 – 1.81 (m, 2H), 1.49 – 1.54 (m, 2H), 0.98 – 1.02 (m, 12H), 0.20 (s, 6H). The ^{1}H NMR spectrum corresponded with the literature.[57]

Synthesis of Compound 28:

To a flask containing aluminum chloride (0.900 g, 6.76 mmol) was added tetrachlorocyclopropene (1.20 g, 6.76 mmol) and CH_2Cl_2 (150 mL). The flask was stirred at r.t. for 20 min and then cooled to -78 °C. Then, a solution of compound **27** (2.60 g, 6.76 mmol) in CH_2Cl_2 (20 mL) was added to the reaction flask and the flask was then stirred at -78 °C for 4 h. The flask was warmed to r.t. and stirred for 1 h before diluting with CH_2Cl_2 (150 mL). Next, 5% HCl $_{(aq)}$ (100 mL) was added to the flask. The organic layer of the crude product was extracted with H_2O (3 x 100 mL) and brine (50 mL), dried with $MgSO_4$, and filtered using gravity filtration. After, the solvent was removed using rotary evaporation to afford compound **28** as a white solid (1.33 g, 45%). ^{1}H NMR ($CDCl_3$, 400 MHz): δ 7.94 – 7.91 (d, J = 12 Hz, 1H), 7.89 – 7.87 (d, J= 8 Hz, 1H), 6.89 – 6.86 (m, 2H), 6.83 – 6.81 (m, 2H), 4.05 – 4.02 (m, 2H), 3.36 – 3.26 (m, 2H), 2.63 – 2.57(m, 2H), 1.82 – 1.75 (m, 2H), 1.55 – 1.46 (m, 2H), 1.03 – 0.97 (m, 12H), 0.25 (s, 6H). The ^{1}H NMR spectrum corresponded with the literature.[57]

Synthesis of Compound 29:

To a flask containing compound **28** (1.20 g, 2.75 mmol) was added 1M TBAF in THF (0.796 mL, 2.75 mmol) and THF (30 mL). The flask was stirred at r.t. for 30 min and was then quenched with $NH_4Cl_{(aq)}$ (30 mL). The reaction mixture was diluted with CH_2Cl_2 (100 mL) and the aqueous layer was extracted with CH_2Cl_2 (3 x 30 mL), dried with $MgSO_4$, and filtered using gravity filtration. After, the solvent was removed using rotary evaporation and the crude product was purified by column chromatography on silica gel using 1:20 CH_3OH: CH_2Cl_2 as the eluent to afford compound **29** as a white solid (0.846 g, 96%). ^1H NMR (DMSO, 400 MHz): δ 10.42 (s, 1H), 7.75 – 7.77 (d, J = 8 Hz, 1H), 7.68 – 7.70 (d, J = 8 Hz, 1H), 7.08 (s, 1H), 6.98 – 7.01 (m, 1H), 6.89 – 6.90 (d, J = 4 Hz, 1H), 6.82 – 6.84 (dd, J = 8 Hz, J = 4 Hz, 1H), 4.06 – 4.09 (t, J = 7 Hz, 2H), 3.34 – 3.44 (m, 2H), 2.43 – 2.7 (m, 2H), 1.70 – 1.75 (m, 2H), 1.41 – 1.48 (m, 2H), 0.93 – 0.96 (t, J = 7 Hz, 3H). The ^1H NMR spectrum corresponded with the literature.[57]

Synthesis of Compound 30:

To a flask containing compound **29** (0.0250 g, 0.0780 mmol) was added ferrocenecarboxylic acid (0.0230 g, 0.101 mmol), DCC (0.0160 g, 0.0780 mmol), DMAP (0.00477 g, 0.0390 mmol), and CH_2Cl_2 (10 mL). The flask was stirred at r.t. for 4 h. After, the solvent was removed using rotary evaporation and the crude product was purified by column chromatography on silica gel using 1:1 EtOAc: CH_2Cl_2 as the eluent to afford compound **30** as fluffy orange solid (0.0380 g, 93%). ^1H NMR (CD_2Cl_2, 400 MHz): δ 8.07 (d, J = 8 Hz, 1H), 7.98 (d, J = 8 Hz, 1H), 7.26 – 7.22 (m, 2H), 6.94 – 6.89 (m, 2H), 4.97 (t, J = 2 Hz, 2H), 4.54 (t, J = 2 Hz, 2H), 4.33 (s, 5H), 4.06 (t, J = 7 Hz, 2H), 3.46 – 3.35 (m, 2H), 2.72 – 2.63 (m, 2H), 1.84 – 1.78 (m, 2H), 1.76 – 1.48 (m, 2H), 1.00 (t, J = 8 Hz, 3H). $^{13}C\{^1H\}$ NMR (CD_2Cl_2, 101 MHz): δ 170.4, 163.0, 153.9, 148.7, 148.0, 136.5, 135.2, 123.7, 121.8, 120.9, 116.7, 113.0, 72.9, 71.2, 70.6, 70.1, 68.7, 37.9, 37.4, 31.7, 30.2, 19.7, 14.1. FT-IR (ATR, ν, cm^{-1}): 3042, 2931, 2370, 1845, 1735, 1607, 1559, 1452, 1366, 1266, 1229, 1218, 1154, 1128, 1089, 1016, 910, 828, 668, 538, 517, 502, 486, 472, 463, 458. ESI-MS calcd for $C_{32}H_{28}FeO_4^+$ $[M]^+$ 532.1337, found 532.1342; difference +0.86 ppm. UV-Vis in CH_2Cl_2 (λ_{max} = 328, 345, 444 nm).

Synthesis of Compound 31:

To a flask containing compound **30** (0.0200 g, 0.0376 mmol) was added CH_2Cl_2 (20 mL). The reaction flask was stirred at r.t. while irradiating with 350 nm light for 10 min. After, the solvent was removed using rotary evaporation to afford compound **31** as fluffy orange solid (0.0190 g, 100%). ^{1}H NMR (CDCl$_3$, 600 MHz): δ 7.32 (d, J = 12 Hz, 1H), 7.24 (d, J = 12 Hz, 1H), 7.15 (d, J = 4 Hz, 1H), 7.07 (dd, J = 4 Hz, J = 12 Hz, 1H), 6.90 (d, J = 4 Hz, 1H), 6.78 (dd, J = 4 Hz, J = 12 Hz, 1H), 4.97 (t, J = 3 Hz, 2H), 4.52 (t, J = 3 Hz, 2H), 4.32 (s, 5H), 3.99 (t, J = 4 Hz, 2H), 3.34 – 3.17 (m, 2H), 2.48 (d, J = 18 Hz, 2H), 1.84 – 1.74 (m, 2H), 1.58 – 1.44 (m, 2H), 0.99 (t, J = 11 Hz, 3H). ^{13}C{^{1}H} NMR (CDCl$_3$, 101 MHz): δ 170.5, 159.2, 155.4, 154.6, 150.1, 127.1, 126.6, 123.2, 122.0, 119.8, 116.9, 115.5, 112.1, 112.1, 109.7, 72.2, 70.8, 70.1, 70.1, 68.0, 36.7, 36.6, 31.4, 19.4, 14.0. FT-IR (ATR, ν, cm^{-1}): 3041, 2927, 2855, 2118, 1733, 1609, 1562, 1487, 1452, 1375, 1366, 1298, 1257, 1218, 1178, 1144, 1109, 1083, 1026, 1018, 911, 823, 493. ESI-MS calcd for $C_{31}H_{28}FeO_3^+$ [M]$^+$ 504,1388, found 504,1393; difference -0.93 ppm. UV-Vis in CH_2Cl_2 (λ$_{max}$ = 305, 322, 444 nm).

2.5.2.4   Compounds 32 – 36

Synthesis of Compound 32:

To a flask containing N-methylmaleimide (0.0200 g, 0.180 mmol) was added CH₃OH (10 mL). The flask was stirred at r.t. and purged with Ar$_{(g)}$ for 20 min. Then, compound **6** (0.0450 g, 0.180 mmol) was added to the reaction flask and the reaction was stirred at r.t. and under inert atmosphere for 2 h. After, the solvent was removed using rotary evaporation and the crude product was purified by column chromatography on silica gel using 1:3 CH₂Cl₂: EtOAc as the eluent to afford compound **32** as a white solid (0.0460 g, 71%). ¹H NMR (CDCl₃, 400 MHz): δ 7.52 – 7.48 (m, 2H), 7.25 – 7.22 (m, 2H), 5.56 (bs, 1H), 4.01 (dd, J = 4 Hz, J = 9 Hz, 1H), 3.57 (s, 2H), 3.35 – 3.28 (m, 4H), 3.15 (dd, J = 9 Hz, J = 19 Hz, 1H), 2.91 (s, 3H), 2.68 (dd, J = 4 Hz, J = 19 Hz, 1H), 1.75 (tt, J = 7 Hz, J = 7 Hz, 2H). ¹³C{¹H} NMR (CDCl₃, 101 MHz): δ 175.8, 174.6, 170.4, 136.4, 135.1, 130.5, 129.8, 49.7, 44.1, 43.5, 37.8, 36.4, 28.7, 25.3. FT-IR (ATR, ν, cm⁻¹): 3253, 3100, 2948, 2102, 1776, 1689, 1630, 1554, 1491, 1436, 1386, 1281, 1198, 1143, 1062, 1015, 950, 807, 774, 690, 577, 494. ESI-MS calcd for C₁₆H₁₉N₅O₃S⁺ [M]⁺ 361.1209, found 361.1208; difference +0.25 ppm.

2.5.2.4   Compounds 32 – 36

Synthesis of Compound 32:

To a flask containing N-methylmaleimide (0.0200 g, 0.180 mmol) was added CH_3OH (10 mL). The flask was stirred at r.t. and purged with $Ar_{(g)}$ for 20 min. Then, compound **6** (0.0450 g, 0.180 mmol) was added to the reaction flask and the reaction was stirred at r.t. and under inert atmosphere for 2 h. After, the solvent was removed using rotary evaporation and the crude product was purified by column chromatography on silica gel using 1:3 CH_2Cl_2: EtOAc as the eluent to afford compound **32** as a white solid (0.0460 g, 71%). ^1H NMR ($CDCl_3$, 400 MHz): δ 7.52 – 7.48 (m, 2H), 7.25 – 7.22 (m, 2H), 5.56 (bs, 1H), 4.01 (dd, J = 4 Hz, J = 9 Hz, 1H), 3.57 (s, 2H), 3.35 – 3.28 (m, 4H), 3.15 (dd, J = 9 Hz, J = 19 Hz, 1H), 2.91 (s, 3H), 2.68 (dd, J = 4 Hz, J = 19 Hz, 1H), 1.75 (tt, J = 7 Hz, J = 7 Hz, 2H). $^{13}C\{^1H\}$ NMR ($CDCl_3$, 101 MHz): δ 175.8, 174.6, 170.4, 136.4, 135.1, 130.5, 129.8, 49.7, 44.1, 43.5, 37.8, 36.4, 28.7, 25.3. FT-IR (ATR, ν, cm^{-1}): 3253, 3100, 2948, 2102, 1776, 1689, 1630, 1554, 1491, 1436, 1386, 1281, 1198, 1143, 1062, 1015, 950, 807, 774, 690, 577, 494. ESI-MS calcd for $C_{16}H_{19}N_5O_3S^+$ [M]⁺ 361.1209, found 361.1208; difference +0.25 ppm.

Synthesis of Compound 33:

To a flask containing compound **32** (0.0190 g, 0.0529 mmol) was added compound **16** (0.0200 g, 0.0529 mmol) and a 1:1 mixture of CH_2Cl_2:CH_3OH (10 mL). The flask was stirred at r.t. for 2 h. After, the solvent was removed using rotary evaporation and the crude product was purified by column chromatography on silica gel using 1:9 CH_3OH: EtOAc as the eluent to afford compound **33** as bright orange solid (0.0370 g, 95%). ^1H NMR ($CDCl_3$, 400 MHz): δ 7.56 – 7.43 (m, 2H), 7.33 – 7.21 (m, 2H), 6.02 (bs, 1H), 4.81 (bs, 2H), 4.40 (bs, 2H), 4.36 – 4.25 (m, 2H), 4.25 – 4.14 (m, 6H), 4.02 (bs, 1H), 3.51 (bs, 2H), 3.27 – 3.04 (m, 4H), 3.01 – 2.80 (m, 4H), 2.76 – 2.58 (m, 2H), 2.35 – 2.21 (m, 2H), 2.06 – 1.91 (m, 2H), 1.76 – 1.50 (m, 3H), 1.45 – 1.29 (m, 2H), 1.18 – 1.01 (m, 2H). $^{13}C\{^1H\}$ NMR ($CDCl_3$, 101 MHz): δ 175.8, 174.6, 171.9, 170.6, 136.5, 134.9, 130.4, 129.7, 71.5, 71.4, 70.3, 70.3, 69.9, 62.0, 45.5, 44.3, 43.5, 36.8, 36.4, 29.8, 29.2, 26.2, 25.3, 23.3, 22.8, 22.4, 20.2, 19.8, 17.9. FT-IR (ATR, ν, cm^{-1}): 3350, 1700, 1543, 1434, 1375, 1276, 1135, 953, 733, 694, 501. ESI-MS calcd for $C_{16}H_{19}N_5NaO_3S^+$ $[M+Na]^+$ 746.2076, found 746.2094; difference -2.47 ppm. UV-Vis in CH_2Cl_2 (λ_{max} = 312, 347, 447 nm).

Synthesis of Compound 34:

To a flask containing compound **32** (0.0220 g, 0.0599 mmol) was added compound **20** (0.0400 g, 0.0499 mmol) and CH_2Cl_2 (10 mL). The flask was stirred at r.t. for 4 h. After, the solvent was removed using rotary evaporation and the crude product was purified by column chromatography on silica gel using 1:9 CH_3OH: CH_2Cl_2 as the eluent to afford compound **34** as shiny purple solid (0.0520 g, 90%). ^1H NMR ($CDCl_3$, 400 MHz): δ 7.72 – 7.64 (m, 2H), 7.58 – 7.54 (m, 1H), 7.46 – 7.36 (m, 4H), 7.36 – 7.30 (m, 1H), 7.26 – 7.22 (m, 2H), 7.20 – 6.84 (m, 2H), 6.74 (bs, 2H), 4.42 – 4.24 (m, 2H), 4.02 – 3.96 (m, 1H), 3.37 – 3.54 (m, 10H), 3.54 – 3.17 (m, 10H), 3.13 – 2.96 (m, 3H), 2.92 – 2.85 (m, 3H), 2.83 – 2.74 (m, 1H), 2.72 – 2.58 (m, 2H), 2.14 (bs, 1H), 2.10 – 1.97 (m, 2H), 1.53 – 1.36 (m, 2H), 1.36 – 1.27 (m, 12H), 1.23 – 1.12 (m, 2H), 1.11 – 0.95 (m, 2H). $^{13}C\{^1H\}$ NMR ($CDCl_3$, 101 MHz): δ 175.8, 174.7, 171.5, 167.7, 157.9, 157.9, 155.9, 155.8, 155.5, 144.7, 134.4, 134.3, 132.3, 130.8, 130.4, 130.3, 130.2, 127.8, 114.3, 96.3, 64.2, 47.5, 46.3, 44.6, 42.8, 41.9, 36.8, 36.6, 30.1, 26.2, 25.3, 23.2, 22.6, 20.5, 17.8, 12.8. FT-IR (ATR, ν, cm^{-1}): 3447,

3054, 2970, 2968, 2369, 1738, 1698, 1646, 1589, 1558, 1466, 1414, 1395, 1380, 1366, 1339, 1277, 1247, 1229, 1217, 1199, 1181, 1132, 1075, 1009, 922, 683. ESI-MS calcd for $C_{59}H_{70}N_9O_7S^+$ $[M - CF_3COO]^+$ 1048.5113, found 1048.5102; difference +1.65 ppm. UV-Vis in CH_2Cl_2 (λ_{max} = 230, 250, 314, 443 nm).

Synthesis of Compound 35:

To a flask containing compound **32** (0.0200 g, 0.0540 mmol) was added compound **18** (0.0200 g, 0.0491 mmol) and CH_2Cl_2 (10 mL). The flask was stirred at r.t. for 4 h. After, the solvent was removed using rotary evaporation and the crude product was purified by column chromatography on silica gel using 1:9 CH_3OH: CH_2Cl_2 as the eluent to afford compound **35** as fine white powder (0.0370 g, 97%). ^1H NMR (CDCl$_3$, 400 MHz): δ 8.38 – 8.27 (m, 1H), 8.24 – 8.19 (m, 2H), 8.19 – 8.13 (m, 2H), 8.11 – 7.97 (m, 4H), 7.49 – 7.42 (m, 2H), 7.25 – 7.20 (m, 2H), 5.92 (bs, 1H), 5.18 (bs, 1H), 5.13 – 5.07 (m, 2H), 4.29 – 4.11 (m, 4H), 4.00 – 3.91 (m, 1H), 3.49 (s, 2H), 3.22 – 3.01 (m, 4H), 2.93 – 2.75 (m, 5H), 2.75 – 2.68 (m, 2H), 2.26 – 2.11 (m, 2H), 1.99 – 1.88 (m, 2H), 1.72 – 1.48 (m, 4H), 1.33 – 1.18 (m, 2H), 1.10 – 0.92 (m, 2H). $^{13}C\{^1H\}$ NMR (CDCl$_3$, 101 MHz): δ 175.8, 174.6, 170.6, 156.6, 136.5, 134.9, 134.9, 133.1, 131.5, 131.4, 130.9, 130.4, 129.7, 128.3, 127.7, 127.5, 127.0, 126.3, 125.6, 125.5, 125.2, 125.0, 124.9, 122.9, 63.0, 53.6, 45.4, 44.3, 43.6, 43.5, 36.7, 36.4, 36.4, 29.1, 26.1, 25.2, 23.1, 22.7, 22.2, 20.1, 19.6, 17.9. FT-IR (ATR, ν, cm^{-1}): 3336, 3089, 2916, 2849, 2244, 1918, 1793, 1703, 1699, 1695, 1684, 1604, 1589, 1520, 1506, 1472, 1456, 1436, 1418, 1366, 1311, 1053, 1026, 1002, 977, 967, 909, 846, 818, 761, 729, 712, 682, 667, 647, 585, 555, 484, 463, 458. ESI-MS calcd for $C_{44}H_{44}N_6NaO_5S^+$ $[M + Na]^+$ 791.2992, found 791.2994; difference -0.36 ppm. UV-Vis in CH_2Cl_2 (λ_{max} = 313, 321, 326, 349, 395 nm).

Synthesis of Compound 36:

To a flask containing compound **32** (0.0140 g, 0.0377 mmol) was added compound **31** (0.0190 g, 0.0377 mmol) and CH_2Cl_2 (10 mL). The flask was stirred at r.t. for 4 h. After, the solvent was removed using rotary evaporation and the crude product was purified by column chromatography on silica gel using 5% CH_3OH in EtOAc as the eluent to afford compound **36** as bright orange solid (0.0290 g, 90%). ^1H NMR (CDCl$_3$, 400 MHz): δ 7.66

– 7.33 (m, 4H), 7.33 – 6.96 (m, 2H), 6.92 – 6.67 (m, 2H), 5.89 (bs, 1H), 4.99 – 4.88 (m, 2H), 4.56 – 4.45 (m, 2H), 4.45 – 4.31 (m, 2H), 4.31 – 4.24 (m, 5H), 4.12 – 3.86 (m, 3H), 3.60 – 3.45 (m, 2H), 3.45 – 3.26 (m, 2H), 3.26 – 2.99 (m, 4H), 2.96 – 2.78 (m, 4H), 2.73 – 2.58 (m, 1H), 2.16 – 1.85 (m, 2H), 1.83 – 1.58 (m, 2H), 1.58 – 1.40 (m, 2H), 1.02 – 0.91 (m, 3H). $^{13}C\{^1H\}$ NMR (CDCl$_3$, 101 MHz): δ 175.8, 174.6, 170.3, 170.3, 160.5, 159.1, 151.9, 150.6, 143.5, 143.1, 139.3, 138.9, 136.4, 135.0, 134.9, 134.7, 133.2, 133.2, 130.5, 130.5, 130.2, 130.2, 129.8, 127.4, 123.8, 123.7, 123.4, 123.3, 122.0, 120.3, 119.7, 117.8, 116.6, 116.0, 113.2, 112.7, 72.3, 72.1, 70.8, 70.7, 70.1, 70.1, 69.7, 68.0, 67.7, 53.6, 49.6, 46.1, 44.3, 43.6, 37.0, 36.9, 36.8, 36.5, 33.2, 33.2, 31.4, 31.4, 29.8, 29.7, 25.3, 19.4, 14.0. FT-IR (ATR, ν, cm^{-1}): 3245, 3030, 2970, 1723, 1717, 1704, 1700, 1668, 1652, 1608, 1559, 1516, 1490, 1455, 1436, 1375, 1366, 1270, 1229, 1217, 1205, 1156, 1110, 1019, 984, 955, 918, 827, 761, 694, 668, 530, 516, 502, 486, 471, 462, 458. ESI-MS calcd for C$_{47}$H$_{48}$N$_5$O$_6$SFe$^+$ [M + C$_4$H$_9$O]$^+$ 866.2675, found 866.2642; difference +3.78 ppm. UV-Vis in CH$_2$Cl$_2$ (λ$_{max}$ = 230, 253, 305, 441 nm).

Chapter 3

# 3   AuNP Synthesis & Interfacial Modifications

3.1   AuNP Synthesis

Moving onto working with AuNPs, inert, base AuNPs were synthesized using thiol **39**. This thiol was synthesized following a literature procedure and was chosen because it produces water soluble AuNPs that are highly stable (Scheme 12). These base AuNPs were also synthesized because the linear nature of thiol **39** allows for dense packing of the organic corona around the gold center, therefore increasing the stability of the AuNPs while maintaining good water solubility. The first transformation was a mono-tosylation of one of the hydroxyl groups of tetraethylene glycol to yield compound **37**. Tetraethylene glycol was used in a great excess to prevent the formation of the ditosylated product. Next, potassium thioacetate participated in a S_N2 reaction with the tosyl group of compound **37** to produce compound **38**. Then the thioacetate group was hydrolyzed to a thiol using NaOH in argon purged ethanol followed by 1 M hydrochloric acid to yield thiol **39**. This thiol was stored in the freezer under an atmosphere of argon gas. To synthesize the AuNPs, the Brust-Schiffrin method was used with $NaBH_4$ as the reducing agent. This synthesis was followed from a paper our group has recently published and the procedure yields AuNPs with an average diameter of 2.9 ± 0.5 nm.[59] Importantly, compound **40** was soluble in both polar organic and aqueous solvents.
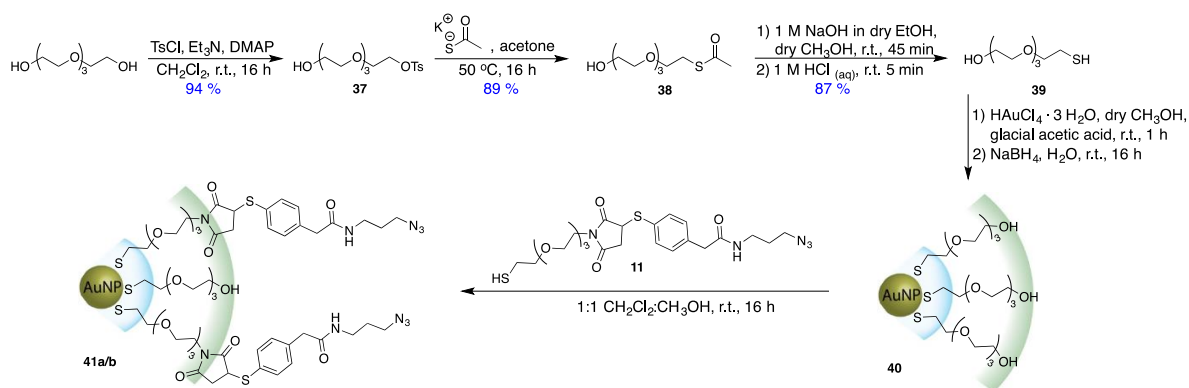
Scheme 12: Synthesis of AuNPs **41a/b** following a literature procedure involving a Brust-Schiffrin particle synthesis and place exchange reaction.[59]

Two different versions of compound **41** were synthesized by reacting compound **40** with varying amounts of thiol **11** in this project. These reactions are called place-exchange reactions and the AuNP products will have both thiols **11** and **39** bound to the colloidal gold core. The ratio of these thiols on the interface of the AuNPs are determined by an equilibrium of the thiol bound to the surface of the particles being displaced off by the introduced thiol and the reverse process as well. The alkyl portion added after the tetraethylene chain on thiol **11** makes it more nonpolar in character compared to thiol **39**, making AuNPs with greater concentrations of **11** added more organic soluble (Scheme 13).
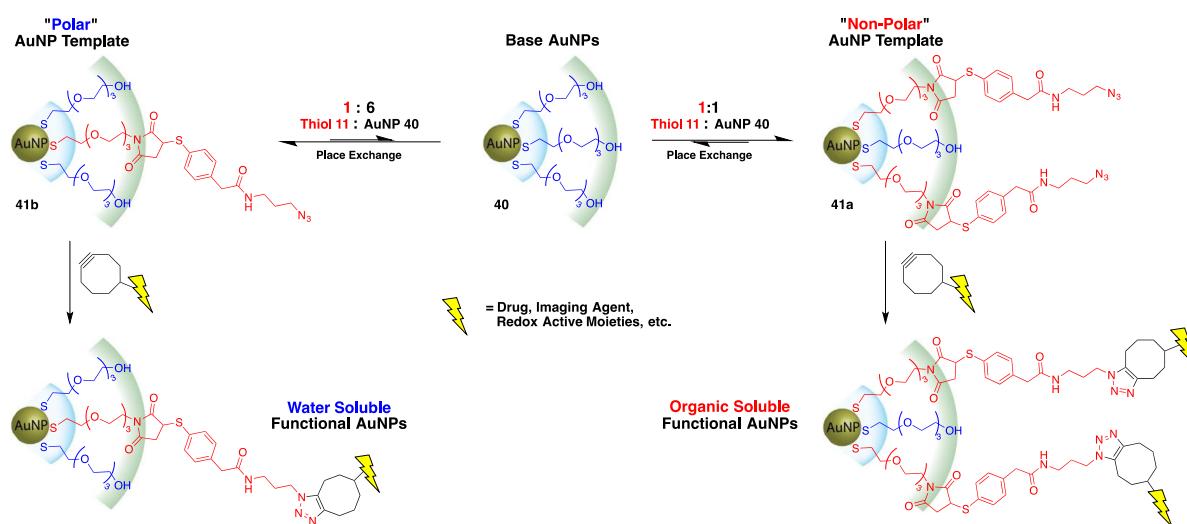

Scheme 13: Tuning solubilities of hydroxyl-terminated AuNPs (**40**) via place exchange reactions with varying quantities of the nonpolar ligand **11** (red) to produce organic soluble (**41a**) and water soluble (**41b**) AuNPs. Equilibria of bound stabilizing ligands to the metallic gold cores are established between the polar hydroxyl-terminated ligands **39** (blue) and the nonpolar azide-terminated ligands to both give polar and nonpolar AuNP templates. These templates can be functionalized with strained alkynes to produce functional water soluble and functional organic soluble AuNPs.

The thiol **11**: particle **40** ratio used to produce AuNPs **41a** was 1:1 by mass. These particles were synthesized to easily characterize the AuNPs because they are more soluble in organic solvents than AuNPs **41b** and the ^{1}H NMR signals for the azide terminated thiol ligand on AuNP **41a** have greater intensity than for AuNP **41b** due to the differences in the thiol ligand: particle ratio. The thiol **11**: particle **40** ratio used to produce AuNPs **41b** was 1:6 by mass. These particles were synthesized because they are fully soluble in aqueous PBS buffer while the AuNPs **41a** are only soluble in water with a little bit of methanol

added. Solubility in PBS buffer is critical for these particles because the glutathione release of MPA off the particles must be performed under physiological conditions. Therefore, AuNPs **41a** are more organic soluble and were used to characterize the nanoparticles with NMR spectroscopy, while AuNPs **41b** are soluble in PBS buffer and will be used in the glutathione release experiments.

3.2 Organic Soluble AuNP Cargo Loading

The organic soluble, azide-terminated AuNPs **41a** synthesized in the last section were subjected to several different strained alkynes to participate in SPAACs, which introduced function (emissive and redox active compounds) to the AuNPs (Scheme 14). While the clicked products of these reactions were not treated with GSH under physiological conditions to trigger the release of the cargo, they were used to determine the efficiency and feasibility of the release experiments. This batch of AuNPs were not suitable for the release experiments because their poor solubility in aqueous solutions like PBS. However, the greater concentrations of the MPA containing ligand bound to the gold core on these AuNPs allowed for more resolved NMR spectra to be obtained. By comparing the NMR spectra of these functionalized AuNPs to those collected in **Section 2.4** of the clicked adducts, it was determined these reactions were clean and successful. These spectra were especially advantageous to examine as their polar, aqueous soluble analogs did not show resolved signals for the MPA containing ligands, due to their lower concentrations of these ligands at the interfaces. The four strained alkynes chosen were compounds **16**, **18**, **20**, and **31**. Compounds **16** and **31** were chosen because they contain ferrocene groups; redox active moieties that were monitored using cyclic voltammetry during the cargo release. Similarity, compounds **18** and **20** were picked for their emissive properties, that can be tracked by utilizing fluorescence spectroscopy. Compound **18** included a pyrene group, a planar, neutral molecule that fluoresces bright blue and compound **20** included a rhodamine B group, a large, charged molecule that fluoresces a vivid pink colour. The strained alkyne present in compounds **16**, **18**, and **20** was BCN, while compound **31** incorporated DIBO instead to depict the versatility of this system. Unfortunately, due to time limitations involved with COVID 19, the depleted reserves of compound **31** could not be replenished and therefore was omitted from this thesis.
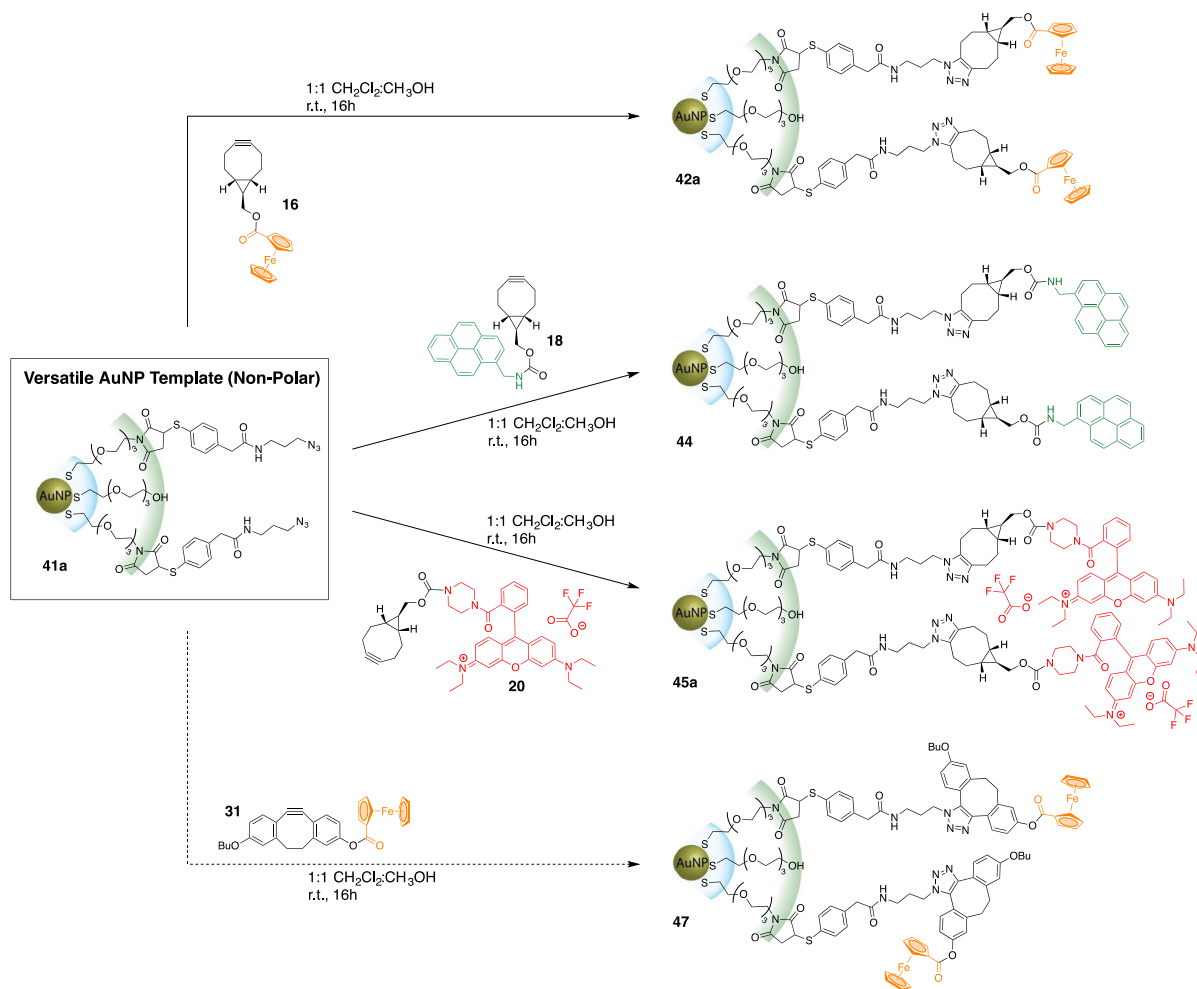
Scheme 14: Reaction schemes depicting versatile, organic soluble AuNPs (**41a**) participating in interfacial SPAACs with strained alkynes **16**, **18**, and **20** to produce functionalized AuNPs. The reaction between **41a** and **31** was not performed due to limitations involved with COVID 19.

Compound **42a** was synthesized from a SPAAC of compounds **41a** and **16**. The dark brown colour of compound **41a** was converted to a dark orange colour in the product **42a** due to the bright orange ferrocene groups covalently bound to the nanoparticle surface. The complex ^{1}H NMR spectrum of compound **42a** was analyzed with the help of the ^{1}H NMR spectrum of compound **33**, the small molecule analogue to the interface of compound **42a**. The comparison below shows that compound **16** was successfully attached onto the surface of the particles because all of the signals in the ^{1}H NMR spectrum of compound **33** were integrated into the ^{1}H NMR spectrum of compound **41a**, but broadened (Figure 5). The signal labelled with an orange circle corresponds to the methyl group on the maleimide

ring of compound **33**. This signal is not present in the spectrum of compound **42a** because it is replaced by ethylene glycol signals labelled with blue circles. All other signals are present in both spectra, indicating once again that compound **16** was successfully attached onto the surface of the particles. Similar NMR spectra comparisons and analysis were performed for AuNPs **44** and **45a** to determine the outcomes of the interfacial SPAACs with strained alkynes **18** and **20**, respectively. The complex ^{1}H NMR spectra of AuNPs **44** and **45a** were analyzed with the assistance of the ^{1}H NMR spectra of their small molecule analogues **35** and **34**, respectively. As a result, the versatile, organic soluble AuNPs **41a** were effectively conjugated with various cargo-loaded strained alkynes via SPAACs and the clicked products were characterized with ^{1}H NMR spectroscopy to determine the effectiveness of the interfacial modifications.
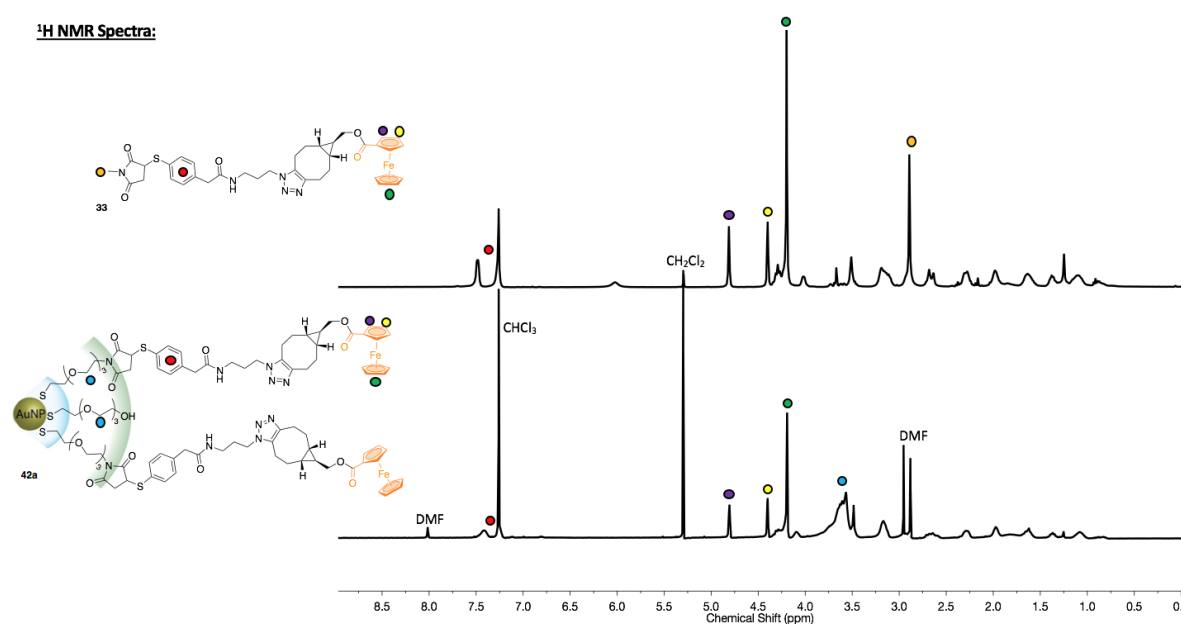
Figure 5: The comparison of the ^{1}H NMR spectra of compounds **33** and **42a** with labelled diagnostic proton assignments. The green, yellow, and purple circles represent the duplicated ferrocene protons.

3.3 Interfacial Modifications of Water Soluble AuNPs

The water soluble, azide-terminated AuNPs **41b** synthesized in Section 3.1 were reacted with compounds **16** and **20** in SPAACs to yield AuNPs **42b** and **45b**, respectively (Scheme 15). Unfortunately, the water-soluble pyrene functionalized AuNPs were not

synthesized due to limitation involved with COVID 19. The pyrene starting material was ordered from Sigma Aldrich in July 2020, but the order was never fulfilled. As previously discussed, the ^{1}H NMR spectra of the water-soluble AuNPs made in this section only cleanly show the tetraethylene signals due to the drastic difference in the proton integrations of this multiplet to all the other signals. The lower azide ligand concentrations on the AuNP gold cores are required to maintain their solubility in PBS for the release experiments. These spectra should have the same chemical shifts and multiplicity as the ^{1}H NMR spectra of their organic soluble counterparts, but with different signal integrations.
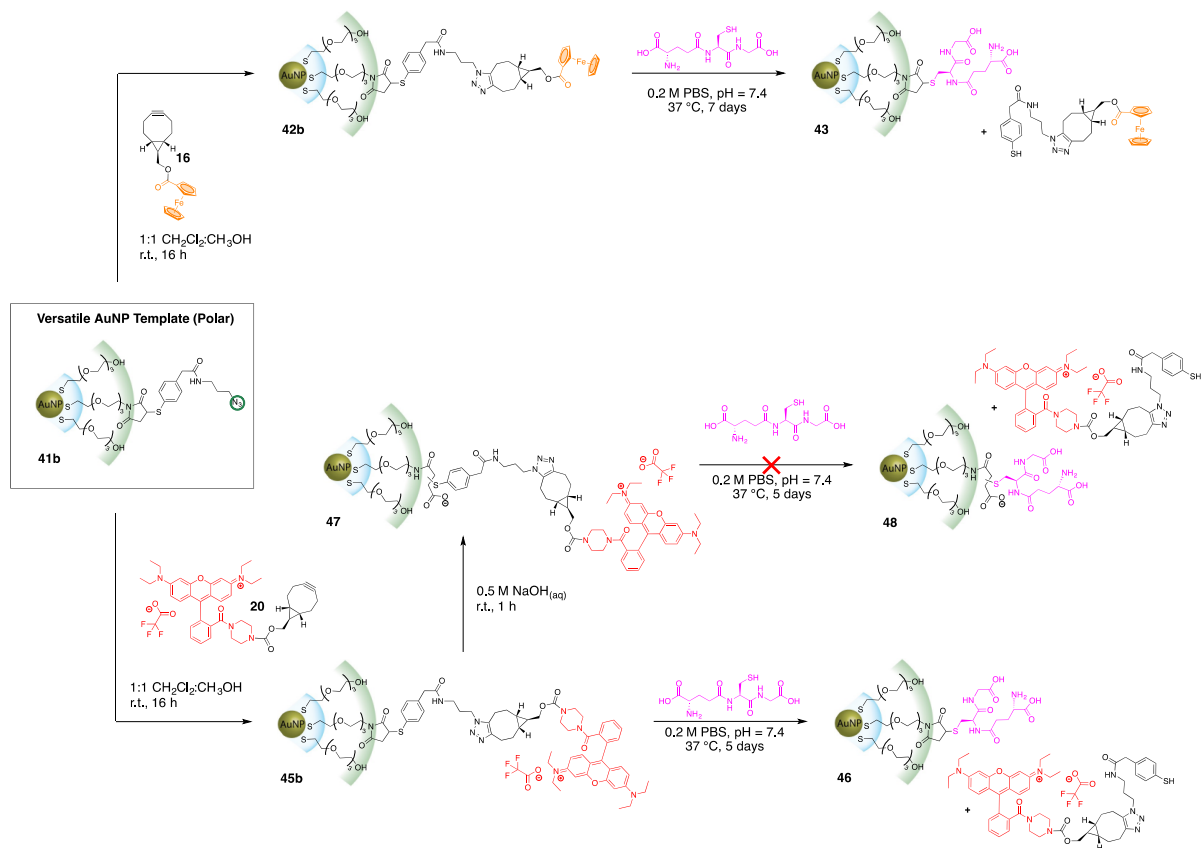
Scheme 15: Interfacial reactions to AuNP **41b** to modify the physical and chemical properties of the nanoparticle surface via SPAACs with strained alkynes **16** and **20**. Functionality was delivered to AuNP **41b** using SPAACs and then the cargo was released using a solution of GSH under physiological conditions. If the maleimide ring is hydrolyzed, GSH triggered release does not occur and the payload is not delivered.

3.3.1   Electrochemical Studies

After successfully synthesizing water-soluble, ferrocene (Fc) terminated AuNPs (**42b**), an experiment was designed to monitor the release of the Fc groups in 0.2M PBS for one week using cyclic voltammetry (CV). The original plan was to perform the release experiment with a bulk batch of AuNP **42b** and collect equal aliquots at 0 h, 6 h, 12 h, 24h, 48 h, 96 h, and 168 h. The aliquots would then be worked up separately and then prepared for cyclic voltammetry to measure the current as a function of potential over one week. While running a small-scale test reaction for this experiment, it was determined that this procedure was not feasible. The two main reasons for this conclusion were: 1) each sample for CV required approximately 10 milligrams of sample and 2) over the gradual release of the Fc groups, the surface chemistry of the AuNPs alter, leading to drastic differences in solubility between the aliquots. The amount of AuNPs needed to collect seven CV plots (approx. 70 mg) was too costly, as these AuNPs require expensive starting materials and are time consuming to synthesize. The disparities in solubility between the aliquots arose as the Fc groups were being replaced by GSH on the nanomaterial interface throughout the length of the experiment (Scheme 16). This made it extremely difficult to isolate the AuNPs from the excess GSH, the released small molecules, and salts from the PBS in each aliquot. Furthermore, each aliquot required its own unique purification method, and it was not possible to determine these conditions with the limited quantities of AuNPs.
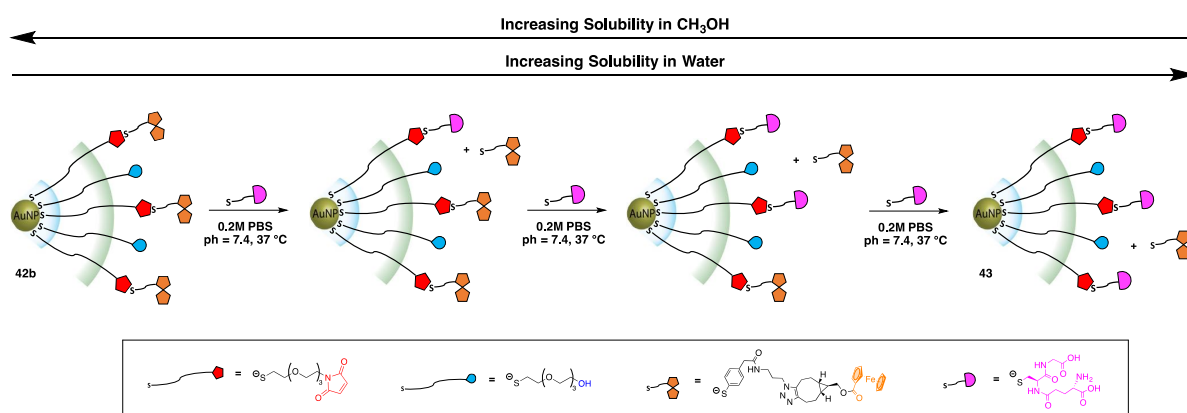
Scheme 16: The changing solubility of water-soluble, Fc terminated AuNP 42b overtime as more nonpolar Fc (orange) groups are displaced by polar GSH (pink) groups. The AuNPs interface becomes gradually more water-soluble overtime creating difficultly in the purification steps of the reaction.

The plan quickly changed to performing the GSH mediated release on a smaller quantity of AuNP **42b** without any aliquots taken, but instead thoroughly purifying the final product **43** after 1 week of release. The crude reaction mixture was extracted with a 1:1 mixture of CH_2Cl_2: hexanes, Et_2O, and a mixture of 1:1 CH_3OH: hexanes to remove any organic, small molecules released off during the reaction. This washing procedure was repeated 5 times and the crude AuNPs were dissolved in CH_3OH and centrifuged at 6000 rpm for 10 min to remove insoluble solid impurities. The AuNPs were then further purified by overnight dialysis to remove any water-soluble salts from the PBS. Then, the sample was dried on high vacuum and passed onto Jonathan Wong from the Ding group to run and collect the CV plots (Figure 6). A three-electrode system was used with a glassy carbon working electrode and two platinum wires which served as the counter and reference electrode. The AuNP samples were dissolved at 3.13 mg/mL in anhydrous DCM and further purged with $Ar_{(g)}$ for 10 minutes. Tetrabutylammonium perchlorate (TBAP) was added into the electrochemical cell as the supporting electrolyte and all potentials were calibrated by an internal ferrocene standard taken at 0.424 V vs SCE.[60-61]
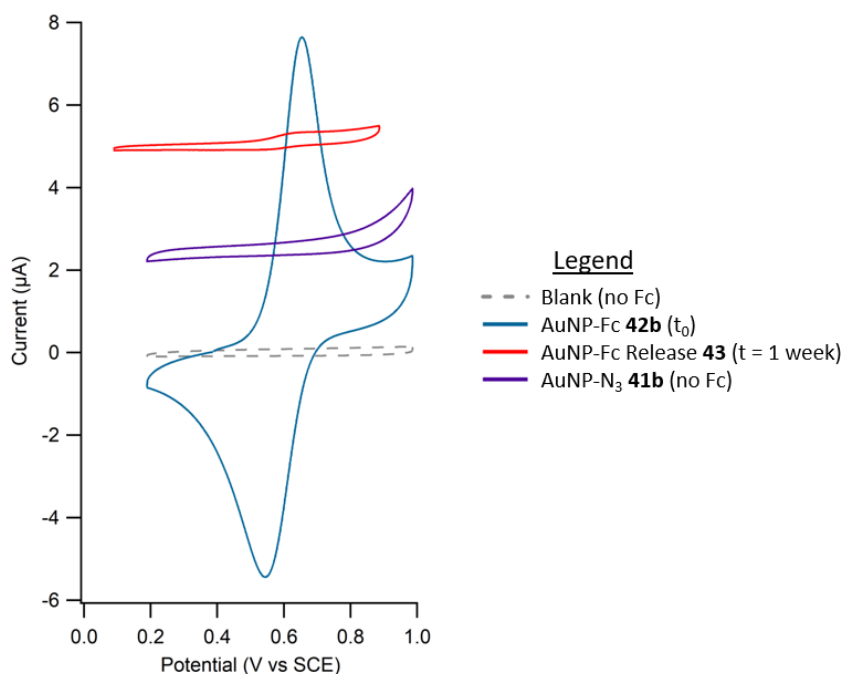
Figure 6: Cyclic voltammetry plots for several water-soluble AuNPs to depict the GSH-mediated release of Fc groups off of AuNP **42b** over 1 week. The current was measured as a function of potential. Azide terminated AuNPs (**41b**) were run for a baseline as there are no Fc groups present, Fc terminated AuNPs

(**42b**) for a time zero because no release has occurred yet, and finally the Fc terminated AuNPs (**43**) after 1 week of GSH-mediated release were run.

Three different AuNPs samples were run along with a blank: azide terminated AuNPs (**41b**) for a baseline as there are no Fc groups present, Fc terminated AuNPs (**42b**) as a time zero because no release has occurred yet, and finally the Fc terminated AuNPs (**43**) after a week of GSH-mediated release. The CV plots show the predicted results. The azide terminated AuNPs do not show any oxidation or reduction curves, due to the lack of redox active molecules in this potential range. The Fc terminated AuNPs exhibit oxidation and reduction waves corresponding to ferrocene-containing species. This data supports the successful attachment of Fc-BCN (**16**) onto AuNP 41b through a SPAAC as well. Finally, the plot for the AuNP **43**, displays a CV curve with very small peaks corresponding to the remaining Fc groups bound to the gold core. By determining the difference in peak areas of the plots for AuNP 42b and 43, it was calculated that approximately 6% of the Fc groups present at t_0 remain after a week of GSH-mediated release. Therefore, the release of redox active moieties on the surface of the Fc terminated AuNPs under physiological conditions works and almost all the releasable groups are displaced by GSH in one week. The gradual release of molecular cargo will be examined in the fluorescence studies.

3.3.2   Fluorescence Spectroscopy

In this section, water-soluble, rhodamine B terminated AuNPs **45b** were reacted with GSH under physiological conditions to monitor the gradual release of emissive small molecules from the nanomaterial interface. This experiment exploited the property of AuNPs, where the fluorescence intensity of emissive molecules bound to its surface are partially quenched.[62-63] It was predicted that overtime the fluorescence intensity would increase as GSH displaces off more and more rhodamine B groups as small molecules via retro-Michael additions. The unbound emissive groups cause the fluorescence count to increase, as the gold core can no longer quench the emission. The residual emission observed was utilized as a baseline of fluorescence for the timed, release experiments. The experiment involved stirring the reaction flask in PBS at 37 °C for seven days and collecting aliquots after 0 h, 6 h, 12 h, 24 h, 48 h, and 96 h to monitor the gradual release of the fluorescent cargo using fluorescence spectroscopy (Figure 7). Each aliquot was

diluted to 10 mL with 0.2M PBS before recording the fluorescence excitation (λ_{ex} = 564 nm) and emission spectra (λ_{em} = 585 nm).
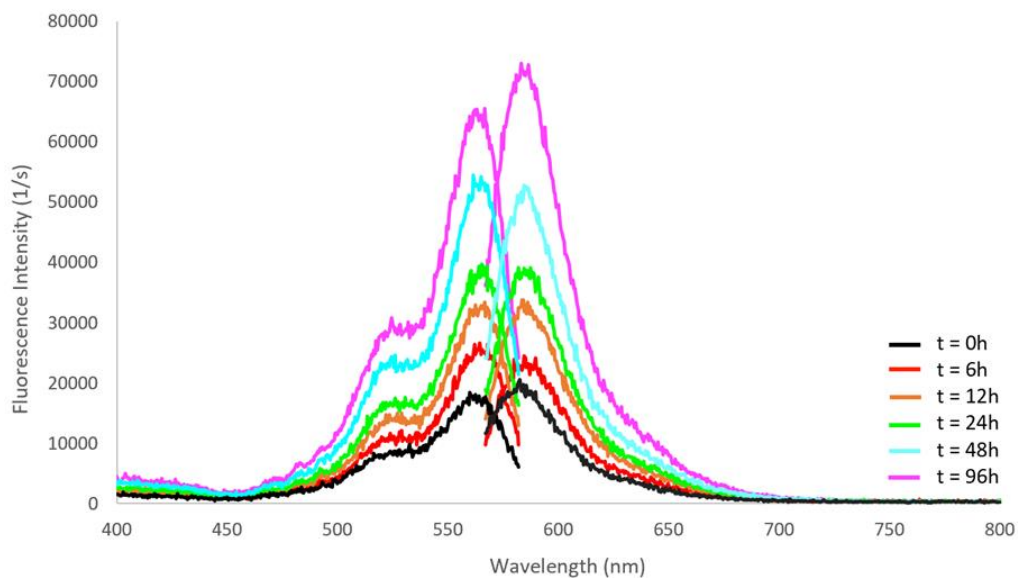

Figure 7: Fluorescence data depicting the gradual, GSH-mediated release of emissive, rhodamine B-containing small molecules off AuNP **45b** recorded over 96 h. All samples were run in 0.2 M PBS (pH = 7.4) with excitation (left) and emission (right) wavelengths at 564 nm and 585 nm, respectively.
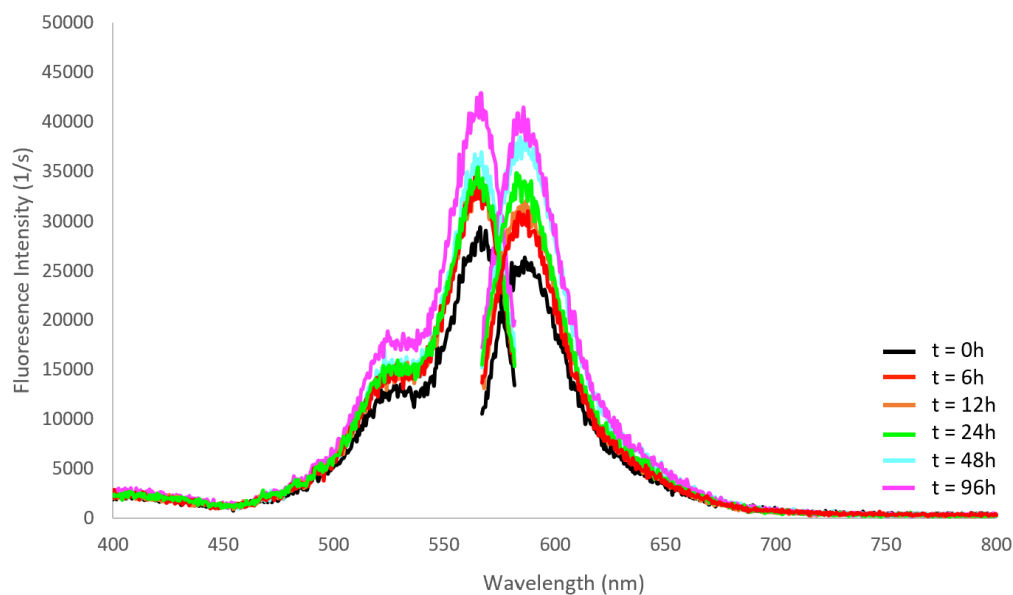

Figure 8: Fluorescence data depicting the GSH-mediated release experiment on "locked" AuNP **47** recorded over 96 h. The fluorescence intensity is not expected to increase for this sample; however, the minimal release

of emissive molecules may be due to the incomplete hydrolysis of AuNP **45b** and/or the dissociation of entire thiol ligands from unwanted place exchange reactions. All samples were run in 0.2M PBS (pH = 7.4) with excitation (left) and emission (right) wavelengths at 564 nm and 585 nm, respectively.

The predicted, gradual increase of fluorescence was qualitatively and quantitively observed upon the addition of GSH in PBS to the AuNP sample, which corresponds to a greater concentration of free emissive dye, unbound from the nanoparticle interface. The fluorescence intensity was roughly quadrupled in 4 days of payload release. Although the release may appear steady overtime, it was seen that there was a gradual decrease in the fluorescence intensity difference between later aliquots within the timespan of this experiment. Another facet of this multi-functional molecular system is the ability to "lock" the maleimide groups on the AuNPs to prevent the GSH-mediated release of its cargo. The "locked" adduct can be formed via hydrolysis of the maleimide ring on the "unlocked" adduct with 0.5 M NaOH(aq.) at r.t. (Scheme 17). The resulting ring openings of the maleimides block the retro-Michael additions with GSH, leading to the retention of the nanoparticles' covalently bound, emissive groups. After AuNP **45b** was hydrolyzed to AuNP **47**, the particles were subjected to the GSH-mediated release conditions for 5 days. The reaction progress was monitored with fluorescence spectroscopy, depicted on the previous page (Figure 8).
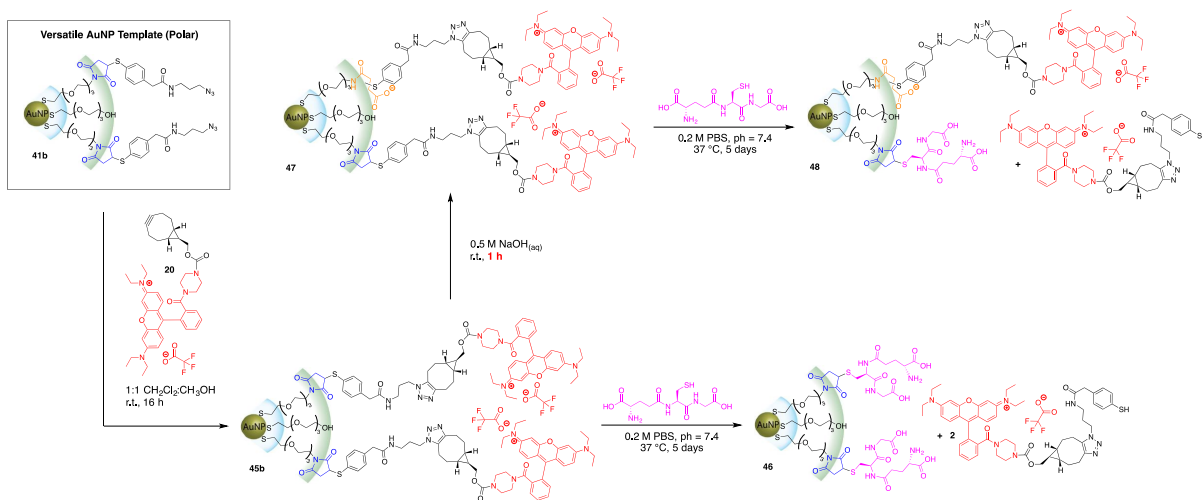
Scheme 17: Reaction schemes describing to the synthesis of "unlocked" AuNPs **45b** and "locked" AuNPs **47** and the corresponding release experiments with GSH under physiological conditions to yield AuNPs **46** and **48**, respectively.

The fluorescence data of the "locked" adduct **47** suggests there was partial release of the fluorophores bound to the nanoparticle interface. There are two hypotheses to explain this result, the incomplete hydrolysis of AuNP **45b** and/or the dissociation of entire thiol ligands from unwanted place exchange reactions. The hydrolysis of AuNP **47** with 0.5 M NaOH$_{(aq.)}$ was only reacted for an hour, which may not have completely locked each of the maleimide rings, leading to accessible sites for GSH-mediated release of the MPA bound rhodamine B groups (Scheme 17). Place exchange reactions between GSH and the thiol ligands bound to the gold core are also possible, although unlikely due to the densely packed AuNP cores. In the chance that a rhodamine B terminated thiol is dissociated from the particles, an increase in fluorescence intensity may be detected. When comparing the fluorescence data for both the "locked" and "unlocked" adducts, it can be observed that the "locked" adduct displays a drastic decrease in fluorescence counts. In conclusion, the release of emissive cargo off both AuNPs **45b** and **47** was monitored via fluorescence spectroscopy, resulting in gradual release for the "unlocked" AuNPs and blocked the release for the "locked" adduct.

3.4   AuNP Synthesis & Interfacial Modifications Experimental

3.4.1   Materials and Methods

All reagents, unless otherwise stated, were purchased from Sigma-Aldrich and used as received. All common solvents, triethylamine (Et_3N), and trifluoroacetic acid (TFA) were purchased from Caledon. Ethanol (EtOH) was purchased from Commercial Alcohols. Dialysis membranes (MWCO 6000-8000 Da) were purchased from Spectra/Por. Glutathione was purchased from Alfa Aesar. ^1H and $^{13}C\{^1H\}$ NMR spectra were recorded on Varian INOVA 400 (or 600) or Bruker AvIII HD 400 spectrometers using $CDCl_3$, CD_2Cl_2 or CD_3OD as solvent. ^1H NMR spectra that were recorded in $CDCl_3$ were referenced against residual protonated solvent at 7.27 ppm. ^{13}C NMR spectra that were run in $CDCl_3$ were referenced to 77.00 ppm. NMR spectra are reported as follows: s (singlet), d (doublet), t (triplet), q (quartet), dd (doublet of doublets), dt (doublet of triplets), tt (triplet of triplets), m (multiplet), bs (broad signal). Coupling constants are reported as J values in Hertz (Hz). The number of protons for a given resonance is indicated as nH and is based on spectral integration values. FT-IR spectra were recorded using an attenuated total reflectance (ATR) attachment using a Bruker Vector 33 FT-IR spectrometer and using standard quartz cells (1 cm path length) with a scan range of 200 to 800 nm. Ultraviolet (UV)-visible spectra were recorded using a Varian Cary 300 Bio spectrometer. ESI MS spectra were recorded on a Micromass LCT mass spectrometer. Photolysis were conducted in a Luzchem LZC-4V photoreactor equipped with 14 UVA (350 nm) 8-watt lamps.

Fluorescence spectroscopic studies were performed on a Photon Technology International (PTI) fluorimeter. Cyclic voltammetry of the AuNP samples were performed to probe the electrochemical features throughout the time release of ferrocene. A three-electrode system was used with a glassy carbon working electrode and two platinum wires which served as the counter and reference electrode. The AuNPs were dissolved at 3.13 mg/mL in anhydrous DCM and further purged with argon gas for 10 minutes. Tetrabutylammonium perchlorate (TBAP) was added into the electrochemical cell as the supporting electrolyte. All potentials are calibrated by an internal ferrocene standard taken at 0.424 V vs SCE.[60-61]

3.4.2 Preparation and Characterization of Compounds (37 – 48)

3.4.2.1 Compounds 37 – 41
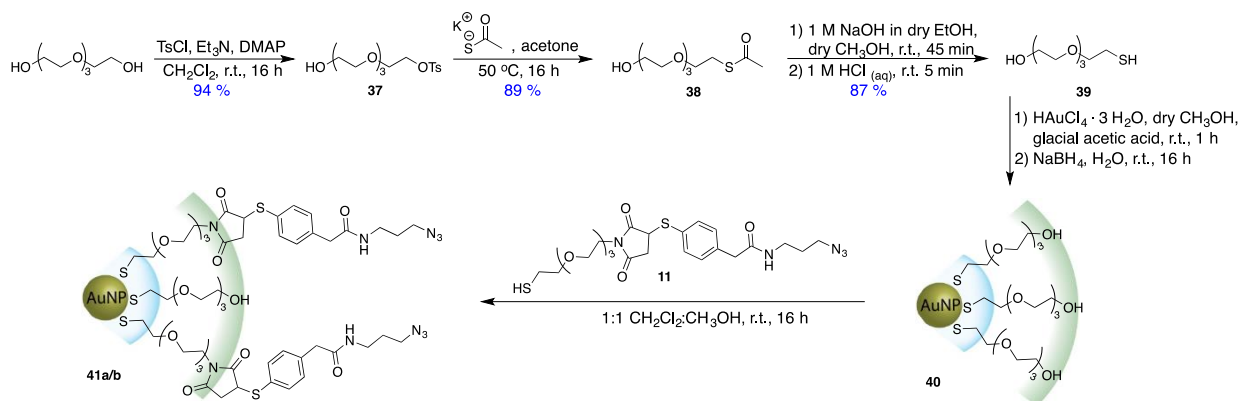
Synthesis of Compound 37:

To a flask containing tetraethylene glycol (26.0 g, 134 mmol) was added tosyl chloride (2.55 g, 13.4 mmol), Et$_3$N (2.80 mL, 20.1 mmol), DMAP (0.122 g, 2.68 mmol), and CH$_2$Cl$_2$ (400 mL). The flask was stirred at r.t. for 16 h. The crude product was extracted with H$_2$O (3 x 200 mL) and brine (50 mL), dried with MgSO$_4$, and filtered using gravity filtration. After, the solvent was removed using rotary evaporation and the crude product was purified by column chromatography on silica gel using EtOAc as the eluent to afford compound **37** as a pale-yellow oil (4.38 g, 94%). ^{1}H NMR (CDCl$_3$, 400 MHz): δ 7.79 – 7.76 (m, 2H), 7.34 – 7.30 (m, 2H), 4.17 – 4.12 (m, 2H), 3.71 – 3.55 (m, 14H), 2.44 (bs, 1H), 2.43 (s, 3H). The ^{1}H NMR spectrum corresponded with the literature.[59]

Synthesis of Compound 38:

To a flask containing compound **37** (9.25 g, 26.5 mmol) was added potassium thioacetate (2.94 g, 34.5 mmol) and acetone (400 mL). The flask was stirred at 50 °C for 16 h. The crude product was extracted with CH$_2$Cl$_2$ (3 x 100 mL) and brine (50 mL), dried with MgSO$_4$, and filtered using gravity filtration. After, the solvent was removed using rotary evaporation and the crude product was purified by column chromatography on silica gel using EtOAc as the eluent to afford compound **38** as a bright yellow oil (5.96 g, 89%).

^{1}H NMR (CDCl$_3$, 400 MHz): δ 3.75 – 3.57 (m, 14H), 3.10 (t, J = 7 Hz, 2H), 2.33 (s, 3H). The ^{1}H NMR spectrum corresponded with the literature.[59]

Synthesis of Compound 39:

To a flask containing compound **38** (5.90 g, 23.4 mmol) was added CH$_3$OH (150 mL) and the flask was stirred at r.t. while purging with Ar$_{(g)}$ for 15 min. In a separate flask, 1M NaOH in EtOH (50 mL) was also stirred at r.t. while purging with Ar$_{(g)}$ for 15 min. Then, the NaOH solution was added to the flask with compound **38** and the solution was stirred at r.t. for 45 min. Meanwhile, 1M HCl in H$_2$O (120 mL) was stirred r.t. while purging with Ar$_{(g)}$ for 15 min. After 20 min of the 45 min had passed, the HCl solution was added to the reaction flask and the mixture was stirred for an additional 5 min. The crude product was extracted with CH$_2$Cl$_2$ (3 x 100 mL), dried with MgSO$_4$, and filtered using gravity filtration. After, the solvent was removed using rotary evaporation and the crude product was quickly purified by column chromatography on silica gel using EtOAc as the eluent. The product is a thiol, which are prone to disulfide formation in the presence of O$_2$ $_{(g)}$. Therefore, the column must be run quickly and with Ar$_{(g)}$ purged eluent to afford compound **39** as a bright yellow oil (4.28 g, 87%). The product was stored in a vial purged with Ar$_{(g)}$ in the freezer. ^{1}H NMR (CDCl$_3$, 400 MHz): δ 3.78 – 3.58 (m, 16H), 2.71 (dt, J = 10 Hz, J = 12 Hz, 2H), 1.94 (bs, 2H), 1.62 (t, J = 12 Hz, 3H). The ^{1}H NMR spectrum corresponded with the literature.[59]

Synthesis of Compound 40:

To a flask containing HAuCl$_4$ · 3H$_2$O (1.46 g, 3.70 mmol) was added a mixture of dry CH$_3$OH (503 mL) and glacial acetic acid (83 mL). Next, compound **39** (2.30 g, 11.0 mmol) was added to the flask. The solution was stirred at r.t. for 1 h. A solution of NaBH$_4$ (1.40 g, 37.0 mmol) in H$_2$O (96 mL) was added dropwise to the reaction mixture while stirring. The mixture turned dark brown immediately. The flask was stirred at r.t. for 16 h and the solvent was removed using rotary evaporation. The resulting film of AuNPs was washed with toluene (30 mL) and the film was remade by dissolving the AuNPs in CH$_3$OH (20 mL) followed by rotary evaporation to remove the solvent. This washing procedure was repeated 6 times. Next, the crude AuNPs were dissolved in H$_2$O and centrifuged at

6000 rpm for 10 min to remove insoluble solid impurities. The crude AuNPs were then further purified by overnight dialysis. ^{1}H NMR (CDCl$_3$, 400 MHz): δ 4.17 – 2.87 (m, 16H). FT-IR (ATR, ν, cm^{-1}): 3309, 1738, 1637, 1635, 1616, 1559, 1456, 1366, 1229, 1217, 1092, 516. The ^{1}H NMR spectrum corresponded with the literature.[59]
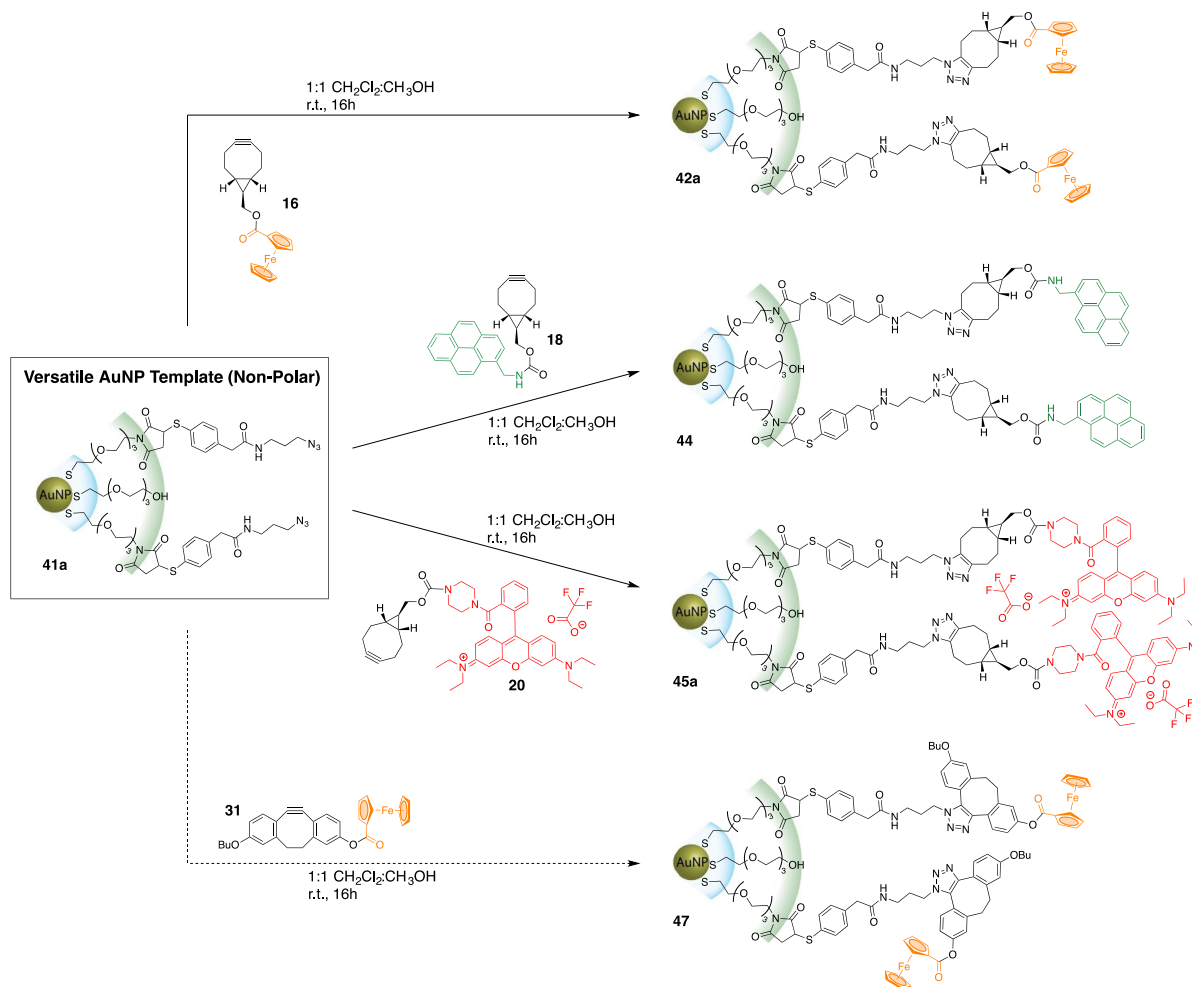
Synthesis of Compound 41a (Nonpolar):

To a flask containing compound **11** (0.0400 g, 0.0741 mmol) was added 1:1 dry CH$_2$Cl$_2$: dry CH$_3$OH (4 mL) and the flask was purged with Ar$_{(g)}$ for 15 mins. Then, compound **40** (0.0400 g) in dry CH$_3$OH (5 mL) was added to the reaction flask and stirred at r.t. for 16 h. After, solvents were removed by rotary evaporation to deposit a film of AuNPs inside a 100 mL round bottom flask. This film was washed with Et$_2$O (30 mL) and the AuNP film was remade by dissolving in CH$_2$Cl$_2$ followed by rotary evaporation. This washing procedure was repeated 5 times and the crude AuNPs were dissolved in CH$_2$Cl$_2$ (10 mL) and centrifuged at 6000 rpm for 10 min to remove insoluble solid impurities. The AuNPs were further purified by overnight dialysis to afford compound **41a** as a dark brown film (0.055 g). ^{1}H NMR (CDCl$_3$, 400 MHz): δ 7.54 – 7.42 (m, 2H), 7.27 – 7.19 (m, 2H), 4.13 – 4.02 (m, 1H), 3.85 – 3.48 (m, 22H), 3.35 – 3.24 (m, 4H), 3.24 – 3.10 (m, 1H), 2.71 – 2.58 (m, 1H), 2.13 – 1.90 (bs, 3H), 1.81 – 1.67 (m, 2H). FT-IR (ATR, ν, cm^{-1}): 3383, 3030, 2924, 2900, 2370, 2096, 1776, 1703, 1699, 1684, 1656, 1652, 1645, 1635, 1559, 1494, 1436, 1398, 1366, 1350, 1277, 1231, 1217, 1199, 1095, 517.

Synthesis of Compound 41b (Polar):

To a flask containing compound **11** (0.0100 g, 0.0185 mmol) was added 1:1 dry CH$_2$Cl$_2$: dry CH$_3$OH (4 mL) and the flask was purged with Ar$_{(g)}$ for 15 mins. Then, compound **40** (0.0600 g) in dry CH$_3$OH (5 mL) was added to the reaction flask and stirred at r.t. for 16 h. After, solvents were removed by rotary evaporation to deposit a film of AuNPs inside a 100 mL round bottom flask. This film was washed with Et$_2$O (30 mL) and the AuNP film was remade by dissolving in CH$_3$OH followed by rotary evaporation. This washing procedure was repeated 5 times and the crude AuNPs were dissolved in CH$_3$OH (10 mL) and centrifuged at 6000 rpm for 10 min to remove insoluble solid impurities. The AuNPs were further purified by overnight dialysis to afford compound **41b** as a dark brown

film (0.050 g). The ^{1}H NMR spectrum for this compound only cleanly shows the tetraethylene signals due to the drastic difference in proton integrations of this multiplet to all the other signals. The spectrum should have the same chemical shifts and multiplicity as the ^{1}H NMR spectrum of compound **41a**, but different integrations.

3.4.2.2   Compounds 42 – 48
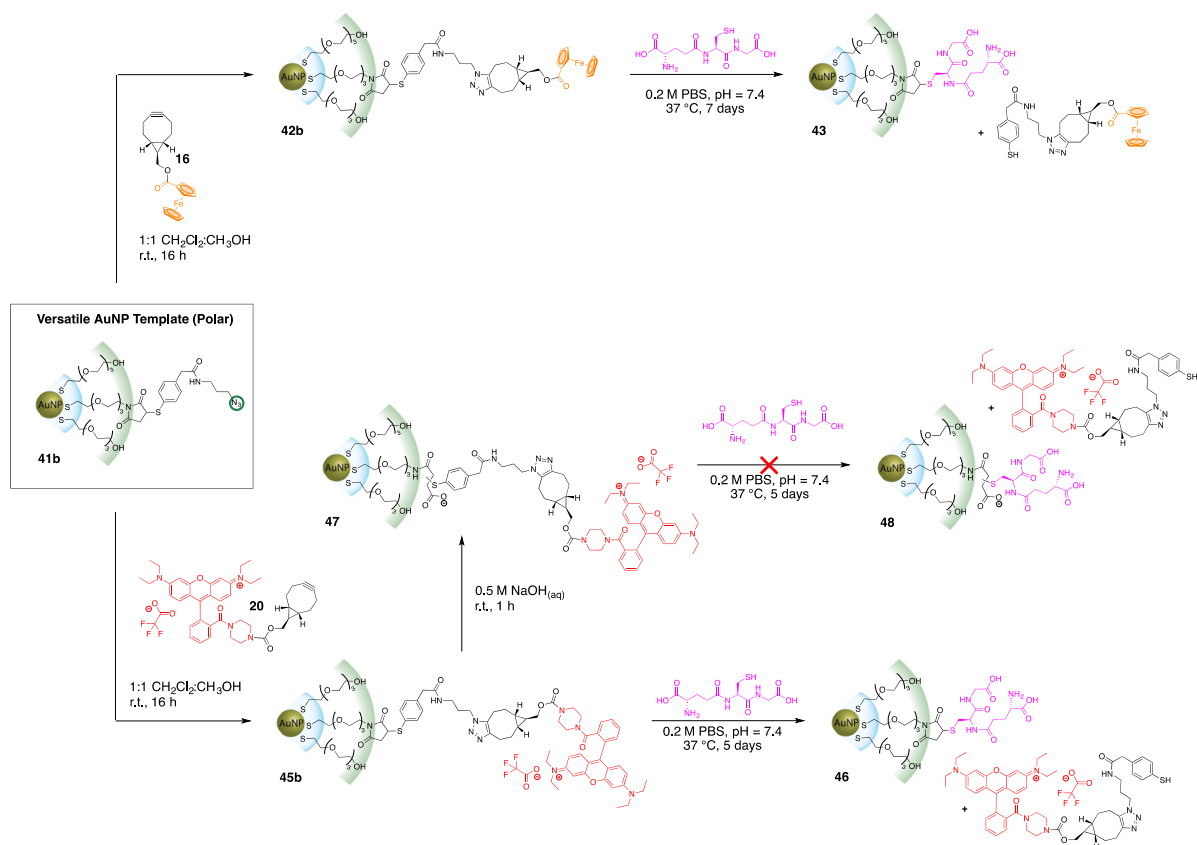
Synthesis of Compound 42a (Nonpolar):

To a flask containing compound **16** (0.0150 g, 0.0397 mmol) was added 1:1 CH$_2$Cl$_2$:CH$_3$OH (4 mL) and the flask was stirred at r.t. for 15 mins. Then, compound **41a** (0.0100 g) in CH$_3$OH (5 mL) was added to the reaction flask and stirred at r.t. for 16 h. After, solvents were removed by rotary evaporation to deposit a film of AuNPs inside a 50 mL round bottom flask. This film was washed with Et$_2$O (30 mL) and a mixture of 1:1 CH$_3$OH: hexanes (30 mL) and the AuNP film was remade by dissolving in CH$_2$Cl$_2$ followed by rotary evaporation. This washing procedure was repeated 5 times and the crude AuNPs were dissolved in CH$_2$Cl$_2$ (10 mL) and centrifuged at 6000 rpm for 10 min to remove insoluble solid impurities. The AuNPs were further purified by overnight dialysis to afford compound **42a** as a yellowish-brown film (0.0130 g). ^{1}H NMR (CDCl$_3$, 400 MHz): δ 7.52 – 7.34 (m, 2H), 7.31 – 7.21 (m, 2H), 4.81 (bs, 2H), 4.40 (bs, 2H), 4.36 – 4.16 (m, 7H), 4.15 – 4.03 (m, 1H), 3.92 – 3.43 (m, 23H), 3.24 – 3.08 (m, 4H), 3.05 – 2.84 (m, 1H), 2.73 – 2.58 (m, 1H), 2.39 – 2.21 (m, 2H), 2.06 – 1.91 (m, 2H), 1.72 – 1.55 (m, 2H),

1.45 – 1.31 (m, 1H), 1.21 – 0.97 (m, 2H). FT-IR (ATR, ν, cm^{-1}): 3308, 1738, 1652, 1635, 1616, 1559, 1539, 1506, 1456, 1366, 1229, 1217, 1092, 585.

Synthesis of Compound 42b (Polar):

To a flask containing compound **16** (0.0050 g, 0.0106 mmol) was added CH$_3$OH (4 mL) and the flask was stirred at r.t. for 15 mins. Then, compound **41b** (0.0250 g) in CH$_3$OH (5 mL) was added to the reaction flask and stirred at r.t. for 16 h. After, solvents were removed by rotary evaporation to deposit a film of AuNPs inside a 50 mL round bottom flask. This film was washed with Et$_2$O (30 mL) and CH$_2$Cl$_2$ (30 mL) and the AuNP film was remade by dissolving in CH$_3$OH followed by rotary evaporation. This washing procedure was repeated 5 times and the crude AuNPs were dissolved in CH$_3$OH (10 mL) and centrifuged at 6000 rpm for 10 min to remove insoluble solid impurities. The AuNPs were further purified by overnight dialysis to afford compound **42b** as a yellowish-brown film (0.0250 g). The ^{1}H NMR spectrum for this compound only cleanly shows the tetraethylene signals due to the drastic difference in proton integrations of this multiplet to all the other signals. The spectrum should have the same chemical shifts and multiplicity as the ^{1}H NMR spectrum of compound **42a**, but different integrations.

Synthesis of Compound 43 (Polar):

To a flask containing compound **42b** (0.040 g) dissolved in 0.2M PBS (890 µL) was added a glutathione solution (0.00614 g in 56 µL of 0.2M PBS) and the flask was stirred at 37 °C for 7 days. The crude reaction mixture was extracted with a 1:1 mixture of CH$_2$Cl$_2$: hexanes (5 x 2 mL) and the excess solvent was removed by rotary evaporation to deposit a film of AuNPs inside the flask. This film was then washed with Et$_2$O (30 mL) and a mixture of 1:1 CH$_3$OH: hexanes and the AuNP film was remade by dissolving in CH$_2$Cl$_2$ followed by rotary evaporation. This washing procedure was repeated 5 times and the crude AuNPs was dissolved in CH$_3$OH and centrifuged at 6000 rpm for 10 min to remove insoluble solid impurities. The AuNPs were then be further purified by overnight dialysis. The purified sample was dried to afford compound **43** (0.0090 g) as a dark brown film. The ^{1}H NMR spectrum for this compound only cleanly shows the tetraethylene

signals due to the drastic difference in proton integrations of this multiplet to all the other signals. Compound **43** was characterized using cyclic voltammetry.

Synthesis of Compound 44 (Nonpolar):

To a flask containing compound **41a** (0.010 g) was be added 1:1 CH_2Cl_2:CH_3OH (4 mL) and the flask was stirred at r.t. for 15 mins. Then, compound **18** (0.015 g, 0.0368 mmol) in CH_2Cl_2 (5 mL) was added to the reaction flask and was stirred at r.t. for 16 h. After, the solvent mixture was removed by rotary evaporation to deposit a film of AuNPs inside a 50 mL round bottom flask. This film was washed with Et_2O (30 mL) and a mixture of 1:1 CH_3OH: hexanes (30 mL) and the AuNP film was remade by dissolving in CH_2Cl_2 followed by rotary evaporation. This washing procedure was repeated 5 times and the crude AuNPs were dissolved in CH_2Cl_2 (10 mL) and centrifuged at 6000 rpm for 10 min to remove insoluble solid impurities. The AuNPs were then further purified by overnight dialysis to afford compound **44** (0.0140 g) as a dark brown film. ^1H NMR ($CDCl_3$, 400 MHz): δ 8.33 – 8.26 (m, 1H), 8.25 – 8.19 (m, 2H), 8.19 – 8.12 (m, 2H), 8.11 – 7.96 (m, 4H), 7.56 – 7.40 (bs, 2H), 7.29 – 7.19 (bs, 12H), 6.48 – 5.89 (m, 7H), 5.81 (bs, 1H), 5.21 (bs, 1H), 5.13 – 5.05 (m, 2H), 4.27 – 4.03 (m, 10H), 4.03 – 3.37 (m, 2H), 2.06 – 1.91 (m, 111H), 3.37 – 3.23 (m, 20H), 3.23 – 2.97 (m, 14H), 2.94 – 2.75 (m, 6H), 2.73 – 2.50 (m, 8H), 2.19 (bs, 3H), 1.99 – 1.45 (m, 30H), 1.09 – 0.91 (m, 3H).

Synthesis of Compound 45a (Nonpolar):

To a flask containing compound **20** (0.0150 g, 0.0187 mmol) was added 1:1 CH_2Cl_2:CH_3OH (4 mL) and the flask was stirred at r.t. for 15 mins. Then, compound **41a** (0.0100 g) in CH_3OH (5 mL) was be added to the reaction flask and stirred at r.t. for 16 h. After, excess solvents were removed by rotary evaporation to deposit a film of AuNPs inside a 50 mL round bottom flask. This film was washed with Et_2O (30 mL) and a mixture of 1:1 CH_3OH: hexanes (30 mL) and the AuNP film was remade by dissolving in CH_2Cl_2 followed by rotary evaporation. This washing procedure was repeated 5 times and the crude AuNPs were dissolved in CH_2Cl_2 (10 mL) and centrifuged at 6000 rpm for 10 min to remove insoluble solid impurities. The AuNPs were further purified by dialysis for 3 days to afford compound **45a** (0.0150 g) as a pinkish-brown film. ^1H NMR ($CDCl_3$, 400 MHz):

δ 7.70 – 7.56 (m, 3H), 7.56 – 7.45 (m, 2H), 7.33 – 7.23 (m, 3H), 7.20 – 7.09 (m, 2H), 6.90 – 6.76 (m, 2H), 6.76 – 6.64 (m, 2H), 5.24 – 5.20 (m, 3H), 4.28 – 3.88 (m, 6H), 3.80 – 2.36 (m, 75H), 2.27 – 1.79 (m, 8H), 1.59 – 1.30 (m, 4H), 1.30 – 0.53 (m, 24H). UV-Vis in PBS (λ_{max} = 335, 532, 567 nm).

Synthesis of Compound 45b (Polar):

To a flask containing compound **20** (0.00667 g, 0.008324 mmol) was added 1:1 CH_2Cl_2:CH_3OH (4 mL) and the flask was stirred at r.t. for 15 mins. Then, compound **41b** (0.0200 g) in CH_3OH (5 mL) was be added to the reaction flask and stirred at r.t. for 16 h. After, excess solvents were removed by rotary evaporation to deposit a film of AuNPs inside a 50 mL round bottom flask. This film was washed with a mixture of 1:1 CH_2Cl_2: hexanes (30 mL) and the AuNP film was remade by dissolving in CH_3OH followed by rotary evaporation. This washing procedure was repeated 5 times and the crude AuNPs were dissolved in CH_3OH (10 mL) and centrifuged at 6000 rpm for 10 min to remove insoluble solid impurities. The AuNPs were further purified by dialysis for 3 days to afford compound **45b** (0.0225 g) as a pinkish-brown film. UV-Vis in PBS (λ_{max} = 335, 532, 567 nm). The ^{1}H NMR spectrum for this compound only cleanly shows the tetraethylene signals due to the drastic difference in proton integrations of this multiplet to all the other signals. The spectrum should have the same chemical shifts and multiplicity as the ^{1}H NMR spectrum of compound **45a**, but different integrations.

Synthesis of Compound 46 (Polar):

To a flask containing compound **45b** (0.0090 g) was added 0.2M PBS (460 µL) and the flask was sonicated to fully dissolve the AuNPs. A glutathione solution (0.00154 g in 50 µL of 0.2M PBS) was added to the flask and it was stirred at 37 °C for 5 days. Aliquots (10 µL) were taken from the reaction flask after 0 h, 6 h, 12 h, 24 h, 48 h, and 96 h to monitor the release of the fluorescent cargo using fluorescence spectroscopy. Each aliquot was diluted to 10 mL with 0.2M PBS before recording the fluorescence excitation (λ_{ex} = 564 nm) and emission spectra (λ_{em} = 585 nm). Each sample of compound **46** will have different ratios of ligands on the surfaces of the AuNPs dependent on the time at which the aliquot was taken. UV-Vis in PBS (λ_{max} = 335, 532, 567 nm). The ^{1}H NMR spectrum for

this compound only cleanly shows the tetraethylene signals due to the drastic difference in proton integrations of this multiplet to all the other signals.

Synthesis of Compound 47 (Polar):

To a flask containing compound **45b** (0.0066 g) was be added an aqueous 0.5M NaOH solution (1.65 mL) and the flask was stirred at r.t. for 1 h. The crude AuNP solution was then purified by overnight dialysis. The excess H_2O was removed and the resulting AuNPs were dissolved in CH_3OH (7 mL) and centrifuged at 6000 rpm for 10 min to remove insoluble solid impurities and afford compound **47** (0.0050 g) as a pinkish-brown film. UV-Vis in PBS (λ_{max} = 335, 532, 567 nm). The ^{1}H NMR spectrum for this compound only cleanly shows the tetraethylene signals due to the drastic difference in proton integrations of this multiplet to all the other signals.

Synthesis of Compound 48 (Polar):

To a flask containing compound **47** (0.0050 g) was added 0.2M PBS (230 µL) and the flask was sonicated to fully dissolve the AuNPs. A glutathione solution (0.0077 g in 25 µL of 0.2M PBS) was added to the flask and it was stirred at 37 °C for 5 days. Aliquots (10 µL) were taken from the reaction flask after 0 h, 6 h, 12 h, 24 h, 48 h, and 96 h to monitor the release of the fluorescent cargo using fluorescence spectroscopy. Each aliquot was diluted to 10 mL with 0.2M PBS before recording the fluorescence excitation (λ_{ex} = 564 nm) and emission spectra (λ_{em} = 585 nm). Each sample of compound **48** will have different ratios of ligands on the surfaces of the AuNPs dependent on the time at which the aliquot was taken. UV-Vis in PBS (λ_{max} = 335, 532, 567 nm). The ^{1}H NMR spectrum for this compound only cleanly shows the tetraethylene signals due to the drastic difference in proton integrations of this multiplet to all the other signals.

4   Conclusions & Future Work

4.1   Conclusions

Previously, work from our group demonstrated the use of bioorthogonal click reactions on maleimide-terminated AuNPs. It was shown that in the presence of GSH, MPA can undergo a retro-Michael addition when bound to a maleimide under physiological conditions. The release of a fluorescent dye directly bound the carboxylic acid group of MPA was studied and the molecular system showed promise for a new multifaceted, functional system on nanomaterial surfaces. This thesis expanded upon this work by incorporating 3-azido-1-propanamine onto the carboxylic acid group of MPA yielding an amide linked to an azide. The modified MPA acted as a Michael donor to combine with maleimides while, the azide introduced an array of functionalization through SPAACs with strained alkynes attached to the desired cargoes.

In Chapter 2, all the small molecules required for the project were synthesized. A single azide terminated thiol ligand **11** was designed capable of reversible functionalization of AuNPs via Michael additions, SPAACs, and GSH-mediated releases. This ligand did not require an interfacial, retro-Diels Alder reaction to afford the reactive AuNP template, circumventing the loss of particles due to aggregation at high temperatures seen in the previous work from our group. Four different strained alkyne cargo were also made to introduce functionality onto the azide nanoparticles via SPAACs. Compounds **16** and **31** were chosen because they contain ferrocene groups; redox active moieties that can be monitored using cyclic voltammetry during the release experiment. Compounds **18** and **20** were picked for their emissive properties, that was tracked by utilizing fluorescence spectroscopy. In addition, the strained alkyne present in compounds **16**, **18**, and **20** was BCN, while compound **31** incorporated DIBO instead to depict the versatility of this system. This section also included test reactions to determine the reaction conditions of the SPAACs with compound **32** and to characterize the clicked products with ^{1}H NMR spectroscopy to compare with their analogous AuNP counterparts in Chapter 3.

In Chapter 3, two versions of the versatile, azide terminated AuNP template were synthesized. AuNPs **41a** were more organic soluble and were used to characterize the

nanoparticles with ^{1}H NMR spectroscopy, while AuNPs **41b** were soluble in PBS buffer and were used in the glutathione release experiments. In the electrochemical studies, the redox active moieties were successfully released off from the surface of the Fc terminated AuNPs **42b** under physiological conditions and determined that almost all the releasable groups are displaced by GSH in a week using cyclic voltammetry. In the fluorescence experiments, the release of emissive cargo off both AuNPs **45b** and **47** was monitored via fluorescence spectroscopy, resulting in gradual release for the "unlocked" AuNPs and blocked the release for the "locked" adduct.

Therefore, the incorporation of bioorthogonal click reactions to develop a multi-functional nanomaterial template was demonstrated, which can be loaded with various, functional cargo through SPAACs with strained alkynes. The system utilized thiol-Michael additions with an azide modified MPA derivative to reversibly functionalize the interface of the AuNPs. Consequently, a single nanomaterial that can undergo an assortment of functionalization with strained alkyne derivatives was synthesized, then the controlled release of desired functionalities was demonstrated in biotic environments using GSH in PBS. The slow release of the molecules generated a molecular system capable of participating in a wide scope of applications. Some of the potential applications include bio-labeling, drug delivery systems, electrochemical catalysis, and more. By continuing to explore the physical and chemical properties of a system such as this, the synthetic toolbox of material sciences will be expanded.

4.2   Future Work

The future of this project involves completing the experiments that were deferred due to the COVID 19 pandemic, before submitting for publication. These experiments include the interfacial studies with the pyrene strained alkyne, and monitoring the release

of this neutral, planar fluorophore off the AuNPs via fluorescence spectroscopy. The photochemistry and reactivity of *hv*DIBO cargo with the AuNPs will be examined as well. Thermal gravimetric analysis (TGA) will also be performed to characterize the ligand distributions on the organic and water-soluble AuNPs and determine the ligand to gold core mass percent difference. This versatile, molecular system may be implemented onto several different nanomaterial architectures as well, such as carbon nanotubes.

Although I am finishing up my time at UWO for my MSc., I am returning to begin a cotutelle PhD program with UWO and the University of Bristol in January 2021. I was able to partially begin this work with the help of the Mitacs Globalink Research Award, which provided me with the opportunity to join the research group of Dr Pierangelo Gobbo at the School of Chemistry of the University of Bristol for three months in 2019. In my PhD, I will work to merge the field of functional nanomaterials with the field of bottom-up synthetic biology and focus on the generation of protocellular materials from AuNP-based colloidosome building blocks. We hope to develop the first inorganic protocellular materials that could be employed for applications in photothermal therapy, biosensing, and drug delivery.

References

1. Li, Z.; Barnes, J. C.; Bosoy, A.; Stoddart, J. F.; Zink, J. I. *Chem. Soc. Rev.* **2012**, *41*, 2590–2605.

2. Cheng, L.; Wang, C.; Feng, L.; Yang, K.; Liu, Z. *Chem. Rev.* **2014**, *114*, 10869–10939.

3. Gawande, M. B.; Goswami, A.; Felpin, F.-X.; Asefa, T.; Huang, X.; Silva, R.; Zou, X.; Zboril, R.; Varma, R. S. *Chem. Rev.* **2016**, *116*, 3722–3811.

4. Jain, P. K.; Huang, X.; El-Sayed, I. H.; El-Sayed, M. A. *Acc. Chem. Res.* **2008**, *41*, 1578–1586.

5. Dest, M. D. *Biochemistry* **2009**, *48*, 6571 – 6584.

6. Fihri, A.; Bouhrara, M.; Nekoueishahraki, B.; Basset, J.-M.; Polshettiwar, V. *Chem. Soc. Rev.* **2011**, *40*, 5181–5203.

7. Kolb, H. C.; Finn, M. G.; Sharpless, K. B. *Angew. Chem. Int. Ed.* **2001**, *40*, 2004 – 2021.

8. Hein, J. E.; Fokin, V. V. *Chem. Soc. Rev.* **2010**, *39*, 1302 – 1315.

9. Thirumurugan, P.; Matsosiuk, D.; Jozwiak, K. *Chem. Rev.* **2013**, *113*, 4905 – 4979.

10. Jewett, J. C.; Bertozzi, C. R. *Chem. Soc. Rev.* **2010**, *39*, 1272 – 1279.

11. Manova, R.; Van Beek, T. A.; Zuilhof, H. *Angew. Chem. Int. Ed.* **2011**, *50*, 5428 – 5430.

12. Nieves, D. J.; Azmi, N. S.; Xu, R.; Levy, R.; Yates, E. A.; Fernig, D. G. *Chem. Commun.* **2014**, *50*, 13157 – 13160.

13. Houseman, B. T.; Gawalt, E. S.; Mrksich, M. *Langmuir* **2003**, *19*, 1522 – 1531.

14. Li, Z.; Seo, T. S.; Ju, J. *Tetrahedron Lett.* **2004**, *45*, 3143 – 3146.b

15. Tornoe, C. W.; Christensen, C.; Meldal, M. *J. Org. Chem.* **2002**, *67*, 3057 – 3064.

16. Rostovtsev, V. V.; Green, L. G.; Fokin, V. V.; Sharpless, K. B. *Angew. Chem. Int. Ed.* **2002**, *41*, 2596 – 2599.

17. Lallana, E.; Riguera, R.; Fernandez-Megia, E. *Angew. Chem. Int. Ed.* **2011**, *50*, 8794 – 8804.

18. Li, S.; Cai, H.; He, J.; Chen, H.; Lam, S.; Cai, T.; Zhu, Z.; Bark, S. J.; Cai, C. *Bioconjugate Chem.* **2016**, *27*, 2315 – 2322.

19. Li, S.; Wang, L.; Yu, F.; Zhu, Z.; Shobaki, D.; Chen, H.; Wang, M.; Wang, J.; Qin,

G.; Erasquin, U. J.; Ren, L.; Wang, Y.; Cai, C. *Chem. Sci.* **2017**, *8*, 2107 – 2114.

20. Agard, N. J.; Prescher, J. A.; Bertozzi, C. R. *J. Am. Chem. Soc.* **2004**, *126*, 15046 – 15047.

21. Poloukhtine, A. A.; Mbua, N. E.; Wolfert, M. A.; Boons, G.-J.; Popik, V. V. *J. Am. Chem. Soc.* **2009**, *131*, 15769–15776.

22. Orski, S. V.; Poloukhtine, A. A.; Arumugam, S.; Mao, L.; Popik, V. V.; Locklin, J. *J. Am. Chem. Soc.* **2010**, *132*, 11024–11026.

23. Arumugam, S.; Orski, S. V.; Mbua, N. E.; McNitt, C.; Boons, G.-J.; Locklin, J.; Popik, V. V. *Pure Appl. Chem.* **2013**, *85*, 1499–1513.

24. Brooks, K.; Yatvin, J.; McNitt, C. D.; Reese, R. A.; Jung, C.; Popik, V. V.; Locklin, J. *Langmuir* **2016**, *32*, 6600–6605.

25. Verdaguer, X.; Moyano, A.; Pericàs, M. A.; Riera, A.; Alvarez-Larena, A.; Piniella, J.-F. *Organometallics* **1999**, *18*, 4275–4285.

26. Poloukhtine, A.; Popik, V. V. *J. Org. Chem.* **2003**, *68*, 7833–7840

27. McNitt, C. D.; Popik, V. V. *Org. Biomol. Chem.* **2012**, *10*, 8200–8202.

28. Prescher, J. A.; Bertozzi, C. R. *Nat. Chem. Biol.* **2005**, *1*, 13 – 21.

29. Patterson, D. M.; Nazarova, L. A.; Prescher, J. A. *ACS Chem. Biol.* **2014**, *9*, 592 – 605.

30. McKay, C. S.; Finn, M. G. *Chem. Biol.* **2014**, *21*, 1075 – 1101.

31. Sletten, E. M.; Bertozzi, C. R. *Angew. Chem. Int. Ed.* **2009**, *48*, 6974 – 6998.

32. Best, M. D. *Biochemistry* **2009**, *48*, 6571 – 6584.

33. Bräse, S.; Gil, C.; Knepper, K.; Zimmermann, V. *Angew. Chem. Int. Ed.* **2005**, *44*, 5188 –5240.

34. Scriven, E. F. V.; Turnbull, K. *Chem. Rev.* **1988**, *88*, 297 – 368.

35. Laughlin, S. T.; Baskin, J. M.; Amacher, S. L.; Bertozzi, C. R. *Science* **2008**, *320*, 664 –667.

36. Kumar, A.; Zhang, X.; Liang, X. *J. Biotechnol. Adv.* **2013**, *31*, 593 – 606.

37. Duncan, B.; Kim, C.; Rotello, V. M. *J. Control Release* **2010**, *148*, 122 – 127.

38. Balasubramanian, S. K.; Yang, L.; Yung, L. Y.; Ong, C. N.; Ong, W. Y.; Yu, L. E. *Biomaterials* **2010**, *31*, 9023 – 9030.

39. Burda, C.; Chen, X.; Narayanan, R.; El-Sayed, M. A. *Chem. Rev.* **2005**, *105*, 1025

– 1102.

40. Jin, Q.; Lin, C.; Chang, Y.; Yang, Y. *Langmuir.* **2018**, *34*, 1256 – 1265.

41. Wang, YQ.; Jin, Y. Y.; Chen, W.; Wang, JJ; Chen, H.; Sun, L.; Li, X.; Ji, J.; Yu, Q.; Shen, L. Y. Chin. *J. Chem. Eng.* **2018**, *358*, 74 – 90.

42. Han, W.; Wu, Z. N.; Li, Y.; Wang, Y. Y. Chin. *J. Chem. Eng.* **2018**, *358*, 1022 – 1037.

43. Gobbo, P.; Workentin, M. S. *Langmuir* **2012**, *28*, 12357 – 12363.

44. Ojea-Jimenez, I.; Puntes, V. *J. Am. Chem. Soc.* **2009**, *131*, 13320 – 13327.

45. Luo, W.; Gobbo, P.; Gunawardene, P. N.; Workentin, M. S. *Langmuir* **2017**, *33*, 1908 –1913.

46. Luo, W.; Gobbo, P.; McNitt, C. D.; Sutton, D. A.; Popik, V. V.; Workentin, M. S. *Chem. Eur. J.* **2017**, *23*, 1052 – 1059.

47. Gobbo, P.; Workentin, M. S. *Synlett* **2016**, *27*, 1919 – 1930.

48. Häkkinen, H. *Nat. Chem.* **2012**, *4*, 443 – 455.

49. Song, Y.; Murray, R. W. J. Am. Chem. Soc. **2002**, *124*, 7096 – 7102.

50. Hong, R.; Fernández, J. M.; Nakade, H.; Arvizo, R.; Emrick, T.; Rotello, V. M. *Chem. Commun.* **2006**, 2347 – 2349.

51. Weissman, M. R.; Winger, K. T.; Ghiassian, S.; Gobbo, P.; Workentin, M. S. *Bioconjugate Chem.* **2016**, *27*, 586 – 593.

52. Mori, T.; Hegmann, T. J. *Nanopart. Res.* **2016**, *18*, 295.

53. Zanchet, D.; Hall, B. D.; Ugarte, D. *J. Phys. Chem. B.* **2000**, *104*, 11013 – 11018.

54. Cui, J. B.; Jiang, R.; Guo, C.; Bai, X. L.; Xu, S. Y.; Wang, L. Y. *J. Am. Chem. Soc.* **2018**, *140*, 5890 – 5894.

55. Dommerholt, J.; Schmidt, S.; Temming, R.; Hendriks, L. J. A.; Rutjes, F. P. J. T.; van Hest, J. C. M.; Lefeber, D. J.; Friedl, P.; van Delft, F. L. *Angew. Chem. Int. Edit.* **2010**, *49*, 9422 –9425.

56. Gobbo, P.; Gunawardene, P.; Luo, W.; Workentin, M. S. *Synlett* **2015**, *26*, 1169 – 1174.

57. Arnold, R. M.; McNitt, C. D.; Popik, V. V.; Locklin, *J. Chem. Commun.* **2014**, *50*, 5307 – 5309.

58. Colangelo, E.; Comenge, J.; Paramelle, D.; Volk, M.; Chen, Q.; Lévy, R.

Bioconjugate Chem. **2017**, *28*, 11 – 22.

59. Luo, W.; Luo, J.; Popik, V. V.; Workentin, M. S. *Bioconjugate. Chem.* **2019**, *30*, 1140 – 1149.

60. Yuan, K.; Wang, X., Mellerup, S. K.; Wyman, I.; Schatte, G.; Ding, Z.; Wang, S. *Organometallics* **2016**, *35*, 3051 – 3059.

61. Stockman, T. J.; Ding, Z. *Can. J. Chem.* **2015**, *96*, 13 – 21.

62. Cannone, F.; Chirico, G.; Bizzarri, A. R.; Cannistraro, S. *J. Phys. Chem. B* **2006**, *110*, 16491 – 16498.

63. Nerambourg, N.; Werts, M. H. V.; Charlot, M.; Blanchard-Desce, M. *Langmuir* **2007**, *23*, 5563 – 5570.

Appendices

Appendix 1: Supporting Information for Chapter 2

A. Characterization of Compound 1
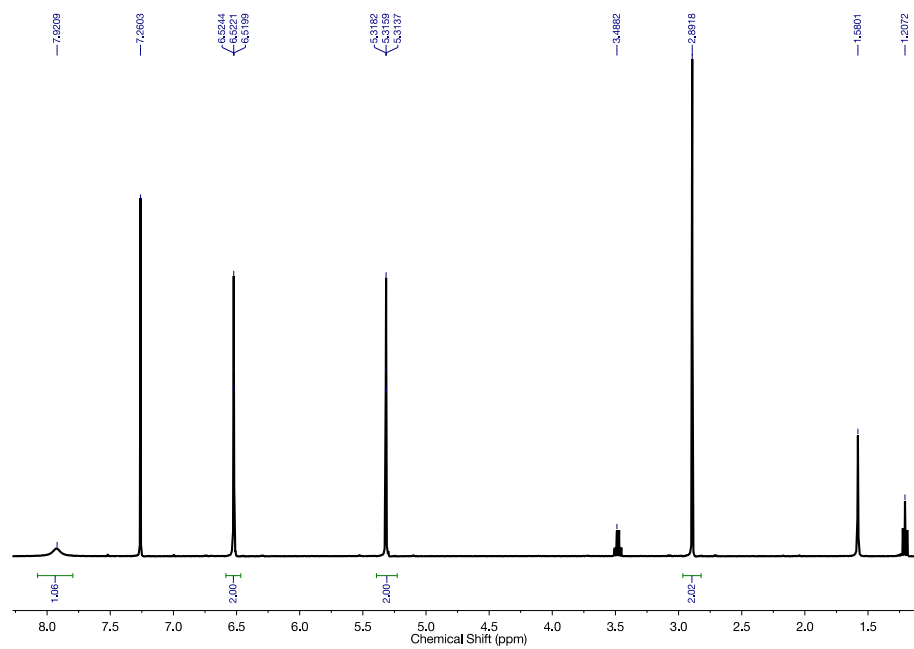
Figure A1: [^1]H NMR spectrum of compound **1**.
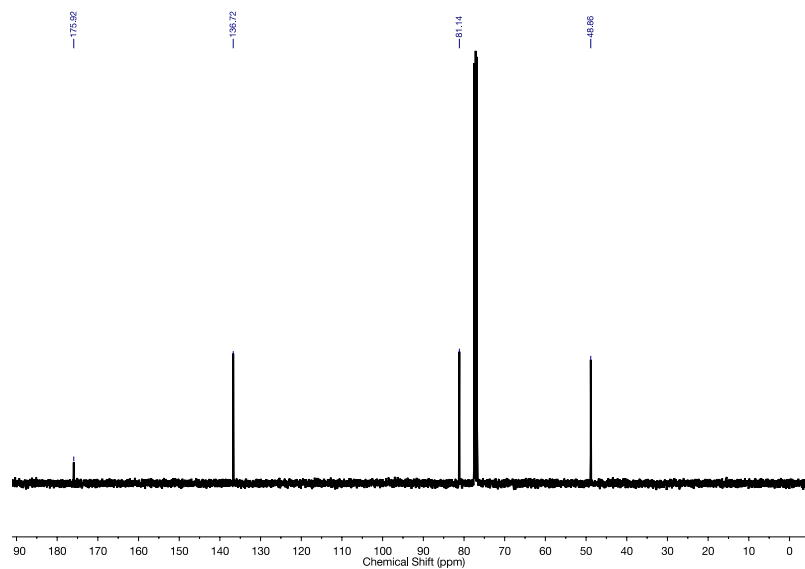
Figure A2: {[^1]H} [^13]C NMR spectrum of compound **1**.

B. **Characterization of Compound 3**
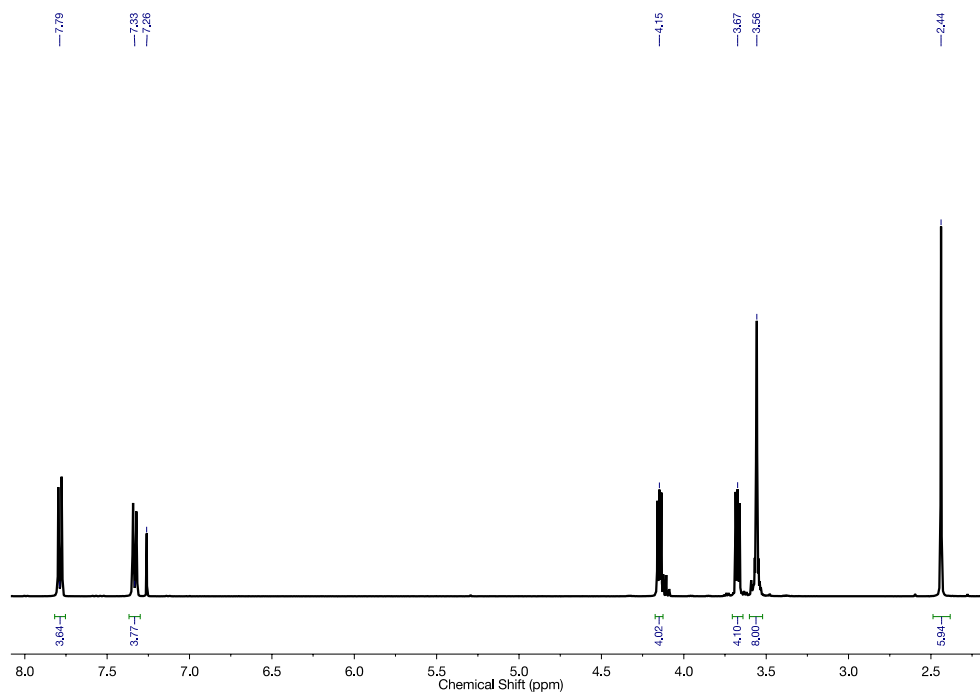
Figure B1: ^{1}H NMR spectrum of compound **3**.
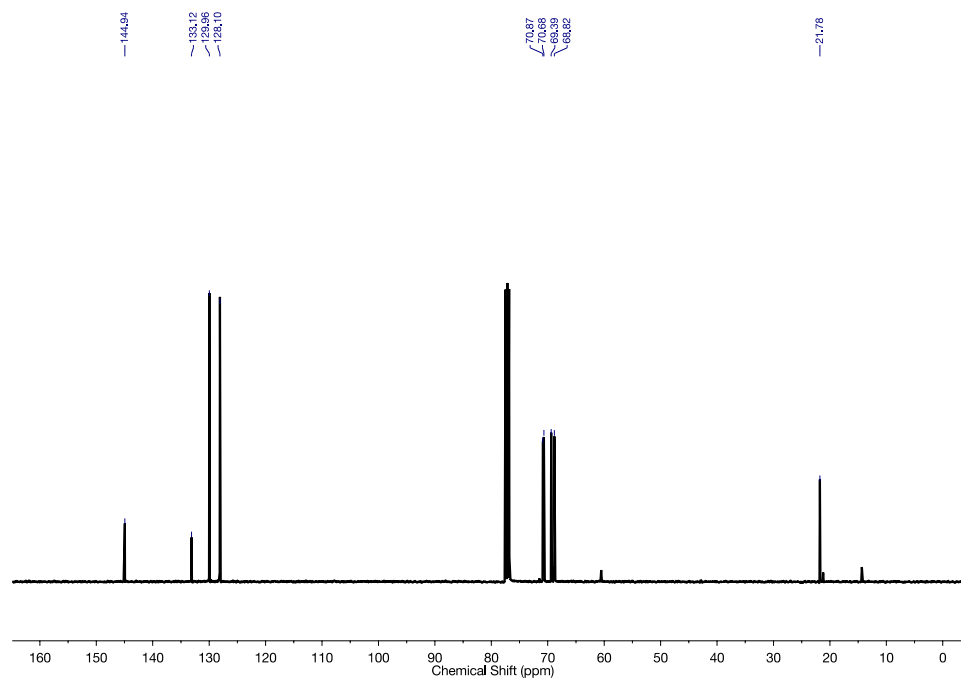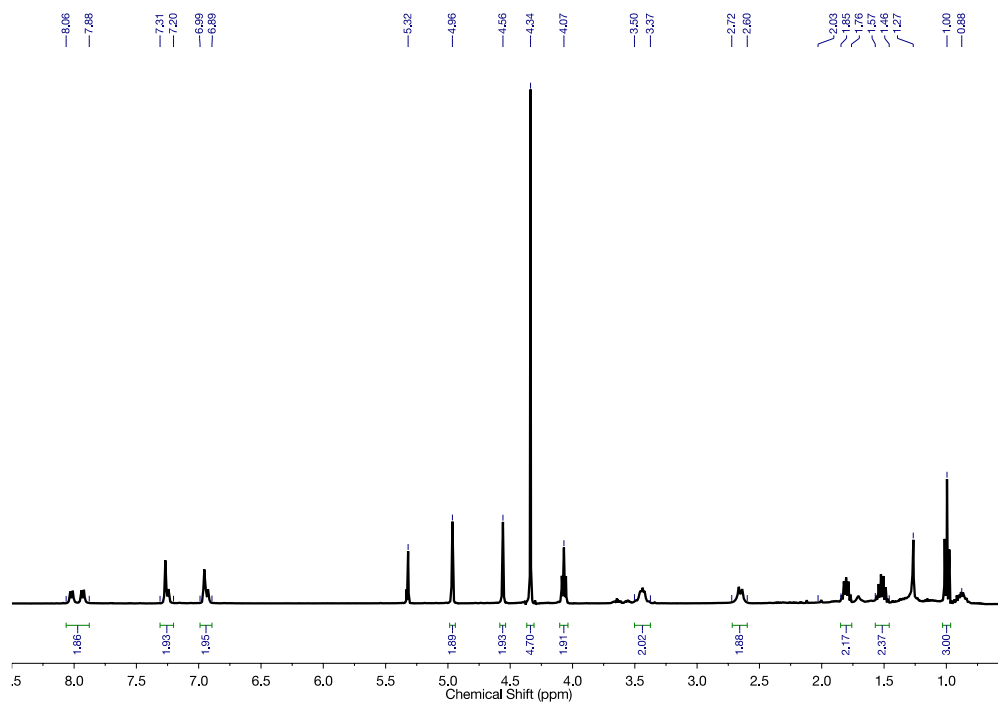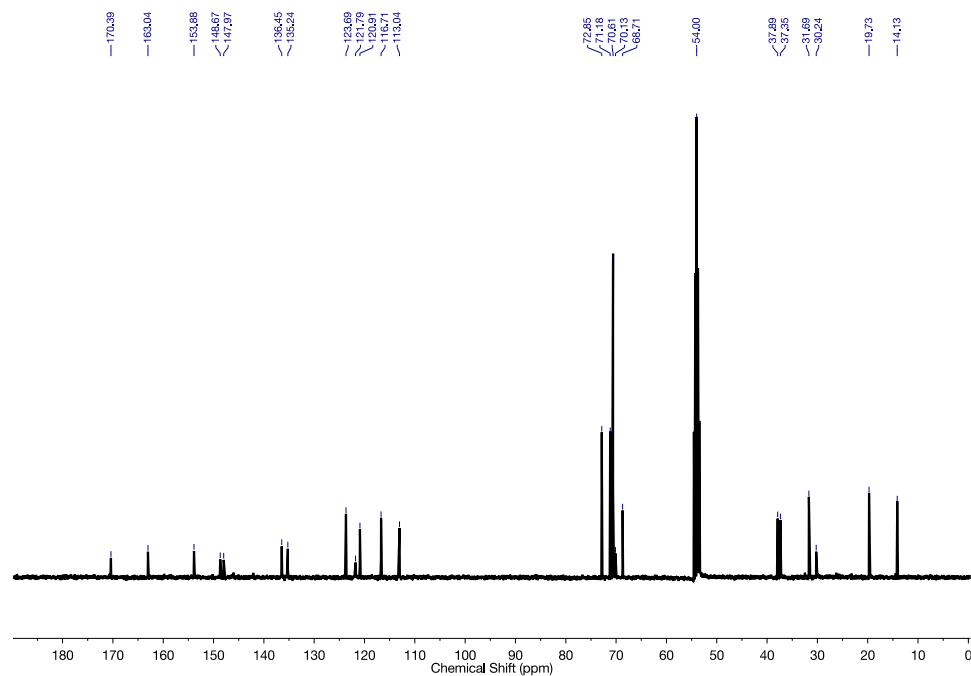

Figure B2: {^{1}H} ^{13}C NMR spectrum of compound **3**.

C. Characterization of Compound 4
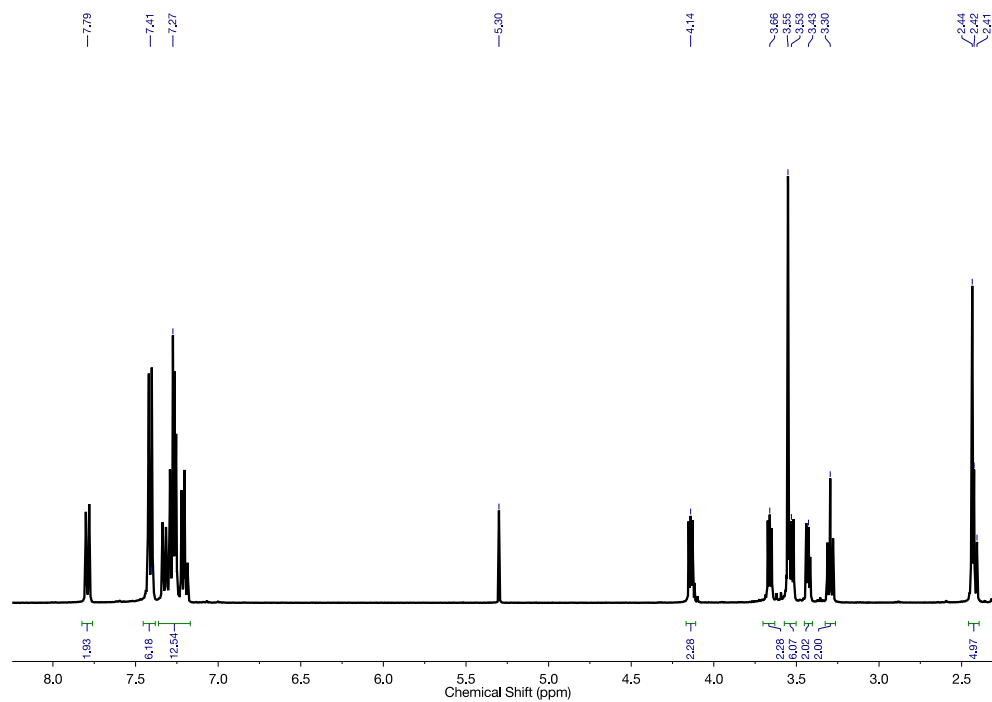
Figure C1: ¹H NMR spectrum of compound **4**.
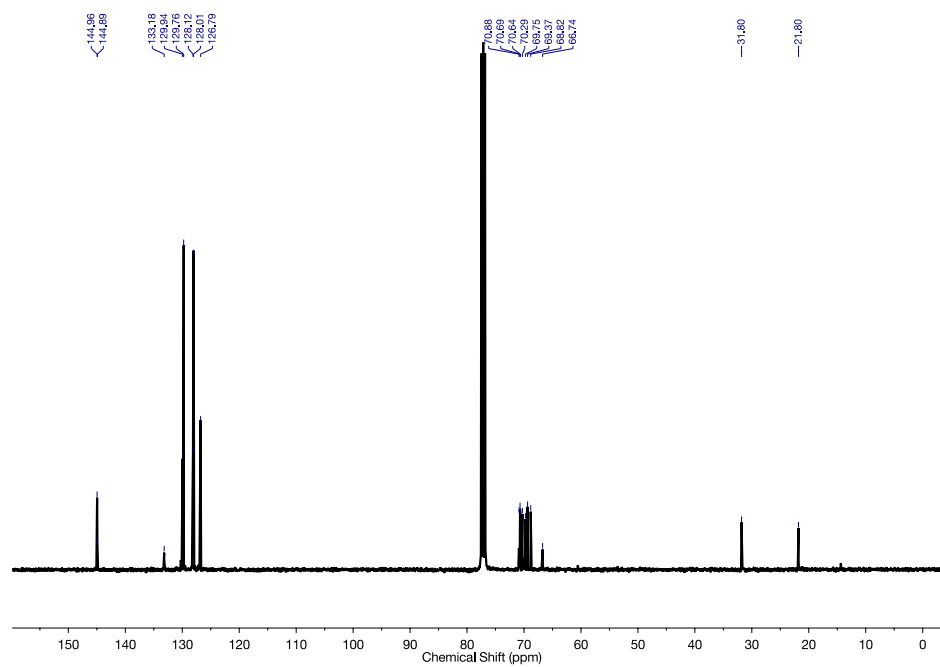
Figure C2: {¹H} ¹³C NMR spectrum of compound **4**.

D. Characterization of Compound 5
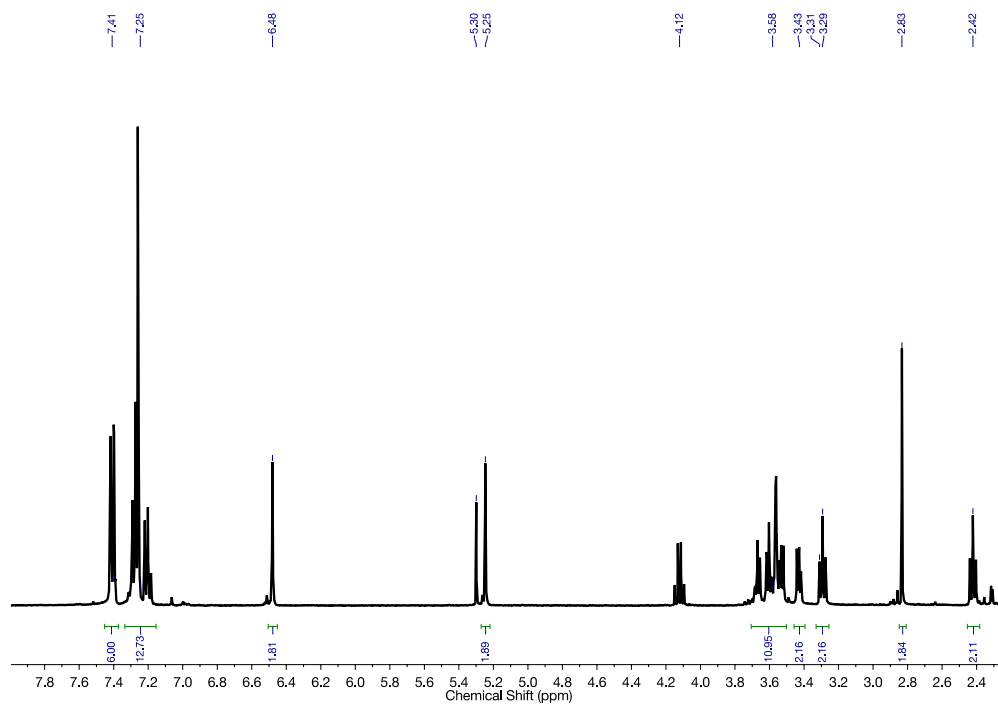
Figure D1: ^{1}H NMR spectrum of compound **5**.
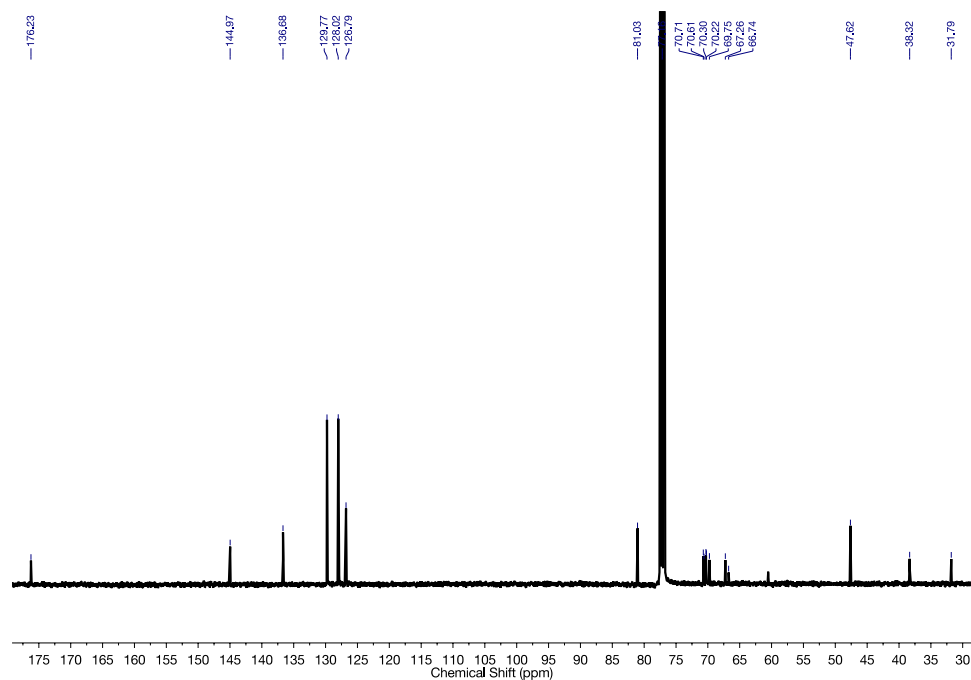
Figure D2: {^{1}H} ^{13}C NMR spectrum of compound **5**.
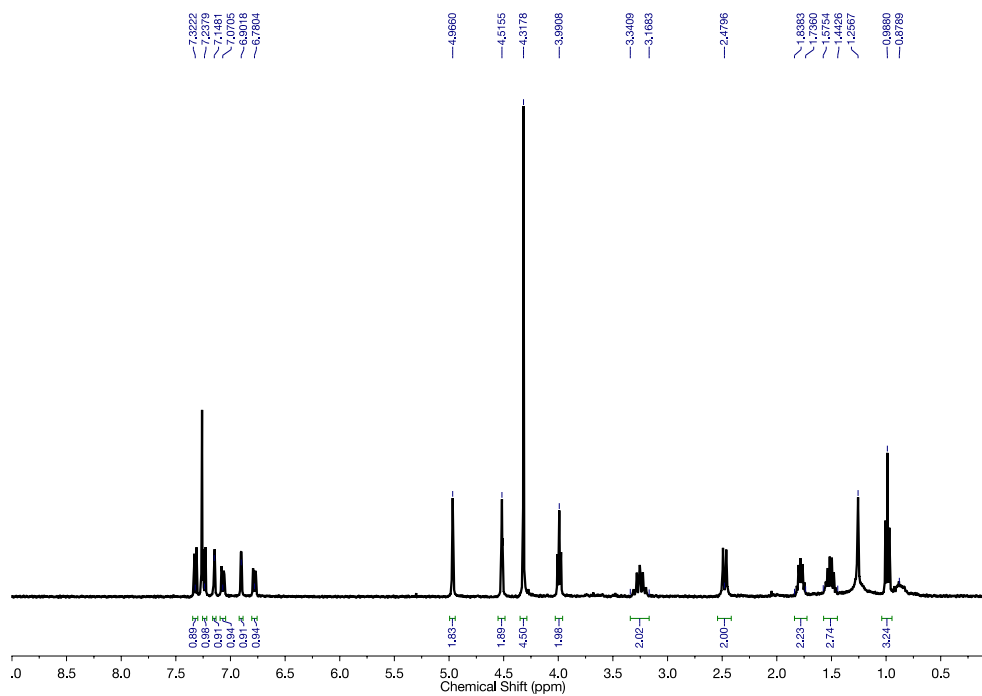
E. Characterization of Compound 6
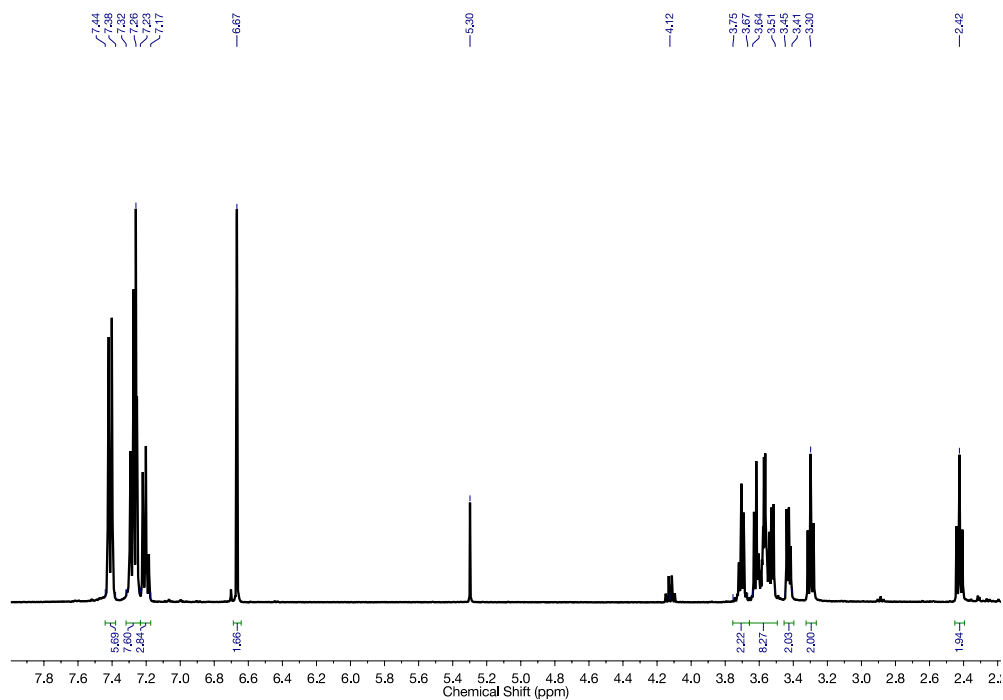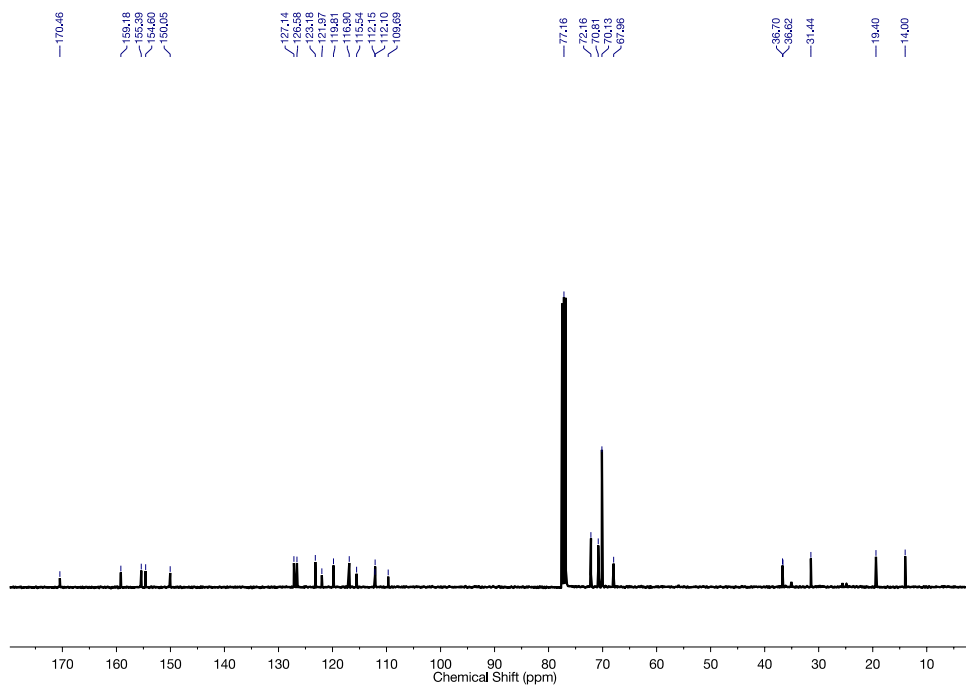
Figure E1: ^{1}H NMR spectrum of compound **6**.
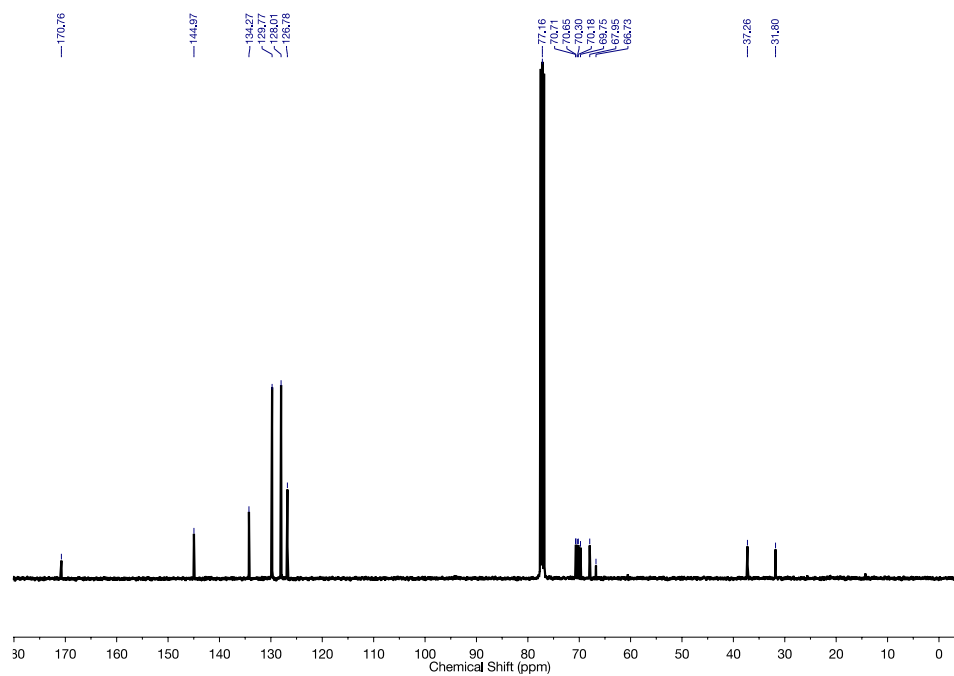
Figure E2: {^{1}H} ^{13}C NMR spectrum of compound **6**.

F. **Characterization of Compound 7**
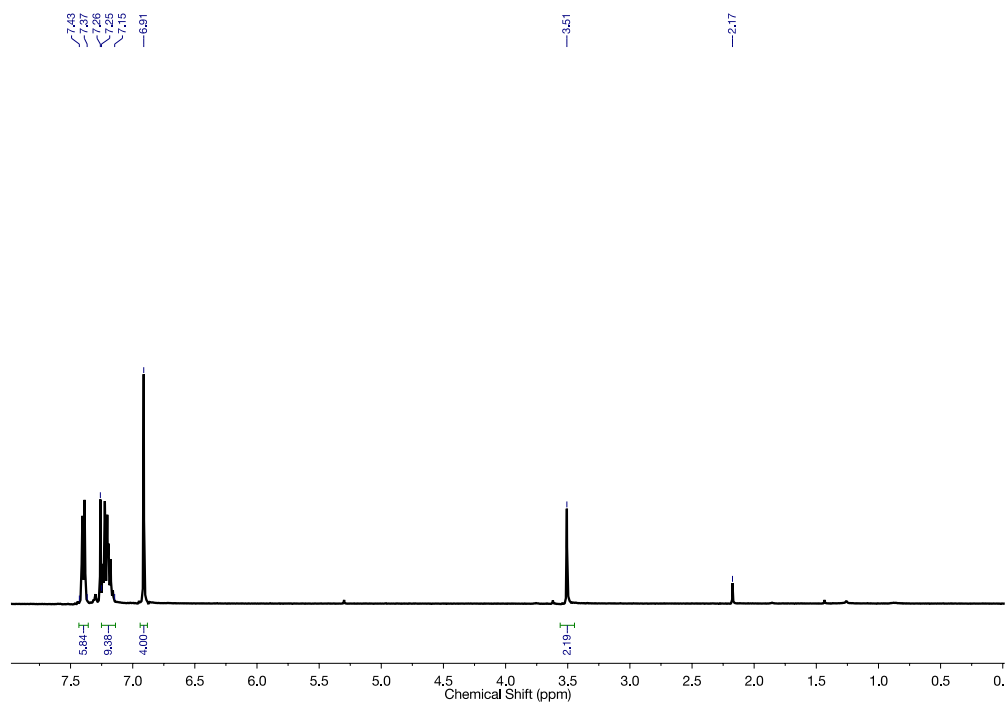
Figure F1: ^{1}H NMR spectrum of compound **7**.
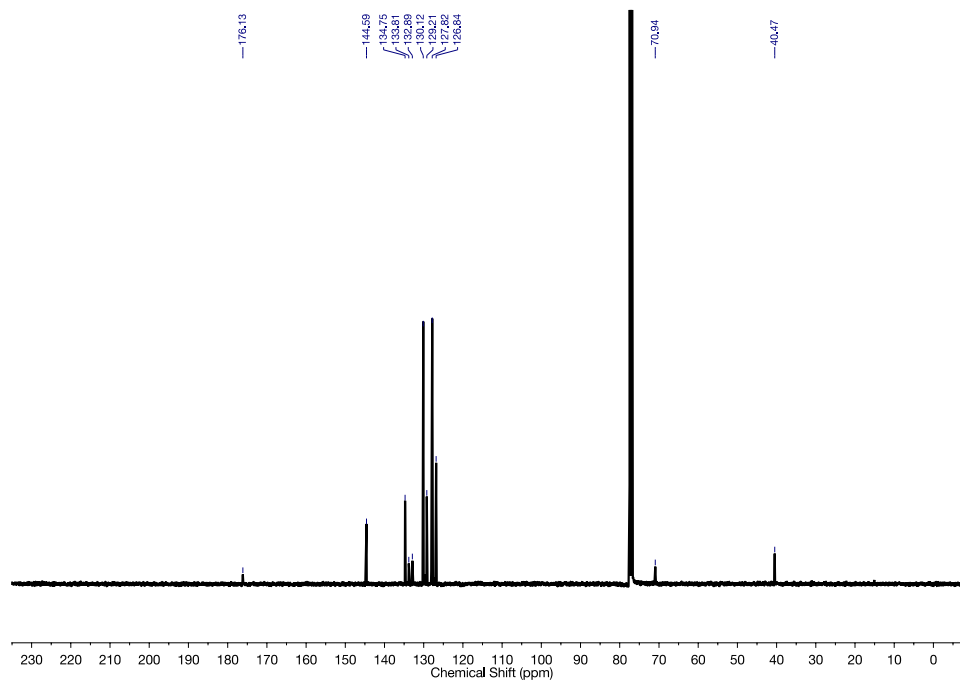
Figure F2: {^{1}H} ^{13}C NMR spectrum of compound **7**.

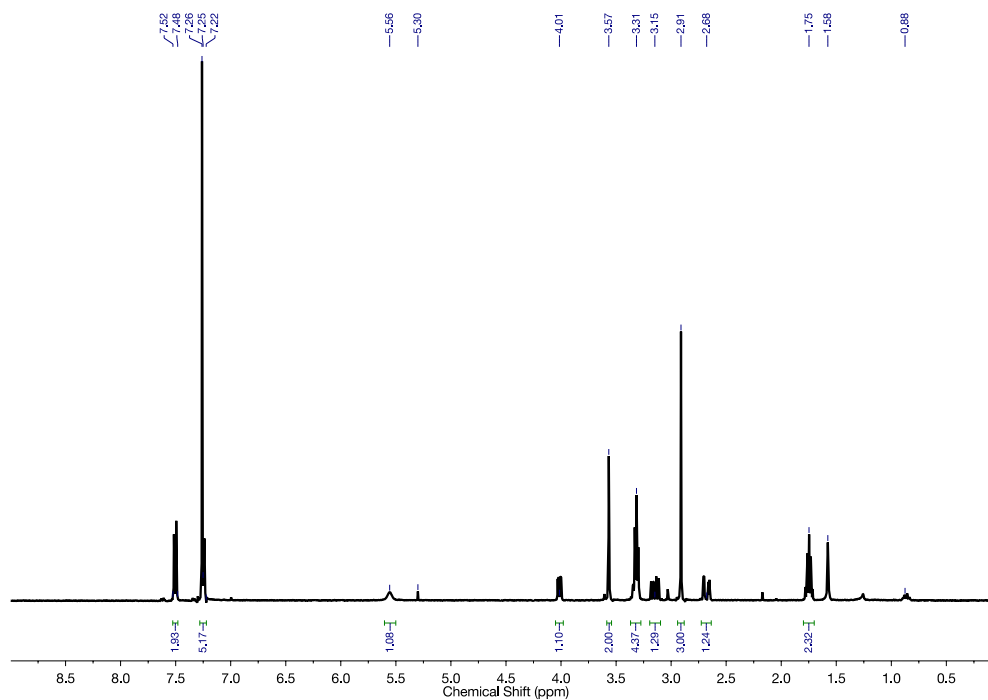### G. Characterization of Compound 8
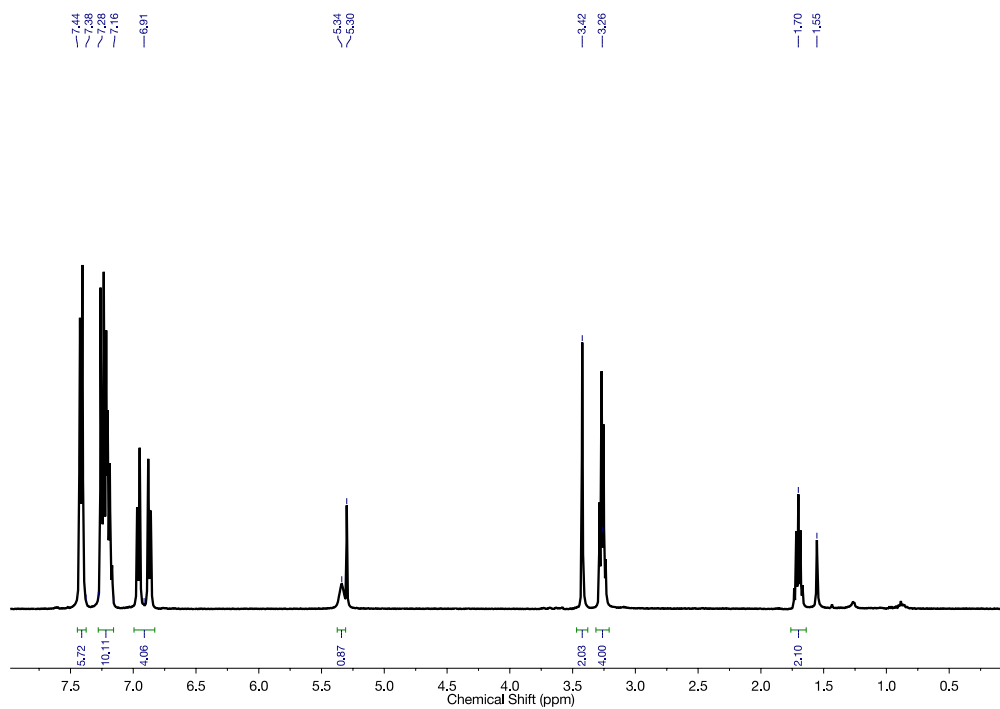
Figure G1: ^{1}H NMR spectrum of compound **8**.
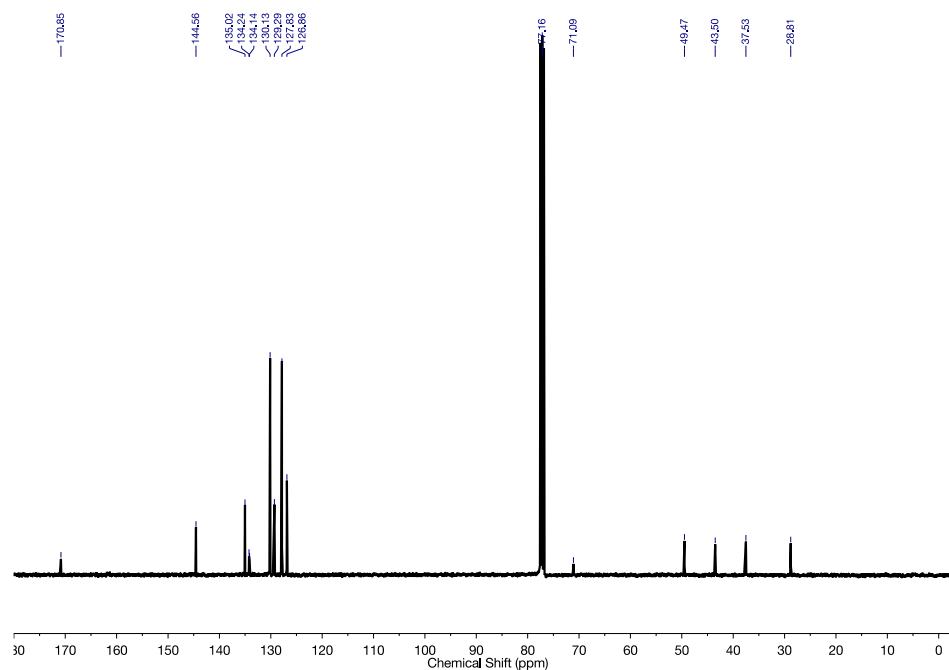
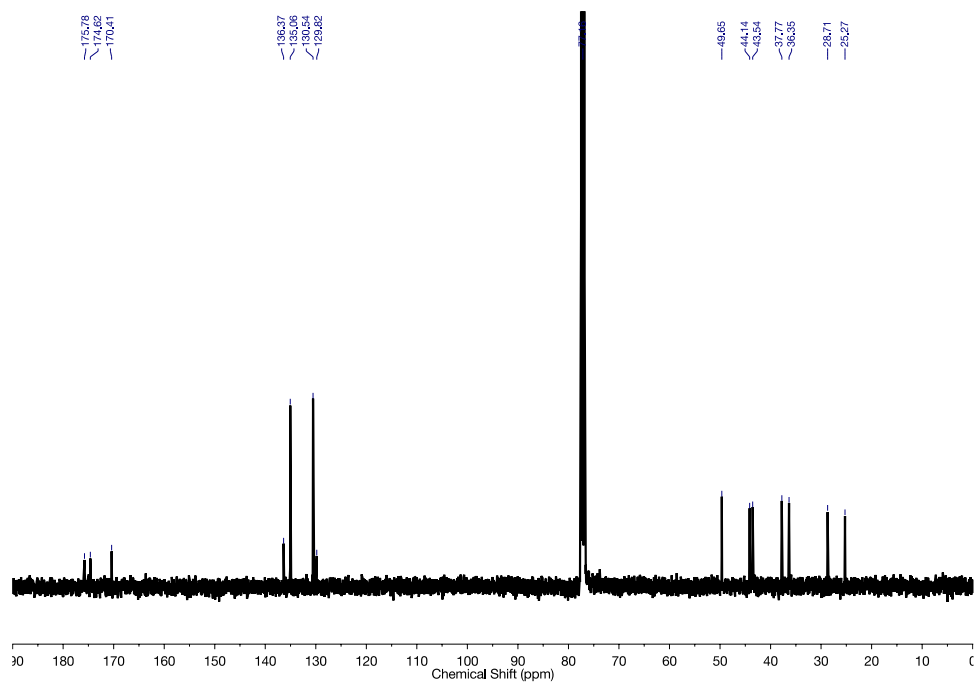**Figure G2:** {^{1}H} ^{13}C NMR spectrum of compound **8**.

H. Characterization of Compound 9
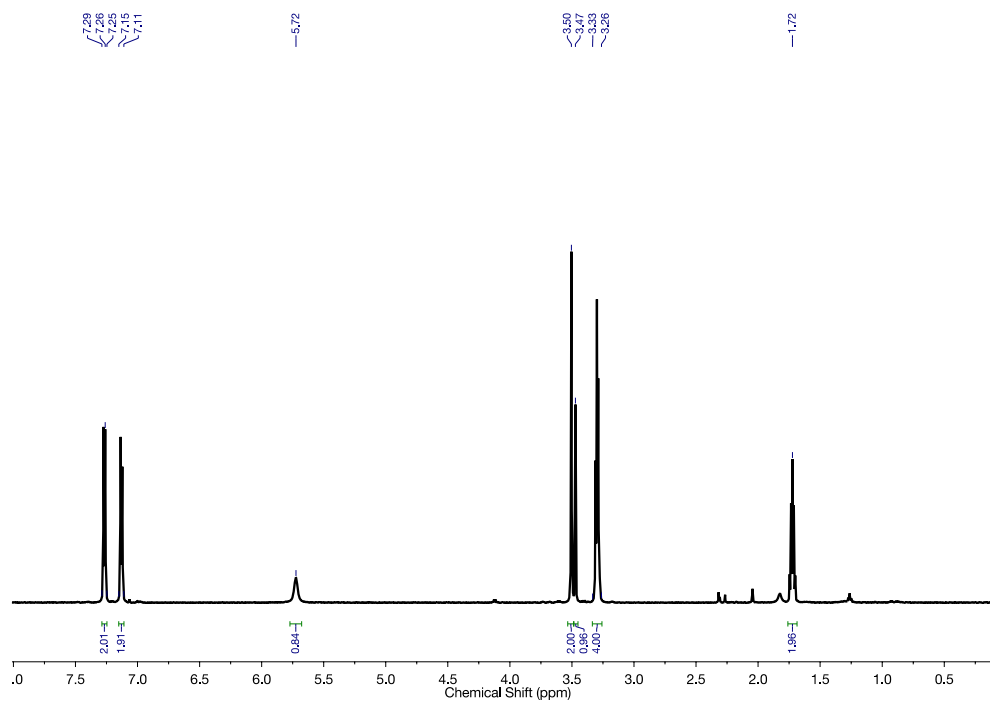
Figure H1: ^{1}H NMR spectrum of compound **9**.
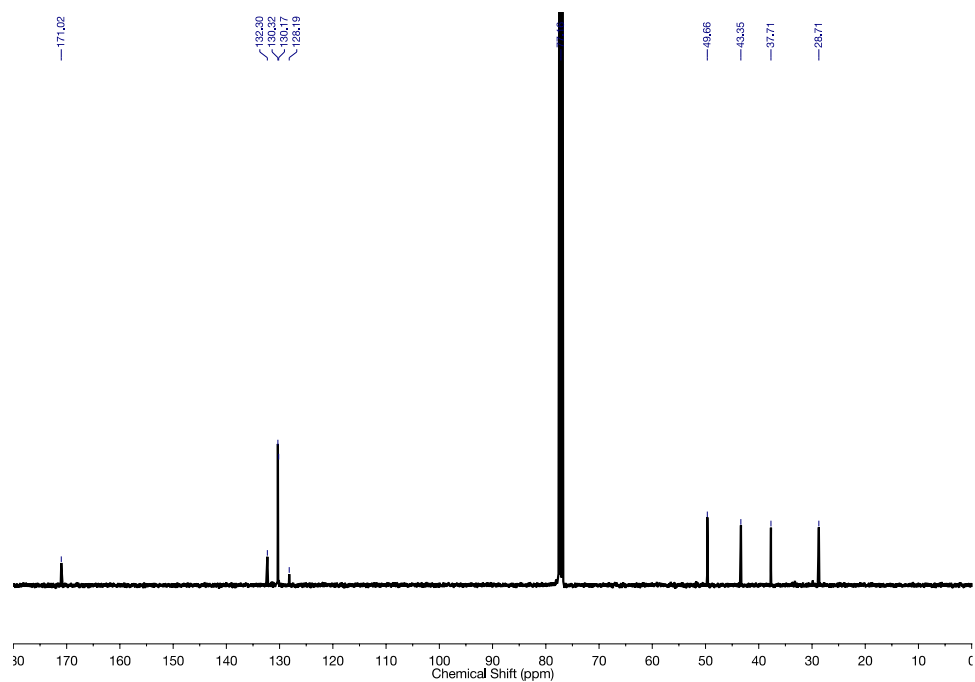
Figure H2: {^{1}H} ^{13}C NMR spectrum of compound **9**.

I.   **Characterization of Compound 10**
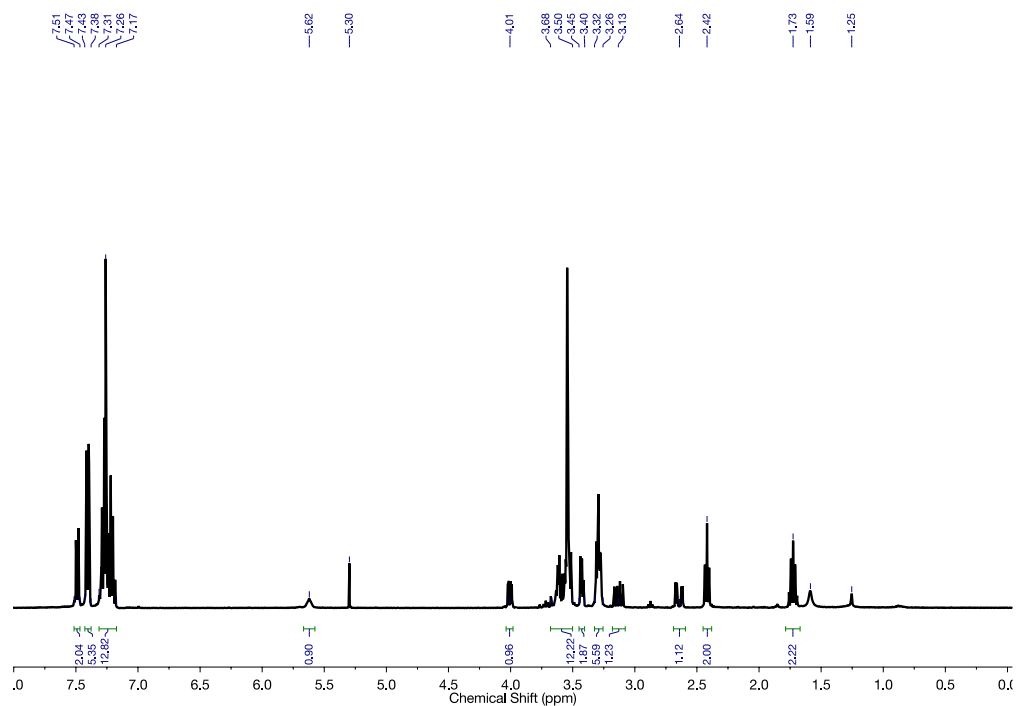
Figure I1: ^{1}H NMR spectrum of compound **10**.
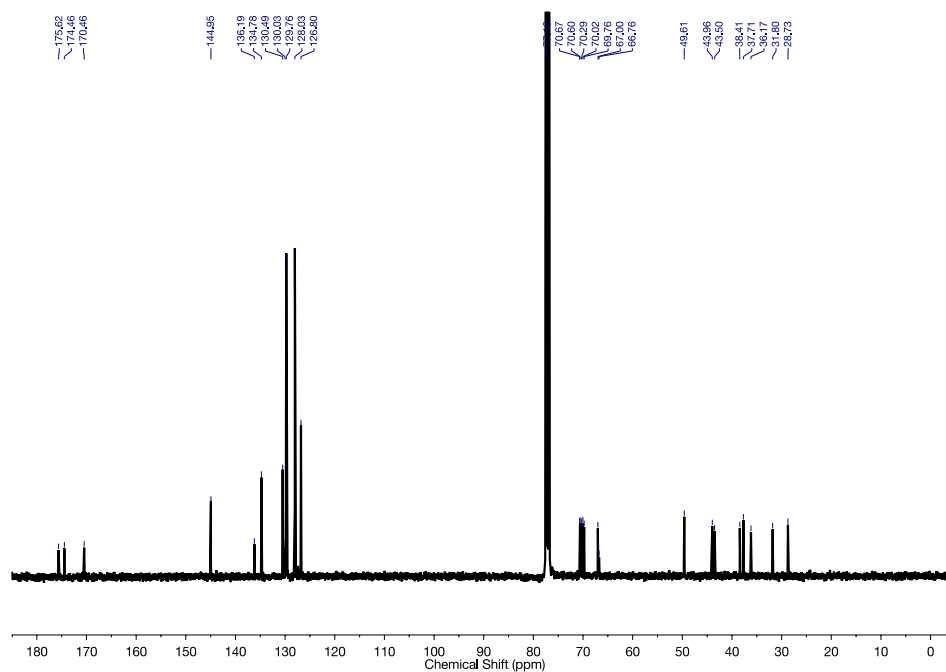
Figure I2: {^{1}H} ^{13}C NMR spectrum of compound **10**.

J. Characterization of Compound 11
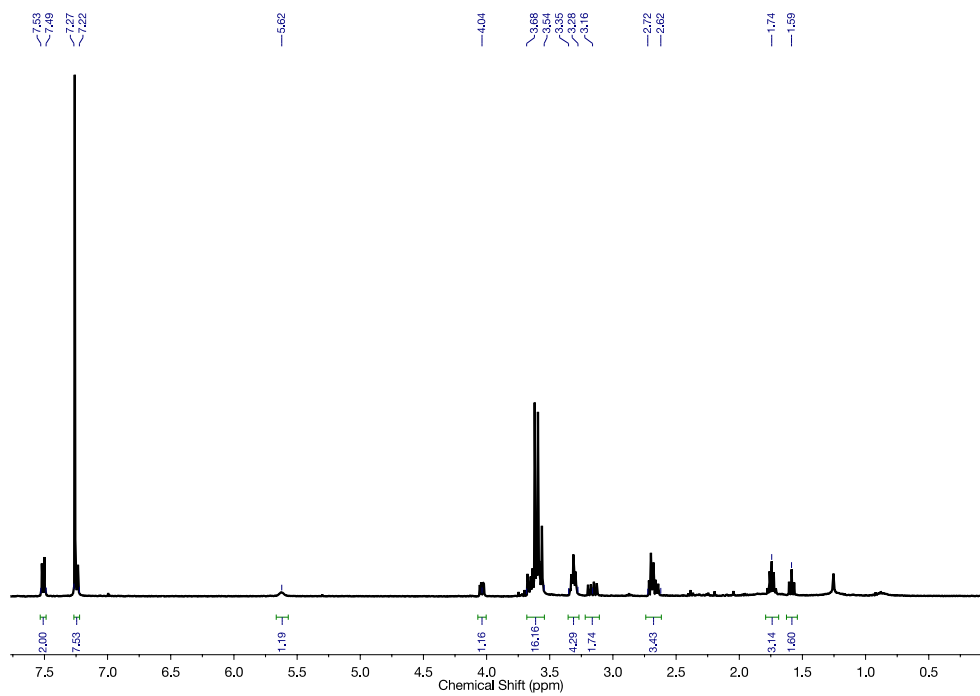
Figure J1: ^{1}H NMR spectrum of compound **11**.
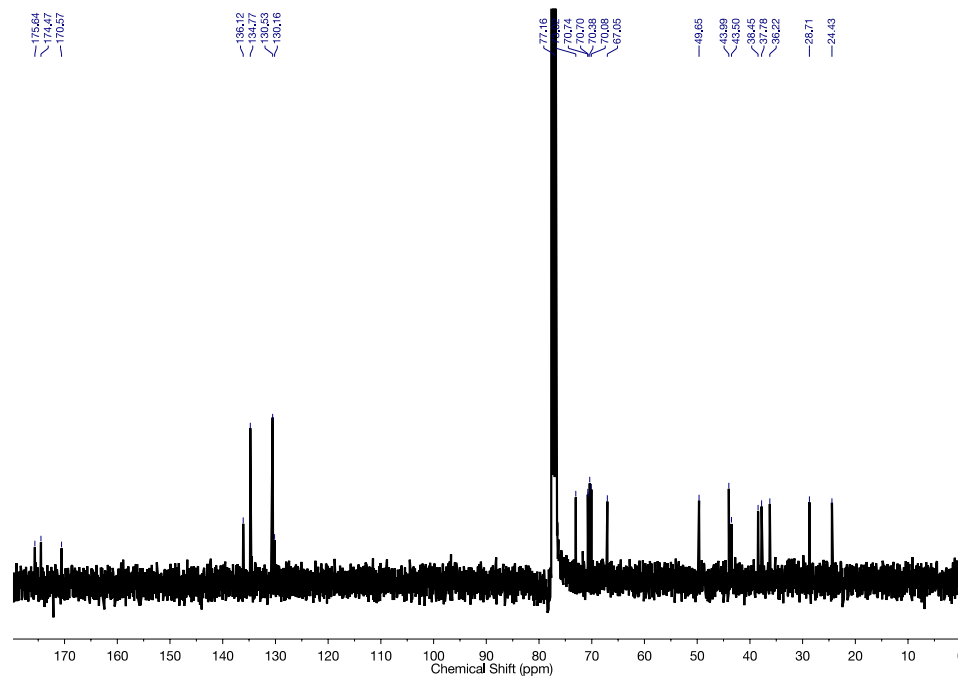
Figure J2: {^{1}H} ^{13}C NMR spectrum of compound **11**.

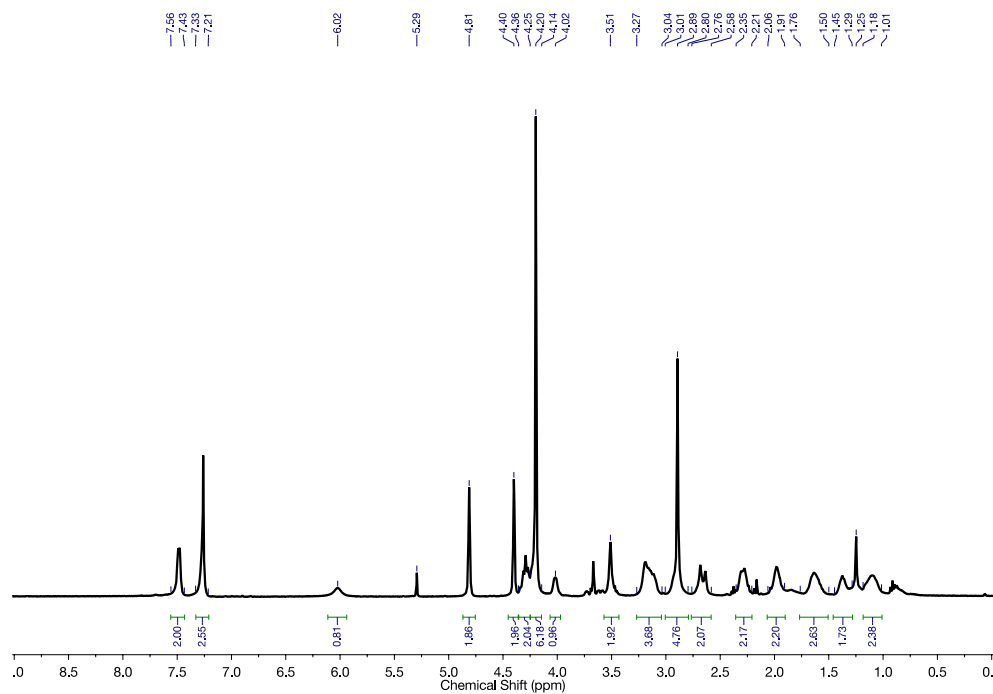### K. Characterization of Compound 16
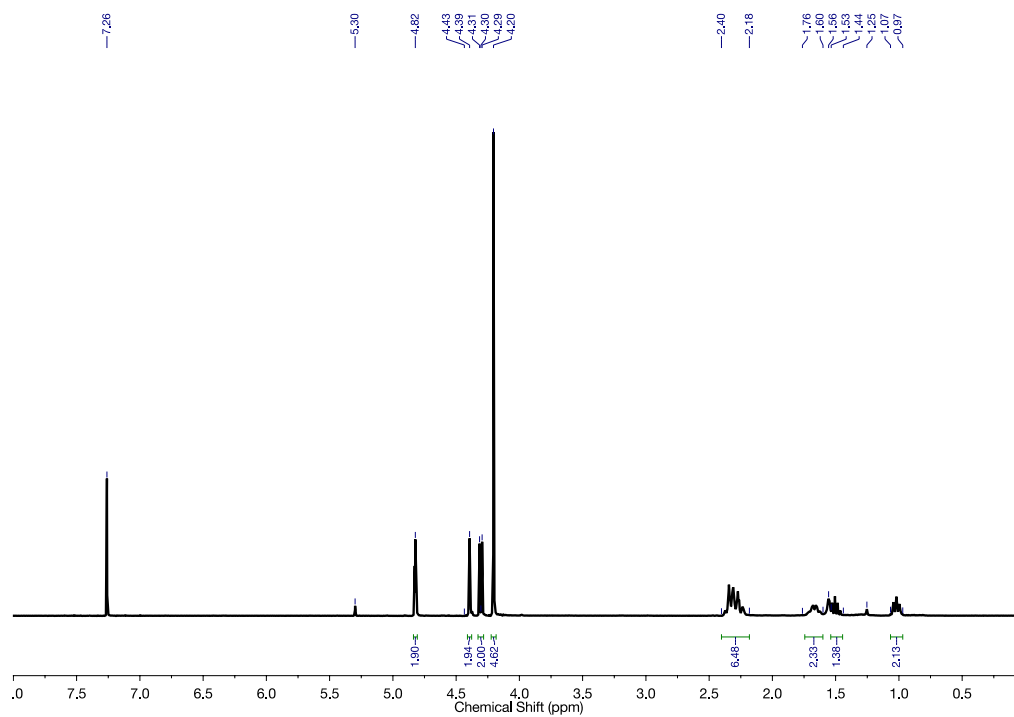
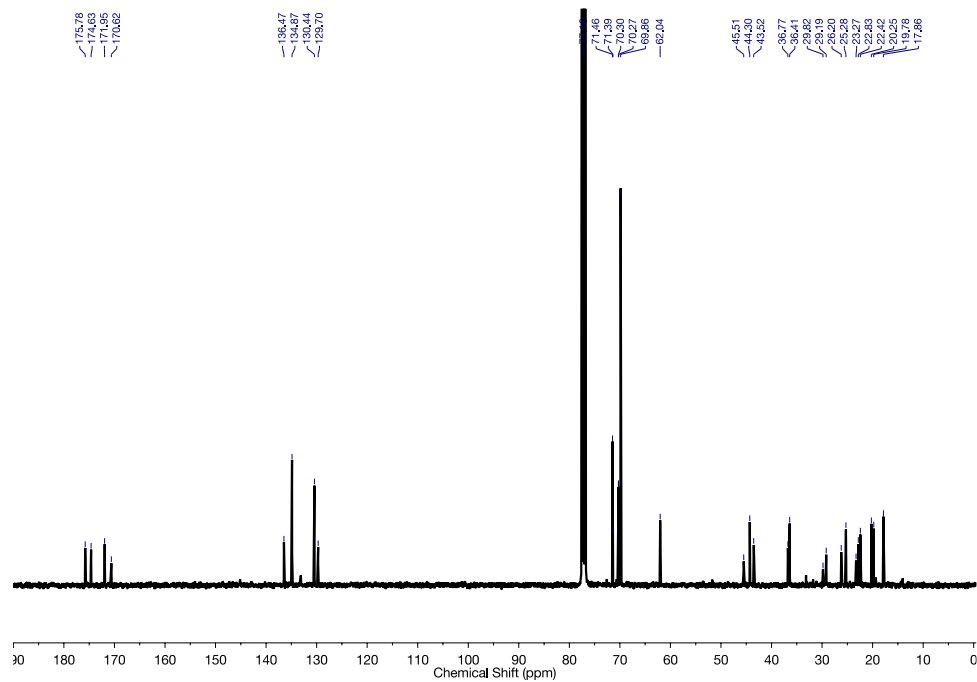**Figure K1:** ^{1}H NMR spectrum of compound **16**.
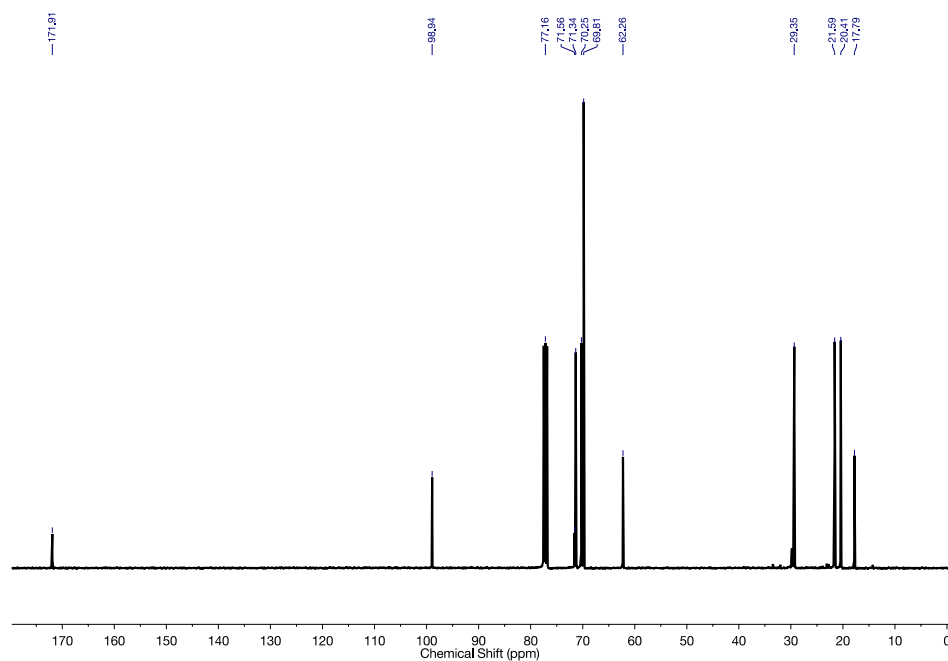
Figure K2: {^{1}H} ^{13}C NMR spectrum of compound **16**.

L. **Characterization of Compound 18**
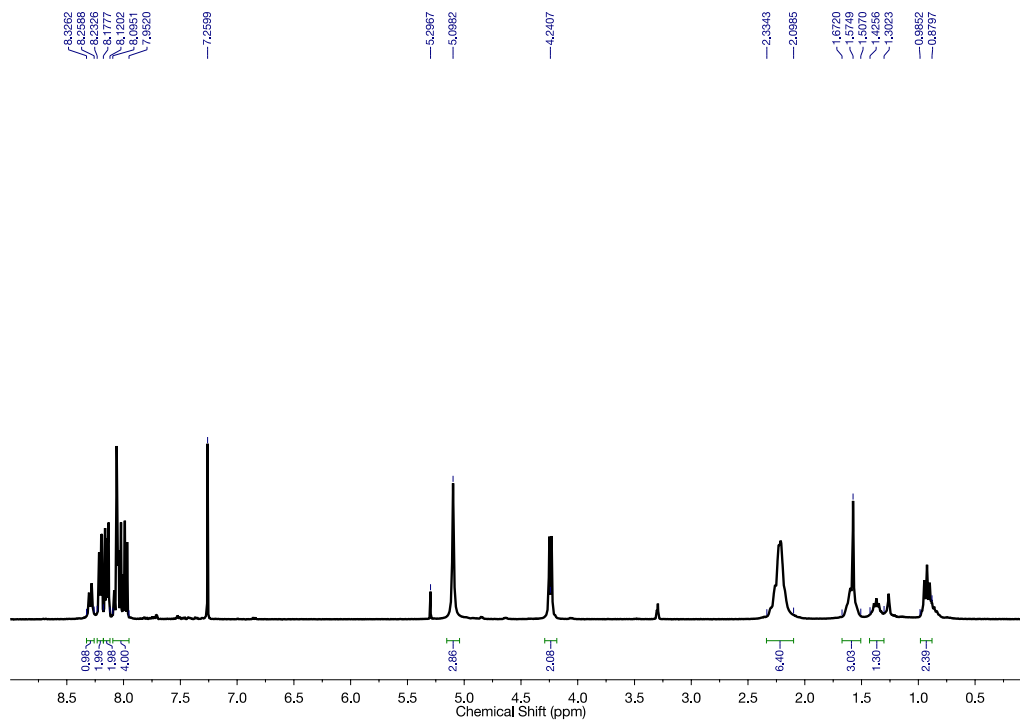
Figure L1: ^{1}H NMR spectrum of compound **18**.
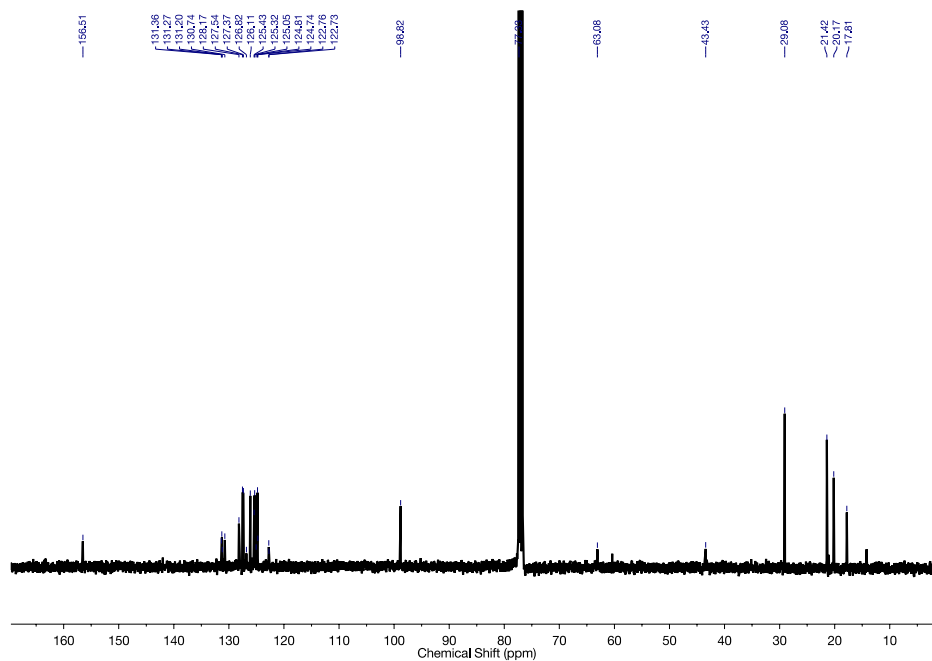
Figure L2: {^{1}H} ^{13}C NMR spectrum of compound **18**.

M. Characterization of Compound 30

Figure M1: ^{1}H NMR spectrum of compound **30**.

Figure M2: {^{1}H} ^{13}C NMR spectrum of compound **30**.

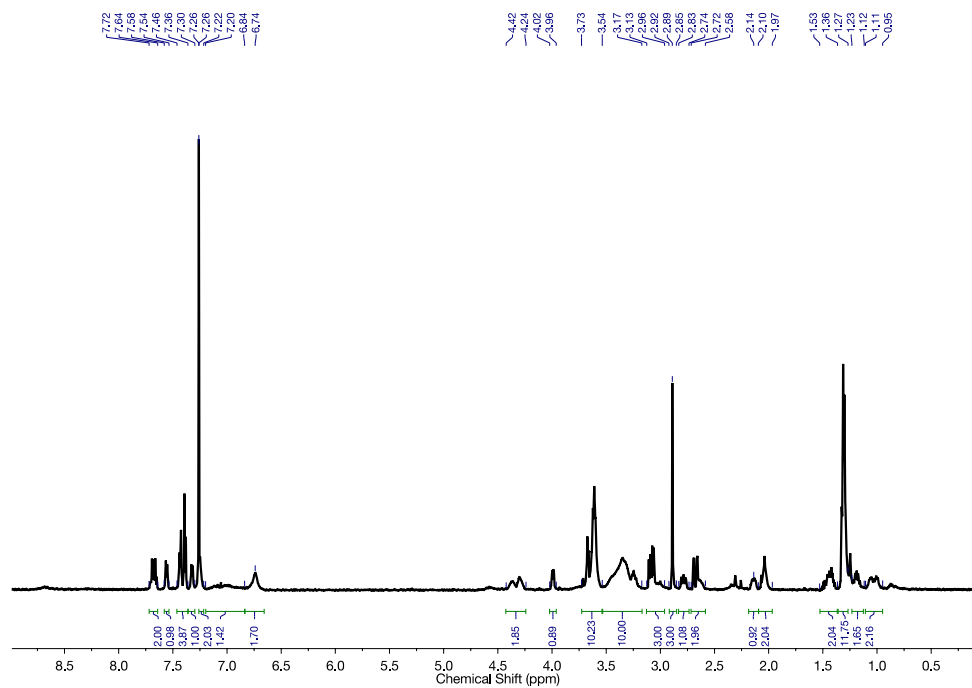### N. Characterization of Compound 31

Figure N1: ^{1}H NMR spectrum of compound **31**.

Figure N2: {^{1}H} ^{13}C NMR spectrum of compound **31**.

O. Characterization of Compound 32

Figure O1: ^{1}H NMR spectrum of compound **32**.

Figure O2: {^{1}H} ^{13}C NMR spectrum of compound **32**.

P. **Characterization of Compound 33**

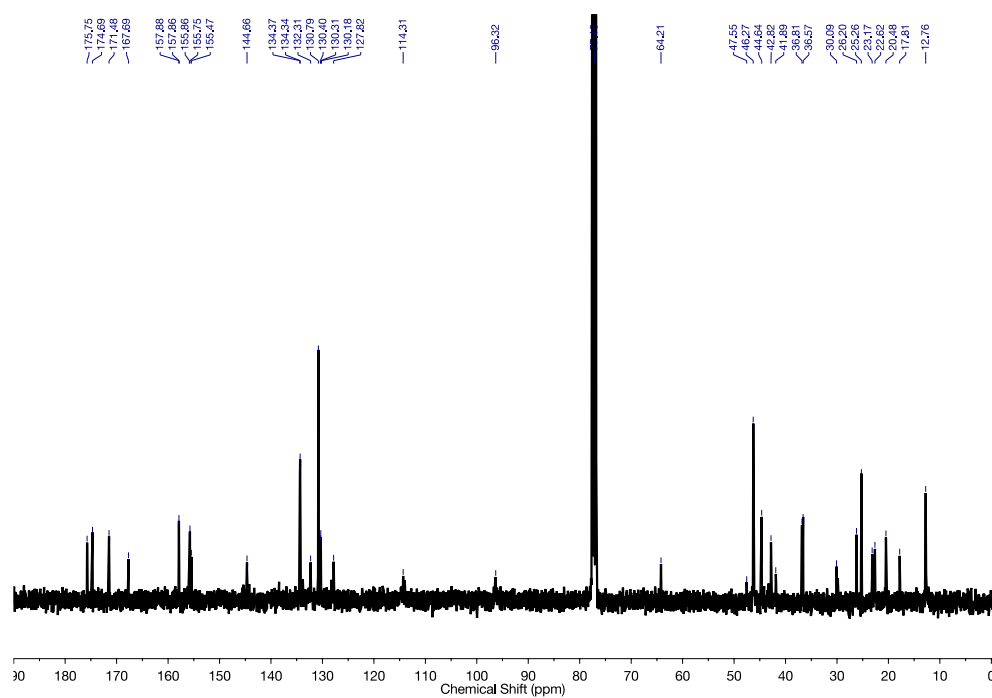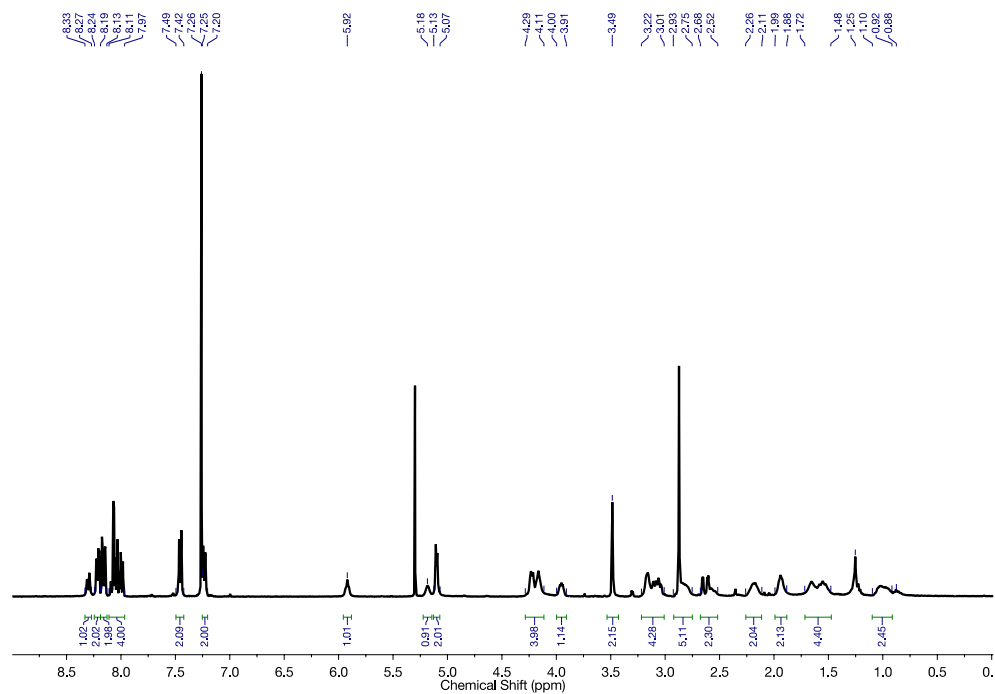**Figure P1:** ^{1}H NMR spectrum of compound **33**.

Figure P2: {^{1}H} ^{13}C NMR spectrum of compound **33**.

Q. Characterization of Compound 34

Figure Q1: ^{1}H NMR spectrum of compound **34**.

Figure Q2: {^{1}H} ^{13}C NMR spectrum of compound **34**.

R. Characterization of Compound 35
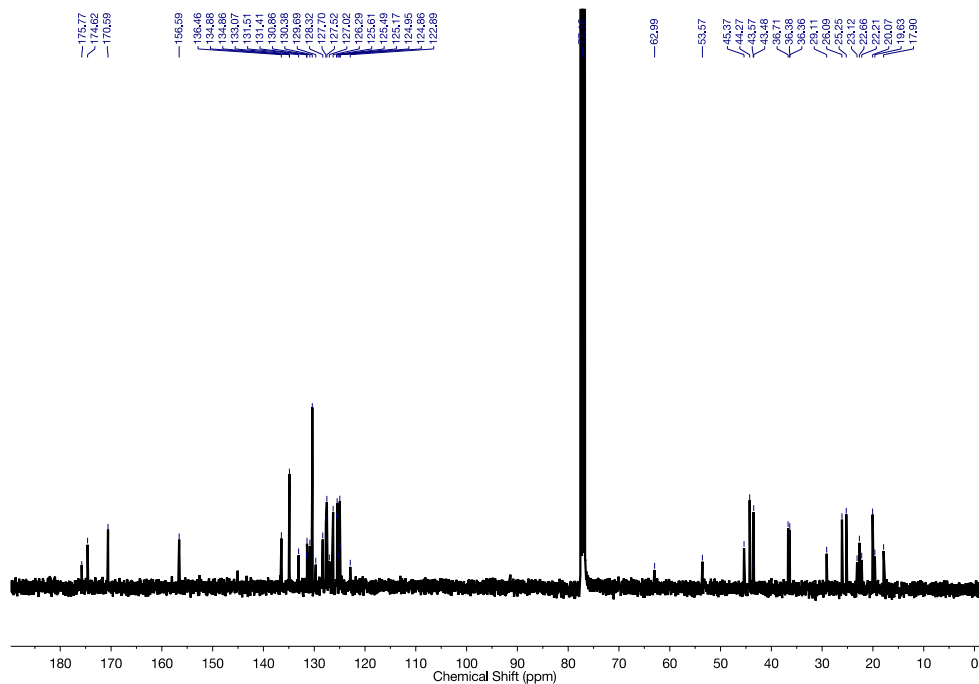
Figure R1: ^{1}H NMR spectrum of compound **35**.

Figure R2: {^{1}H} ^{13}C NMR spectrum of compound **35**.
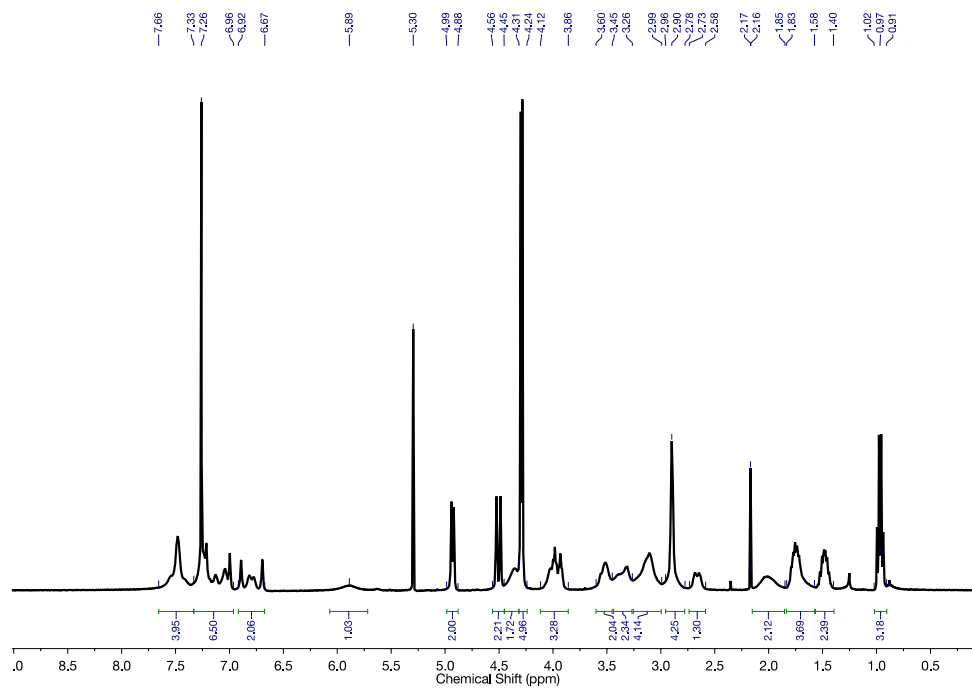
S. Characterization of Compound 36

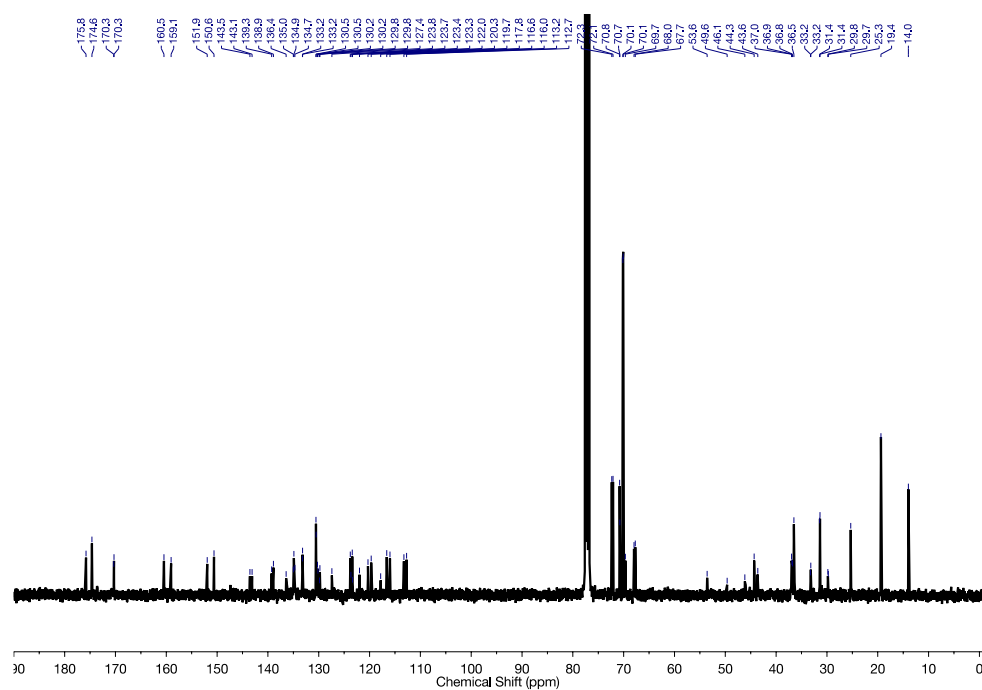**Figure S1:** ^{1}H NMR spectrum of compound **36**.

Figure S2: {^{1}H} ^{13}C NMR spectrum of compound **36**.

Appendix 2: Supporting Information for Chapter 3
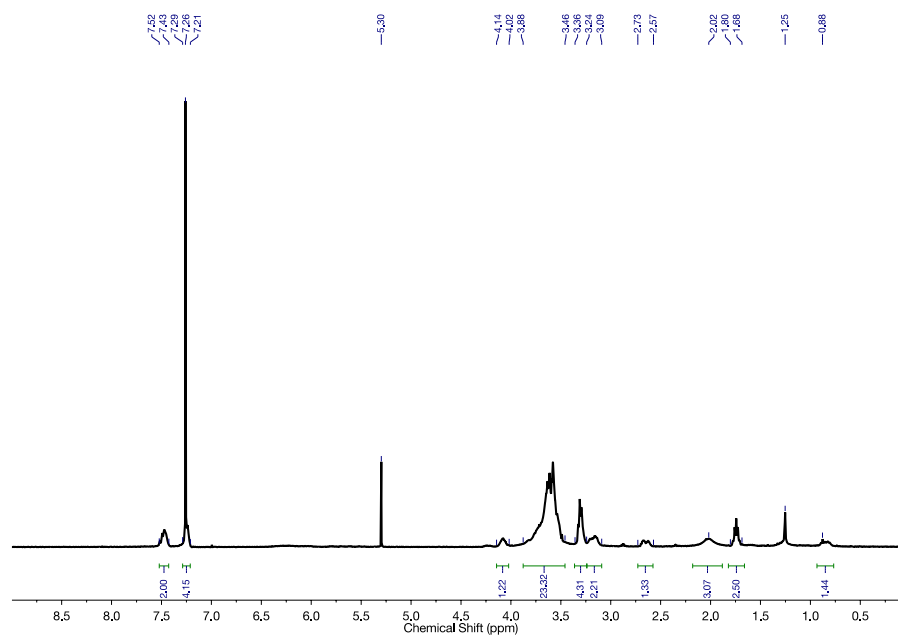
A. Characterization of Compound 41

Figure T1: ^{1}H NMR spectrum of compound **41**.
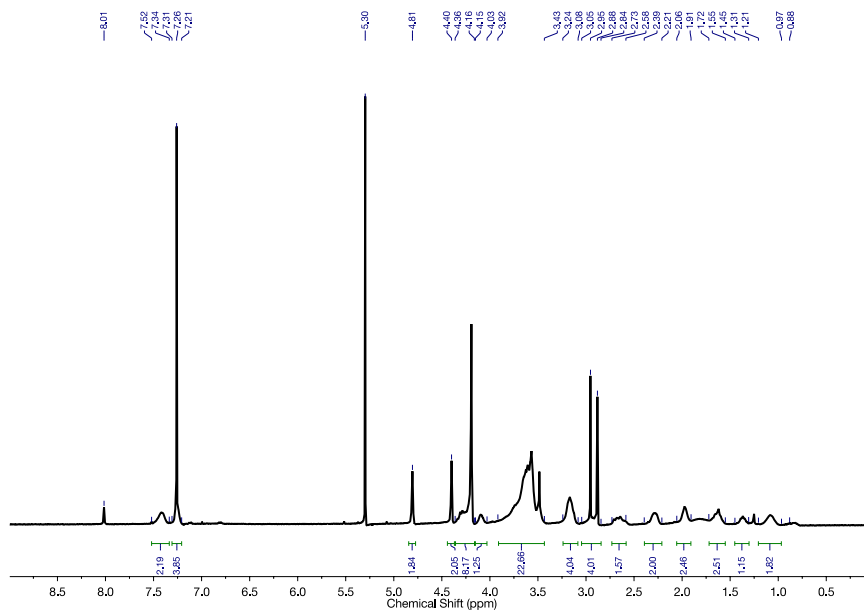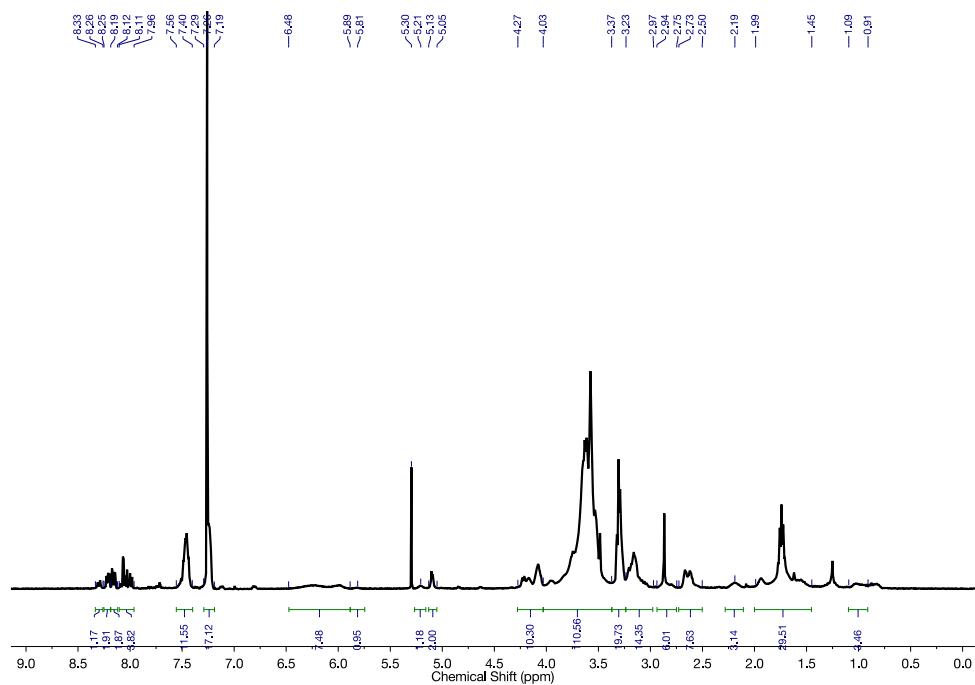
B. Characterization of Compound 42

Figure U1: ^{1}H NMR spectrum of compound **42**.

C. Characterization of Compound 44

Figure V1: ^{1}H NMR spectrum of compound **44**.
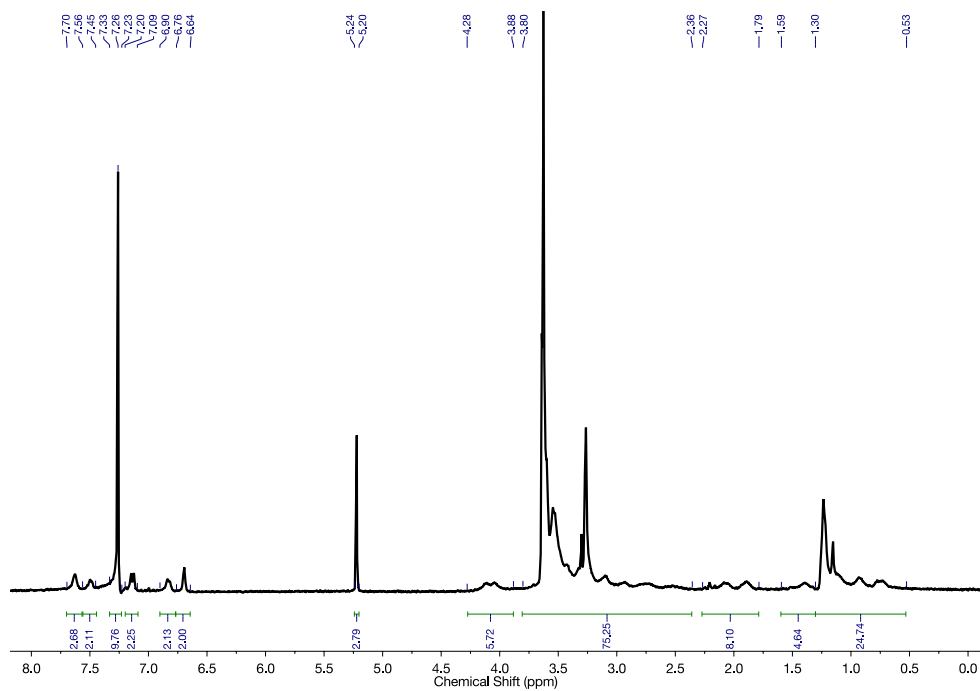
D. Characterization of Compound 45a

Figure W1: ^{1}H NMR spectrum of compound **45a**.

Curriculum Vitae

Name: Jun-Hyeong Park

Post-secondary   The University of Western Ontario
Education and   London, Ontario, Canada
Degrees: 2014 – 2018 B.Sc.
                Chem 4491E Supervisors: Dr. Mark Workentin,
                Dr. Paul Ragogna, and Dr. Michael Kerr

                The University of Western Ontario
                London, Ontario, Canada
                2018 – Present (2020) M.Sc.
                Supervisor: Dr. Mark Workentin

Honours and   Mitacs Globalink Research Award
Awards: 2019

                Aspire Travel Award
                2019

                Science International Engagement Fund
                2019

                QCAM CCCE 2019 Materials Poster Prize
                2019

                Theodor Ackermann Continuing Award
                2016-2017

Related Work   Resource Room Teaching Assistant (Chem 2213A)
Experience   Laboratory Teaching Assistant (Chem 2283G)
                The University of Western Ontario
                2018-2020

                International Research Collaboration
                Visiting Graduate Researcher
                The University of Bristol
                2019
                Supervisor: Dr. Pierangelo Gobbo

                Research Assistant
                The University of Western Ontario
                2016-2017
                Supervisor: Dr. Johanna Blacquiere

Presentations: Aspire & Science International Engagement Fund Presentation (Departmental): Jun-Hyeong Park, Dr. Pierangelo Gobbo, and Dr. Mark S. Workentin. Development of Gold Nanoparticle based Photo-Responsive Colloidosomes, The University of Western Ontario, London, ON, Canada, March 5, 2020.

Conference Poster Presentation (National): Jun-Hyeong Park and Dr. Mark S. Workentin. Development of Multi-Functional Molecular Systems Based in Reversible Thiol-Michael additions to Maleimide Gold Nanoparticles, 102nd Canadian Chemistry Conference and Exhibition, Quebec City, QC, Canada, June 3 – June 7, 2019.

Course Work: Chem 9503R – Advanced NMR I (82%)
Chem 9563Q – Total Synthesis (92%)
Chem 9603T – Advanced NMR II (100%)
Chem 9651S – Organometallic Bond Activation (88%)
Chem 9657Y – Pass (Average grade = 88%